Generation and characterisation of a nociceptor specific Cre expressing mouse

Lucy Caroline Stirling

A Thesis submitted for the degree of Doctor of Philosophy to the University of London

Department of Biology, University College London

February 2004

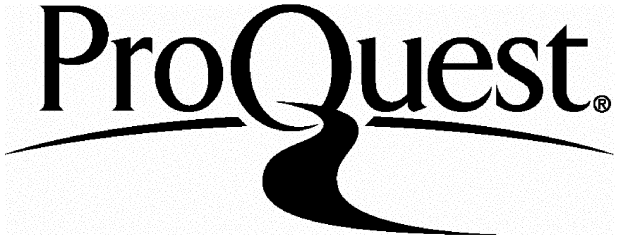

Contents

Figures and Tables

Chapter 2

Chapter 3

Chapter 4

Acknowledgments

I would like to thank Professor John Wood for the opportunity to undertake a PhD in his laboratory and for his support and guidance during this time. My thanks to my teacher, Dr. Mohammed Nassar, a man of integrity, kindness and patience, are huge.

Many other past and present members of the Molecular Nociception Group have been a great support throughout - thanks are due particularly to Anjan, Bjarke, James, Karen, Kenji, Liam, Louisa, Louise, Manue, Mark, Paolo, Sam and Veronika. Dr. Greta Forlani, from Milan, kindly helped with the project when time was pressured.

Intermittent visits to Professor Giorgio Gabella have been welcome interludes, and resulted in superb technical help and many enjoyable discussions. Professor Stephen Hunt and members of his laboratory have given much helpful advice. Thanks are also due to my second supervisor, Dr. Karl Peter Giese.

May I take something of what I have learnt to patients, the prime motivators to explore the world of pain.

My parents, sisters and brother have yet again and as ever been sources of invaluable verbal and non-verbal support. Wonderful friends, Columba, Jax, Mala, Maureen and Miranda have provided patient ears at the end of the 'phone and masses of reviving laughter, care and encouragement. These were all vital.

This thesis is dedicated to Hans, a precious, wise anchor of patience, trust and understanding. My thanks are endless.

Lara and Alice, your simplicity, complexity, abject honesty, love and laughter have been my sanity checks throughout.

Abbreviations

ATP	Adenosine triphosphate
AMPA	α-amino-3-hydroxy-5-methyl-4-isoazolepropionic acid
BAC	Bacterial artificial chromosome
BDNF	Brain-derived neurotrophic factor
BK	Bradykinin
bp	base pair
cAMP	cyclic adenosine monophosphate
CFA	Complete Freund's Adjuvant
CGRP	Calcitonin gene related peptide
CMV	Cytomegalovirus
CNS	Central nervous system
DNA	Deoxynucleic acid
DRG	Dorsal root ganglion
ES cells	Embryonic stem cells
GABA	γ-amino butyric acid
GDNF	Glial-derived neurotrophic factor
GFP	Green fluorescent protein
HSV	Herpes Simple Virus
H	Histamine
5HT	5-Hydroxytryptamine
IB_4	Isolectin B_4
IPANs	Intrinsic primary afferent neurons
IRES	Internal ribosomal entry site
LBD	Ligand binding domain
MGlu	Metabotrophic Glutamate receptors
NF200	Neurofilament-200
NGF	Nerve growth factor
NK1	Neurokinin-1
NMDA	N-methyl-D-aspartate
OHT	4-hydroxytamoxifen
PAC	Phage artifical chromosome
PBS	Phosphate buffered saline
PCR	Polymerase chain reaction
PKC	Protein kinase-C
hPLAP	Human placental alkaline phosphatase
PNS	Peripheral nervous system
R26R	ROSA26 reporter
RNA	Ribonucleic acid
rpm	Revolutions per minute
SCG	Superior cervical ganglion
siRNA	Small interfering RNA
SP	Substance P
TRP	Transient receptor potential
TTX	Tetrodotoxin
3'UTR	3' untranslated region
VGSC	Voltage gated sodium channel
YAC	Yeast artifical chromosome

Summary

Examination of mouse null mutants provides useful insights into gene function, but perinatal lethality or developmental compensatory mechanisms may obscure behavioural phenotypes. The bacteriophage Cre-*loxP* system provides a method of producing deletion of genes in specific tissue. The tetrodotoxin-resistant voltage gated sodium channel, $Na_V1.8$, is expressed exclusively in a subset of primary afferent neurons, more than 85% of which are nociceptors. The heterozygous $Na_V1.8$ mouse has been shown to have a normal electrophysiological and behavioural phenotype.

In this project gene targeting was used to insert the Cre-recombinase gene into the translational start of $Na_V1.8$ in embryonic stem cells and transgenic mice expressing Cre under the control of the $Na_V1.8$ promoter were generated. The expression pattern of functional Cre was examined using ROSA26 reporter mice and was found to be identical to $Na_V1.8$. Expression started at E13 and was limited to small diameter neurons in dorsal root ganglia, trigeminal ganglia and nodose ganglia. There was no expression in non-neuronal cells or in the central nervous system. This pattern of expression did not alter in adult animals.

Examination of the $Na_V1.8$ mediated TTX-resistant current in small diameter dorsal root ganglion neurons from heterozygote $Na_V1.8$Cre animals revealed that it was identical to that in wild type neurons. In addition, the nociceptive behavioural phenotype of adult heterozygote $Na_V1.8$Cre mice both in tests of mechanical and thermal thresholds and in models of inflammatory and neuropathic pain, was identical to that of wild type mice.

These findings demonstrate that the $Na_V1.8$Cre mouse line is a suitable tool to examine the effects of nociceptor specific gene deletion on pain behaviour, and so provide insights into the role of widely expressed genes in nociception.

Chapter 1

General Introduction

This chapter will provide a general introduction to the neurobiology of pain. Specific introductions will be given at the beginning of the ensuing chapters.

1.1. Overview of the nervous system

The nervous system can be subdivided anatomically into the central nervous system (CNS) that comprises the spinal cord and brain, and the peripheral nervous system (PNS) that comprises neuronal tissue outside these organs. Functionally, it can be subdivided into the motor nervous system, in which information controlling bodily function is conveyed from the CNS to the periphery via efferent neurons, and the sensory nervous system, in which sensory information is conveyed to the CNS from the periphery in afferent neurons. The motor nervous system is further divided into the somatic motor system that controls skeletal muscle function, and the autonomic nervous system that controls smooth muscle, cardiac muscle and glandular function. The main components of the autonomic system are the sympathetic and parasympathetic nervous systems. In addition, the enteric nervous system controls the physiological function of the gastrointestinal tract.

The cell bodies of PNS neurons cluster together to form ganglia, and peripheral axons are grouped together to form nerves that are enveloped by glial cells (Schwann cells). Sensory ganglia lie adjacent to the spinal cord or brain and extend axons to the periphery that terminate in specialised end organs. These end organs contain specialised receptors that transduce sensory information into electrical stimuli.

1.2. Pain

One of the most common reasons for seeking medical attention is the experience of pain. Pain profoundly affects quality of life, interfering with physical activity, causing anxiety and fear, and undermining confidence in one's health. A World Health Organization survey of almost 26,000 primary health care patients across 14 countries (Gureje et al., 1998) revealed that a mean of 22% of adult patients reported

persistent (i.e. for over 6 months) pain, and that when compared with patients without pain, these patients were significantly more likely to have a psychological disorder, to rate their health as moderate or poor and to experience significant interference with their work because of pain.

Pain is the most common symptom in patients with cancer; it is present in 30-45% of patients at diagnosis and affects 65-90% with advanced disease. Globally, ten million new cases of cancer were diagnosed in 2000, and cancer accounted for 12% of all deaths (WHO, 2003). In England, more than one in three people will develop cancer during their lives, and one in four will die of cancer (DOH, 2000).

An assessment of a patient with pain involves an evaluation of the physical and non-physical factors contributing to the experience of pain. Management includes interventions directed at the primary cause of pain (for example, anti-neoplastic treatment or antibiotics in the case of cancer or infection respectively), pharmacological and non-pharmacological interventions directed at the relief of pain, and close monitoring and follow-up. Currently available pharmacological agents include non-opioid (paracetamol and cyclo-oxygenase inhibitors) and opioid (e.g. codeine, morphine, diamorphine, fentanyl) analgesics, and adjuvant analgesics. Adjuvant analgesics are by definition agents whose primary indication is for conditions other than pain but which have been shown to have analgesic effects - anticonvulsants, antidepressants, corticosteroids, muscle relaxants and antispasmodic agents. Non-pharmacological interventions include local and regional neurolysis, local anaesthesia and psychological therapies.

The pathological process(es) underlying pain direct the choice of analgesic intervention. However, multiple mechanisms and multiple factors contribute to the generation and experience of pain, these factors are dynamic, and within a disease category the pathological process may not be consistent. Further, concomitant illness, genetic variability, and psychosocial factors play a significant role in the generation and experience of pain, and the response to a given analgesic agent. These factors combined with the relatively small armamentarium of agents available to treat pain mean that a proportion of patients with chronic, particularly neuropathic pain do not obtain complete relief from the agents prescribed (Dunn et al., 2001;

Sindrup and Jensen, 1999). Studies have shown that approximately 10-20% of cancer patients do not experience adequate pain control or that it is accompanied by significant side effects (Meuser et al., 2001; Ventafridda et al., 1987). The very presence of persistent non-malignant pain (Gureje et al., 1998) highlights the inadequacy of available treatment modalities.

Pain is defined as an emotional and sensory experience caused by potential or actual tissue damage (IASP, 1994). Nociception refers to the activation of damage sensing neurons, nociceptors, following a noxious, i.e. tissue damaging insult, and the transmission of this information to the central nervous system.

Pain can be classified into physiological and pathophysiological pain. Physiological or nociceptive pain refers to pain evoked by a noxious stimulus. Information is transmitted to the brain and acts as a warning to prevent further injury. The afferent input activates a withdrawal reflex, an increase in arousal and emotional and autonomic responses. A classical example is the experience of pain following a needle prick injury.

Pathophysiological pain may be inflammatory, occurring following tissue damage, infection, tumour growth etc., or neuropathic, occurring following neuronal damage or dysfunction, for example diabetic/HIV neuropathy, spinal cord compression, or post-herpetic neuralgia.

One of the key characteristics of the nervous system is its ability to modulate its response to a given stimulus (Woolf and Salter, 2000). This neuronal plasticity within the nociceptive pathway is responsible for the pain syndromes encountered in patients with pathophysiological pain – hyperalgesia, an augmented response to a painful stimulus, allodynia, a painful response to a non-painful stimulus, and spontaneous pain, the presence of pain in the absence of a stimulus.

In vitro experiments and animal models of pathophysiological pain have provided much insight into the changes that occur following tissue or nerve damage both in the phenotype of primary sensory neurons and within the central nervous system.

1.3. Nociceptors

Nociceptors are primary sensory neurons that are activated by stimuli capable of causing tissue damage. They are responsible for transducing a noxious insult into a train of action potentials, and for conducting and transmitting this signal faithfully to the central nervous system. The end organs of nociceptors are free nerve endings that are located in peripheral tissues, and the cell bodies are in the trigeminal and dorsal root ganglia, innervating tissues of the head and body respectively.

Anatomical and functional criteria subdivide primary sensory neurons into three main groups, Aα/β–, Aδ– and C. Aα/β primary sensory neurons have large cell bodies, heavily myelinated axons and conduct action potentials rapidly to the spinal cord. Most Aα/β primary sensory neurons are activated by innocuous mechanical stimuli in skin, muscle and joints and do not contribute to the perception of pain, although recently, Aα/β nociceptive neurons have been reported (Lawson, 2002). In contrast, C and Aδ primary sensory neurons are primarily responsible for the transmission of nociceptive information, responding to noxious thermal (hot or cold), mechanical or chemical stimuli. C-fibre nociceptors have small cell bodies and their axons are unmyelinated resulting in slow action potential conduction. They comprise about 60% of all nociceptors, and most are polymodal, i.e. they respond to all noxious stimulus modalities. In addition there is a group of C-fibres that respond to noxious heat only, and a group, the 'silent nociceptors', that is only activated when sensitised by tissue injury. The cell bodies of Aδ nociceptors are intermediate in size and their axons are thinly myelinated resulting in more rapid signal conduction. Based on their response to thermal stimuli, Aδ nociceptors can be further subdivided into type I nociceptors that have a thermal threshold of ~53°C, and type II nociceptors that are activated at ~43°C. This subdivision is based on the expression pattern of members of the transient receptor potential (TRP) family of non-selective cation channels - type I Aδ nociceptors express TRPV2 (Caterina et al., 1999) and type II Aδ nociceptors express TRPV1 (Tominaga et al., 1998). Aδ nociceptors mediate the rapid sharp, 'first' pain experienced following an insult

whereas C-fibre nociceptors mediate the delayed, more diffuse 'second' pain (reviewed in Julius and Basbaum, 2001).

Neurochemically, nociceptors can be divided into peptidergic and non-peptidergic populations. The peptidergic population expresses the neurotransmitters substance P (SP) and calcitonin gene related peptide (CGRP), and TrkA, the high affinity tyrosine kinase receptor for nerve growth factor (NGF). These neurons are supported by NGF throughout embryogenesis and postnatally. In contrast, the non-peptidergic population contains no SP and expresses a surface carbohydrate group that selectively binds to a plant lectin called isolectin B_4 (IB_4). This IB_4 positive population of nociceptors also expresses the adenosine triphosphate (ATP) - gated ion channel $P2X_3$ and the tyrosine kinase receptor for glial-derived neurotrophic factor (GDNF), c-ret. These neurons are supported by NGF during embryogenesis and by GDNF postnatally. Aα/β neurons express TrkB and TrkC, the high affinity tyrosine kinase receptors for brain-derived neurotrophic factor (BDNF) and neurotrophin-3 respectively.

1.4. Nociception

There are a variety of specialised receptors on the peripheral terminals of nociceptors that are activated by stimuli of differing types. Noxious thermal insults, both hot and cold, activate members of the TRP family of non-selective cation gated ion channels; TRPV1 and TRPV2 are activated by noxious heat, and TRPM8 and ANKTM1 are activated by noxious cold (Patapoutian et al., 2003).

The proteins responsible for the transduction of noxious mechanical stimuli have not yet been clearly identified. Several potential candidates have been reported: there is evidence to suggest that members of the acid sensing ion channel (ASIC) group of cation channels, that are also gated by low pH and peptides, and of the TRP channel family, and of the purinergic receptor family are involved (reviewed in Ernstrom and Chalfie, 2002).

Following tissue damage, a host of chemical mediators are released from damaged tissue, from recruited inflammatory cells (mast cells, neutrophils, platelets etc.), and

from the peripheral nociceptor ending. These mediators activate a variety of receptors located on the nociceptor peripheral terminal and induce local tissue changes that result in the generation of inflammatory pain. Damaged tissues release ATP and protons that activate purinergic, ASIC and TRPV1 receptors respectively. Inflammatory cells release a multitude of factors - bradykinin (BK), cytokines (tumour necrosis factor (TNF-α), interleukin-1 and -6 (IL-1, IL-6)), nerve growth factor (NGF), serotonin (5HT) histamine (H), arachidonic acid and its prostaglandin metabolites - each of which activate specific receptors (BK_2, TrkA, IL, 5HT, H1 and EP receptors) found on the surface of the nociceptor. Several of these factors directly activate nociceptors, whereas others induce plastic changes in the nociceptor that result in a lowered threshold of activation and augmented response of the nociceptor to a given stimulus. This process is known as peripheral sensitisation. In addition, the activation of some receptors following tissue damage results in the release of neurotransmitters substance P (SP) and calcitonin gene related peptide (CGRP) from the peripheral nerve ending, a process called neurogenic inflammation. SP and CGRP cause a variety of local effects including vasodilation, plasma extravasation and degranulation of mast cells, resulting in a further augmentation of the inflammatory response.

Post-translational changes that contribute to the generation of peripheral sensitisation involve the activation of intracellular secondary messenger mediated pathways through tyrosine kinase (e.g. TrkA) and G-protein coupled (e.g. BK_2, H1) receptor activation. These in turn lead to protein kinase A and protein kinase C mediated phosphorylation of a variety of channels – the voltage gated sodium channel $Na_V1.8$ (Fitzgerald et al., 1999), TRPV1 and TRPV2 (Cesare and McNaughton, 1996) – resulting in a lowered threshold of nociceptor activation. In addition, transcriptional changes are induced following inflammation, primarily via NGF. After binding to its high affinity tyrosine kinase receptor TrkA, NGF is retrogradely transported to the cell body where changes in the transcription of proteins are initiated; an increase in levels of the TTX-resistant voltage gated sodium channels $Na_V1.8$ and $Na_V1.9$, TRPV1, opioid receptors and BK_2 receptors is seen at the peripheral terminal and there is a increase in the synthesis and release of SP and

CGRP both peripherally and centrally. These changes contribute to the generation of peripheral sensitisation and the clinical experience of inflammatory pain, classically including hyperalgesia and spontaneous pain (Costigan and Woolf, 2000; Julius and Basbaum, 2001; Kidd and Urban, 2001).

Following nerve injury, the main pathological process that occurs in afferent sensory neurons is the development of spontaneous and abnormal activity in injured and uninjured afferent neurons (Chul Han et al., 2000). Nerve injury interferes with the supply of the trophic factors NGF and GDNF on which neurons depend for their differentiation and survival. This initiates a series of phenotypic changes in injured and adjacent uninjured neurons that contribute to the generation of spontaneous neuronal activity and the clinical syndrome of neuropathic pain. Some of these changes, for example the expression of $Na_V1.3$ and galanin, are indicative of a reversion to an immature neuronal phenotype. Several studies have shown that there is a significant redistribution of voltage-gated sodium channels (VGSCs) in injured and uninjured sensory nerves following injury. In injured neurons, protein (Decosterd et al., 2002) and transcript (Dib-Hajj et al., 1996) levels of the TTX-resistant channels $Na_V1.8$ and $Na_V1.9$ (Decosterd et al., 2002) fall and levels of the embryonic TTX-sensitive channel $Na_V1.3$ increase (Black et al., 1999a). Gold *et al.,* (Gold et al., 2003) recently showed that in the axons of adjacent uninjured neurons there is an increase in $Na_V1.8$ protein and in the $Na_V1.8$ mediated TTX-resistant current. In injured animals these changes and the behavioural manifestations of neuropathic pain are reversed by the intrathecal administration of the growth factors GDNF and NGF (Boucher et al., 2000; Cummins et al., 2000; Leffler et al., 2002).

Other changes in afferent sensory nerves that have been reported following nerve damage, that may contribute to neuropathic pain, include a down regulation of voltage gated potassium channels in injured DRG neurons, (Kim et al., 2002) an increase in the levels of TRPVI (Hudson et al., 2001), an increase in pacemaker currents in myelinated neurons (Chaplan et al., 2003), and an increase in the $\alpha 2\delta$-1 subunit of voltage gated calcium channels (Luo et al., 2002).

Some changes observed in afferent sensory neurons occur in both inflammatory and neuropathic pain, for example an increase in opioid receptors (Stein et al., 2003), in TRPV1, and in cyclo-oxygenase-1 and –2 and prostaglandins (Samad et al., 2002).

1.5. Central processing of nociceptive information

Information about a noxious insult is transduced into action potentials in the peripheral nociceptor ending, conducted via the nociceptor axon, and transmitted to neurons in the dorsal horn of the spinal cord, which can be subdivided into six layers, or laminae, based on their neuronal cytological features. The synaptic processing of information within the dorsal horn involves a highly complex interaction between primary sensory neurons, dorsal horn interneurons, descending neurons from the brain and spinal neurons. Nociceptive information is primarily transmitted to laminae I, II and V. Lamina I contains mostly nociceptive specific neurons that project directly to the brain, and some wide dynamic range neurons that respond to both noxious and non-noxious inputs. Lamina II contains excitatory and inhibitory interneurons that respond to noxious and non-noxious inputs and lamina V contains primarily wide dynamic range neurons. Peptidergic C and Aδ nociceptors project to lamina I and lamina II_{outer} whereas the non-peptidergic population synapse primarily in lamina II_{inner} of the dorsal horn. C and Aδ nociceptors also synapse in lamina V (Stucky et al., 2001). Aα/β sensory neurons synapse in laminae III, IV, V, and VI.

The main neurotransmitter released by sensory neurons is glutamate, although nociceptors also release the peptidergic neurotransmitters SP and CGRP. In addition, the neurotrophic factor BDNF is present in the central terminals of a subset of peptidergic nociceptors. The receptors for glutamate on dorsal horn neurons are ionotrophic α-amino-3-hydroxy-5-methyl-4-isoazolepropionic acid (AMPA), kainate and *N*-methyl-D-aspartate (NMDA) receptors, and metabotrophic glutamate (mGlu) receptors. At rest, NMDA receptors are blocked by magnesium (Mg^{2+}), so, normally glutamate released from nociceptor central terminals activates AMPA receptors, generating fast excitatory post-synaptic potentials. The dorsal horn post-

synaptic membrane is depolarised and on reaching the threshold, action potentials are generated that signal the nature, intensity and location of noxious injury. More intense nociceptor activation results in the release of SP, which activates NK1 receptors, generating slow excitatory post-synaptic potentials and sustained depolarisation of the dorsal horn neurons. BDNF is released after bursts of C-fibre activity and activates high affinity tyrosine kinase TrkB receptors.

Persistent and enhanced activity in nociceptors following both tissue and nerve damage induces plastic changes in the dorsal horn of the spinal cord. This process, central sensitisation, is characterised by increased synaptic efficacy, a lowered threshold for activation and a widening of the receptive field of dorsal horn neurons (reviewed in Sah et al., 2003; Woolf and Mannion, 1999). Several different phenomena are observed. A barrage of activity in nociceptors induces an augmented persistent response of dorsal horn neurons to the afferent input that outlasts the period of afferent activity and that also occurs at synapses with non-nociceptive afferents. These changes occur almost immediately after the onset of nociceptor activity. Persistent low frequency activity in nociceptors results in wind-up – a summating dorsal horn response in which the same afferent input induces increasing dorsal horn action potential generation. Wind-up does not persist beyond the duration of the stimulus. A third phenomenon, dorsal horn long term potentiation, in which brief high frequency activity in nociceptors results in long lasting synaptic facilitation, has also been demonstrated (Ji et al., 2003).

Post-translational and transcriptional changes contribute to the development of central sensitisation. Persistent depolarisation of the post-synaptic membrane results in removal of the Mg^{2+} ion from the pore of NMDA receptors, permitting the influx of cations, predominantly calcium, resulting in a progressive increase in the action potential response to each stimulus, seen in wind-up (Thompson et al., 1990). In addition, persistent and augmented nociceptor activity results in the activation of metabotrophic glutamate receptors, NK1 receptors and TrkB receptors. These receptors activate secondary messenger mediated cascades primarily resulting in the activation of intracellular kinases. Phosphorylation of NMDA and AMPA receptors by protein kinase C, protein kinase A and extracellular-signal receptor kinase

induces conformational changes that augment channel opening time, further augmenting the post-synaptic depolarisation (Chen and Huang, 1992; Lu et al., 1999). The influx of calcium through NMDA receptors also leads to the activation of intracellular signal transduction kinases. Thus the dorsal horn response is augmented and outlasts the duration of the stimulus. Intracellular kinase activation in turn leads to the phosphorylation of cAMP-response-element binding protein (CREB), inducing the transcription of *c-fos* and other immediate early genes (Hunt et al., 1987; Iadarola et al., 1988).

Following inflammation there is a dramatic, NGF dependent, increase in the level of BDNF in nociceptors (Pezet et al., 2002). In addition, Fukuoka *et al.,* demonstrated that following spinal nerve ligation, there is an increase in BDNF in small diameter uninjured neurons (Fukuoka et al., 2001). BDNF is released after bursts of high frequency C-fibre nociceptor activity. Binding to its high affinity tyrosine kinase TrkB receptors that are localised on the presynaptic terminals of medium and large diameter sensory neurons and on dorsal horn neurons, results in the activation of different intracellular transduction pathways including MAP kinase pathways and protein kinase C (Pezet et al., 2002).

It has also been shown that after inflammation and nerve injury, myelinated Aβ sensory neurons begin to express SP on their central terminals, thereby enhancing synaptic transmission in the spinal cord and exaggerating the response to innocuous stimuli (Neumann et al., 1996).

There are a host of other factors that contribute to the spinal cord processing in the dorsal horn. Descending facilitatory and excitatory pathways synapse in the dorsal horn and release the neurotransmitters noradrenaline, dopamine, 5-HT and acetylcholine. Local inhibitory interneurons also modulate the signal, releasing γ-amino butyric acid (GABA) and glycine. μ–, δ– and κ opioid receptors are present in this region, as well as in the periphery and brain, and have a predominantly inhibitory effect on neurotransmitter release and dorsal horn excitability. Ligand-gated purinergic P2X ion channels are localised on the presynaptic terminals of nociceptors and on dorsal horn neurons and have a facilitatiory effect - activation augments the presynaptic release of neurotransmitters and augments postsynaptic

dorsal horn excitation (Dunn et al., 2001). The α2δ-1 subunit of voltage gated calcium channels, that modulates the function of the pore forming α1 subunit, is upregulated in the spinal cord and or in DRGs in animal models of neuropathic pain (Luo et al., 2002) and inhibition by the anticonvulsant gabapentin has an analgesic effect. It is now known that spinal glial cells are activated in inflammatory and neuropathic pain models and that they release many neurotransmitters and neuromodulators that augment the nociceptive process (Watkins et al., 2001). Increased production of prostaglandins and synthesis of cyclo-oxygenase 1 and 2 in the spinal cord after inflammation and nerve injury also augment the nociceptive process (Samad et al., 2002).

Information is conveyed to the brain primarily via two pathways. The spinothalamic tract originates in the deeper layers of the dorsal horn, synapses within the ventroposterior and ventrobasal thalamus and projects to the cortex. A second pathway, the spinobrachial pathway originates in the most superficial layer of the spinal cord, synapses in the parabrachial area and the periaqueductal grey and projects to the hypothalamus and amygdala. The spinothalamic tract is thought to convey discriminatory information about the nature of the stimulus, whereas the spinobrachial tract is thought to convey information about the intensity of the stimulus and the emotional/affective aspects of pain (reviewed in Hunt and Mantyh, 2001). In addition, there is now growing evidence that the primary and secondary somatosensory cortices, the anterior cingulate cortex and the insular cortex are the areas of the brain primarily involved in pain perception. Descending pathways, both excitatory and inhibitory, arise mainly from periaqueductal grey and rostroventral medulla.

1.6. Project outline

Although much is now known about the neurobiological processes involved in the generation of pathophysiological pain, the urgent need for better and more specific analgesics remains. Nociception is a complex, plastic process and there are many

potential targets for analgesic development, but before new drugs are developed, the precise role of a given target must be defined. In the last 10 years one of the major advances has been an improved understanding of the changes that occur in nociceptors following tissue or nerve damage, and several gene products in these cells are very attractive drug targets. However, many of these proteins have an expression pattern that is not restricted to nociceptors, precluding the use of conventional methods, such as pharmacological manipulation or the generation of null mutant mice, from defining their role in pathophysiological pain.

The goal of this thesis is the development of a murine model system that allows specific gene deletion exclusively in the nociceptor cell population. This model system will be suitable to determine the role of individual molecules in nociceptors, increasing our understanding of the molecular pathways of pain perception and providing a rational basis for the development of targeted analgesic agents.

Chapter 2

Generation of a nociceptor specific Cre expressing mouse

2.1. Introduction

This chapter describes the generation of a mouse line in which the bacteriophage Cre recombinase gene is knocked-in to the translational start site of the voltage gated sodium channel (VGSC) $Na_V1.8$. In the introduction I will describe the principles of gene targeting, site-specific recombinases and the Cre-*loxP* system. I will then examine the expression pattern of potential target genes found in nociceptors.

2.1.1. Gene Targeting

Gene targeting refers to the alteration of a chosen (target) gene in a predetermined way using homologous recombination (reviewed in (Bronson and Smithies, 1994; Capecchi, 1989; Muller, 1999). Homologous recombination refers to the intrinsic ability of mammalian cells to mediate recombination between homologous DNA sequences. Thus, when exogenous DNA is introduced into a cell, it can locate and recombine with the endogenous homologous sequences (Lin et al., 1985). The use of gene targeting in embryonic stem (ES) cells has facilitated the generation of a vast array of genetic alterations in the mouse that have contributed significantly to our understanding of health and disease. ES cells, first isolated over 20 years ago (Evans and Kaufman, 1981; Martin, 1981) are pluripotent cells derived from the inner cell mass of mouse blastocysts that have two characteristics that make them ideal candidates for gene targeting. They can contribute to all embryonic tissues in chimeric mice, including the gametes, and they can be maintained in an undifferentiated state *in vitro* in certain culture conditions.

Gene targeting involves the generation of a targeting vector in which the desired alteration of the target locus is introduced using recombinant DNA technology. The targeting vector is then linearised, and introduced into ES cells where homologous recombination incorporates the modification into the ES cell genome. Screening is used to select those ES cell clones in which homologous recombination has occurred. The ES cells are microinjected into the blastocyst of a mouse embryo and the blastocyst transferred into the uterus of a pseudopregnant mouse. Generally, 129

ES cell lines and C57Bl/6 blastocysts are used. Chimeric offspring are selected by coat colour and are then crossed to suitable mice to check that the ES cells have contributed to the formation of the germ line.

Targeting vectors have three specific features - the desired genetic modification, selection markers, and two stretches of mouse genomic DNA that are homologous to the desired integration site, known as the arms of homology– see Figure 2.1.

Homologous recombination is a relatively rare event (~$1/10^4$ cells electroporated); non- homologous integration of the targeting vector into random sites within the genome, often in tandem repeats, occurs much more frequently. The frequency of homologous recombination is related to the extent of the homology between exogenous and host DNA and occurs in almost every introduced molecule when the arms of homology are over 5kb in length (Thomas and Capecchi, 1987). It is also more likely to occur if the targeting vector is constructed from DNA that is isogenic with the ES cell line used in the targeting experiment (te Riele et al., 1992). When the arms of homology are non-isogenic, DNA mismatch repair machinery interferes with homologous recombination.

The inclusion of positive and negative selection markers in the targeting vector allows detection of the rare correct targeting events. Mansour *et al.,* first described their combined use in the selection of cells that contained targeted disruptions of the *hprt* and *int-2* genes (Mansour et al., 1988). A positive selection marker is positioned within the arms of homology and selects for those ES cells in which the targeting vector is present. In addition, a negative selection marker is positioned outside the arms of homology; it is therefore lost when there is correct targeting, but is present when random integration occurs. Selection for ES cells that contain the positive selection marker and against cells that contain the negative selection marker will isolate those in which homologous recombination has occurred. The most commonly used positive selection marker is the neomycin phosphotransferase gene that encodes resistance to geneticin (G418). The Herpes Simplex Virus thymidine kinase gene, that encodes sensitivity to the antiviral agent gancyclovir, is widely used for negative selection.

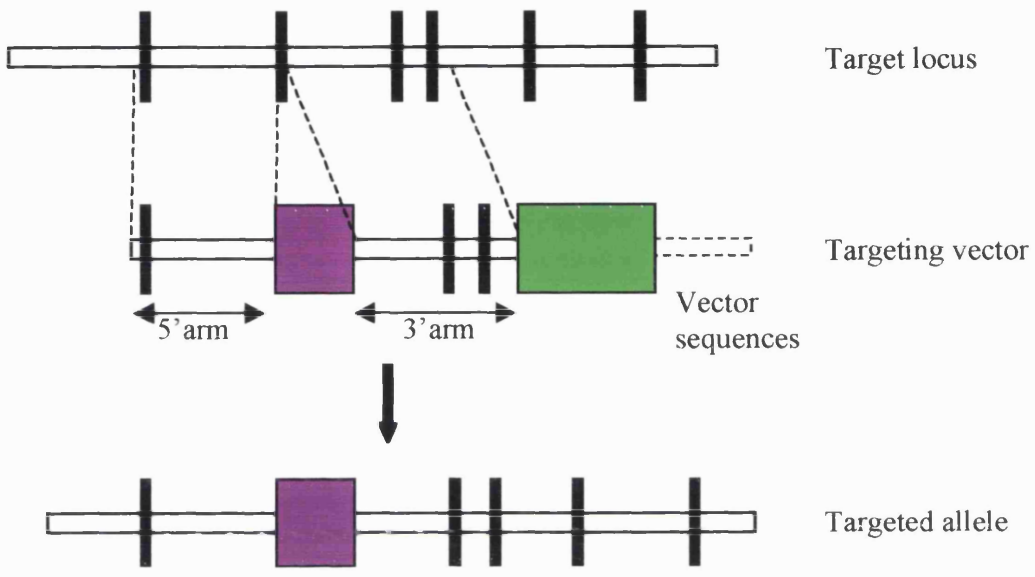

Figure 2.1: Gene targeting with a replacement vector.
White boxes indicate introns and black boxes exons. Purple and green boxes indicate positive and negative selection markers respectively. Homologous recombination between the target locus and the arms of homology (5' arm and 3' arm) of the targeting vector results in a targeted allele in which an exon is replaced by the positive selection cassette.

The most widely used application of the gene targeting approach is the generation of null mutant animals in which a specific gene is disrupted throughout ontogeny. Study of the phenotype of null mutant animals has provided much useful insight into the role of the gene of interest. However this approach has several limitations (Joyner and Guillemot, 1994). For some gene inactivations, the resulting phenotype is lethal to the embryo or soon after birth, precluding investigation of the genes' role later in life. In addition, gene inactivation during foetal development may trigger alteration in the expression and function of other genes resulting in masking of the phenotype attributable to the deleted gene. Finally, inactivation of genes expressed in several tissues and/or in several cell types will result in global loss of function making it difficult to study the function in specific tissues and cell types.

2.1.2. Site-specific recombinases

Because of the potential problems with global gene deletion, strategies in which the location and timing of genetic mutation can be controlled have been developed. Two such systems are available for use in the mouse, the Cre-*loxP* and Flp-*FRT* site-specific recombinases (reviewed in Lewandoski, 2001; Nagy, 2000; Sauer, 1998).
I will give a brief summary of the Flp-*FRT* system before describing the Cre-*loxP* system in more detail

2.1.2.1. Flp-*FRT* system

Flp recombinase, encoded by the yeast *Saccharomyces cerevisiae,* mediates recombination between two *FRT* (Flp recognition target) sites (Dymecki, 1996). *FRT* consists of a unique 8-base pair (bp) spacer region surrounded by two 13-bp inverted repeats which serve as the binding sites for Flp. Utilisation of Flp has been limited by its low level of activity at 37°C. More recently, a more thermostable Flp (Jung et al., 1993) has been developed, termed FLPe, and has been shown to be 3-5 times more efficient at recombination in mammalian cells (Buchholz et al., 1998). Rodriguez *et al,* have shown that FLPe is effective in germ cell lines (Rodriguez et al., 2000). In this project I have used the Flp-FRT system to remove the positive selection marker present in the targeting vector.

2.1.2.2.Cre-*loxP* system

Site-specific recombinases comprise two elements: the recombinase enzyme and a small stretch of DNA that it specifically recognises – see Figure 2.2. Two recognition sequences are required for recombinase activity. The recombinase cleaves DNA at one recognition sequence and ligates it to the second cleaved recognition sequence. The orientation of the recognition sequences determines the nature of the modification catalysed by the recombinase. When they are in the same orientation, the intervening DNA region is excised and forms a circular segment, whereas when they are in the opposite orientation, the intervening DNA segment is inverted. Alternatively, the sites can be located on separate DNA molecules resulting in translocation of the DNA distal to the sites. Recombination is carried out with absolute fidelity and does not require any accessory host factors. These features make these systems extremely attractive for conditional gene targeting.

In vivo, two mouse strains are frequently used – one in which the site and/or timing of recombinase expression is controlled, and the other in which the recognition sequences flank functionally important exons of the target gene. In the F1 progeny, the pattern of the recombinase activity will determine the pattern of target gene modification.

Cre, the 38-kDa product of the *cre* (*c*yclization *re*combination) gene, is a site-specific DNA recombinase of the P1 bacteriophage that catalyses the recombination between two *loxP* sites. The *loxP* sites are 34bp in size and consist of two 13-bp inverted repeats that flank an 8-bp nonpalindromic core region that gives the *loxP* site directionality. The *loxP* sequence is large enough so that it is unlikely to occur by chance in the mammalian genome, but small enough so that its presence does not usually interfere with gene expression. A Cre molecule binds to each of the inverted repeats, and the core region is the site of cleavage, exchange and ligation.

It was thought that the mouse genome contains no endogenous *loxP* or *FRT* sites, but Thyagarajan *et al.,* (Thyagarajan et al., 2000) have shown that both Cre and FLP can mediate recombination between degenerate *loxP* or *FRT* sites and that there are pseudo-*loxP* sites within the mouse genome. Indeed there have been *in vitro* and *in*

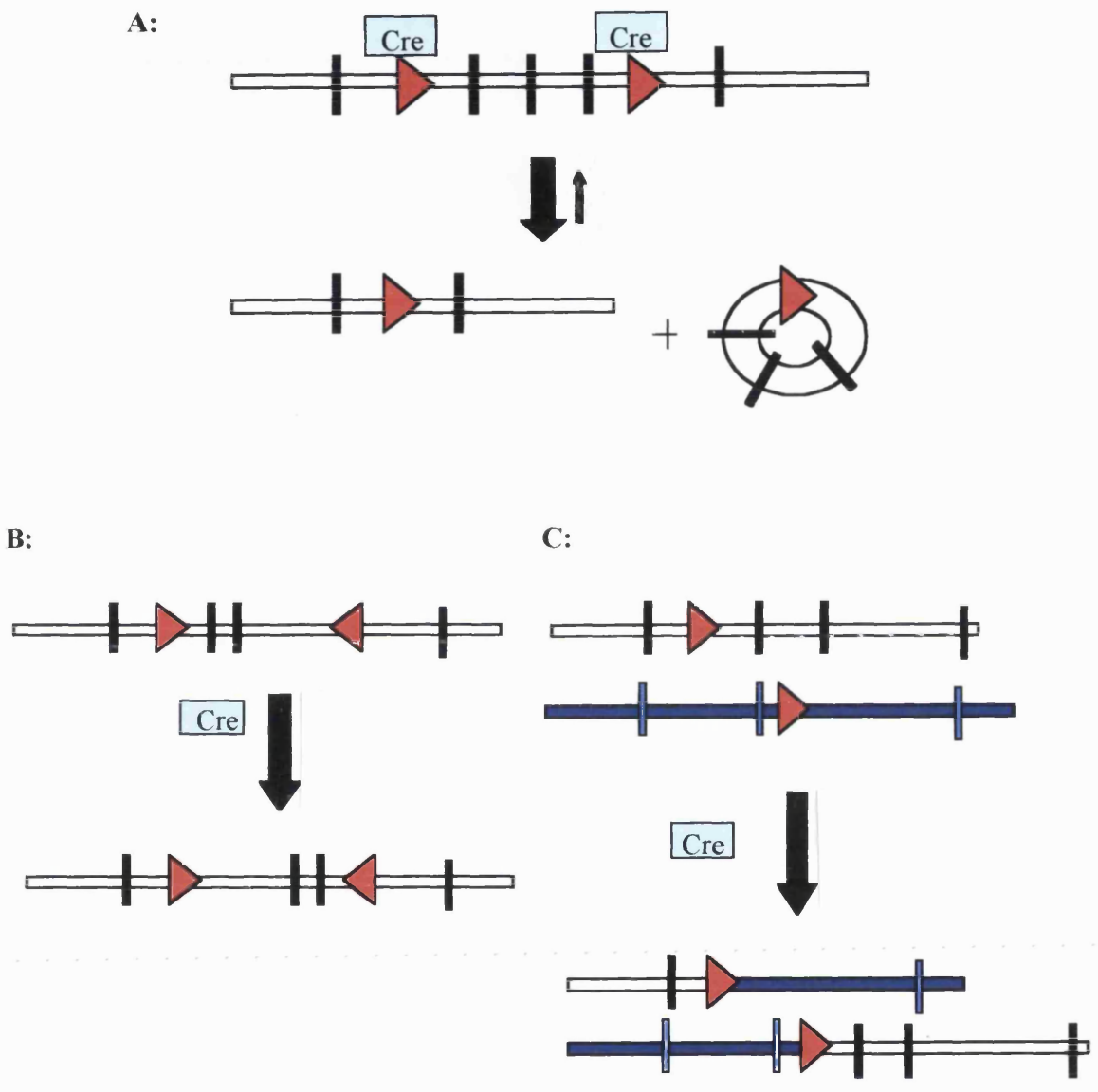

Figure 2.2: The Cre-*loxP* system.
A: Cre mediated gene deletion. The *loxP* sites (shown in red) are in the same orientation, resulting in loss of the intervening DNA sequence. **B:** Cre mediated gene inversion. When the *loxP* sites are head-to-head, inversion of the intervening sequence results. **C:** Cre mediated gene translocation. Positioning of the *loxP* sites on different chromosomes results in translocation of the DNA distal to the sites.

vivo studies that indicate that Cre can mediate recombination between these sites (Loonstra et al., 2001; Schmidt et al., 2000). However the widespread effective use of Cre indicates that these events are likely to be very rare.

Sauer and Henderson first used Cre *in vitro* (Sauer and Henderson, 1988) to excise a *loxP* flanked kanamycin resistance gene in a mouse cell line. Gu *et al.,* (Gu et al., 1993) then showed that transient expression of Cre in ES cells results in recombination between *loxP* sites and successful germ line transmission of the deleted gene.

The most common use of the Cre-*loxP* system is to generate tissue specific knock-out mice (Gu et al., 1994). *LoxP* sites are targeted to the gene of interest and positioned around functionally essential exons. An animal in which Cre expression is driven by a promoter with the desired tissue specificity is then used to delete the floxed gene segment. The pattern of Cre mediated target gene deletion in the F1 progeny of these animals will follow that of the promoter.

Three methods have been used to generate tissue specific Cre expressing animals. In the transgenic approach, a promoter with the desired tissue specificity is selected and cloned. Recombinant DNA technology used to insert the Cre gene immediately downstream of the promoter. The resulting transgene is then injected into fertilised eggs where it is randomly integrated into the genome, and Southern blotting or PCR used to detect those offspring carrying the transgene. Founder lines with the desired Cre expression are then used. Alternatively the knock-in approach can be utilised, in which gene targeting is used to insert Cre into a gene with the desired tissue specificity, so that the endogenous regulators of gene expression are utilised to control the pattern of Cre expression.

Another method that has been developed in the last ten years and can be used to introduce Cre into the mouse genome is the use of bacterial artificial chromosome (BAC), P1 artificial chromosome (PAC) or yeast artificial chromosome (YAC) transgenic mice. BACs, PACs and YACs are large fragments of genomic DNA cloned into vectors derived from bacteria, phage P1 or yeast respectively, that allow the propagation of large lengths of DNA. BACs and PACs can carry ~200kb of genomic DNA and are propagated in bacteria whereas YACs carry much larger

fragments and are propagated in yeast. A BAC or PAC that contains the gene of interest, flanked on both sides by ~50kb of DNA is chosen. The desired modification or exogenous gene (e.g. *Cre*, *lacZ*), flanked by very small (~50-500bp) arms of homology, is then electroporated into the BAC directly or within a shuttle vector and is integrated via homologous recombination. The modified BAC is then introduced using pronuclear injection and suitable founder lines selected (Heintz, 2001).

In addition to site-specific gene deletion, there are several other ways in which the Cre-*loxP* system can be used:

1. The Cre-*loxP* system has been used to mediate large gene deletions or translocations. However the frequency of recombination across such large distances is very low. To aid selection of clones in which it has occurred, the Hypoxanthine phosphoribosyl transferase (Hprt) mini-gene has been utilised (Ramirez-Solis et al., 1995). One half of this bi-partite gene is placed on one side of each *loxP* sites. Hprt negative ES cell lines are used to select for Cre mediated recombination. When it occurs, the two halves of the Hprt gene are brought together restoring the gene function.

2. A further use of the Cre-*loxP* system is Cre mediated gene repair. Lakso *et al.*, (Lakso et al., 1992) demonstrated that Cre can be used to activate gene expression; they inserted a floxed 1.3kb Stop signal between a promoter and coding sequence of the desired transgene preventing gene expression. Cre mediated excision of the Stop signal switched on gene expression. A floxed neomycin cassette can also be targeted so that it interferes with or prevents endogenous gene function. The phenotype of the resulting mouse is examined and then a lineage specific Cre expressing mouse used to restore gene function (Arin et al., 2001).

3. It is now known that the strong promoters that drive expression of the neomycin cassette used in gene targeting experiments can interfere with the expression of surrounding genes. Reduction in the level of expression of the target gene can occur (Fiering et al., 1995), and also of genes surrounding (Olson et al., 1996) and distant from the target site (Pham et al., 1996). It is therefore important to consider removing it before analysing the phenotype due to the targeted disruption.

Removal of a positive selection marker that is flanked by *loxP* or *FRT* sites can be achieved using the Cre-*loxP* or Flp-*FRT* system respectively either at the ES cell stage or using ubiquitous Cre/Flp expressing mice. Using the Cre-*loxP* system, three *loxP* sites are inserted, two flanking the target gene and a third flanking the selection marker. Cre is transiently transfected in ES cells to excise the selection cassette, a mouse in which the target gene is floxed is generated, and crossed to the Cre expressing mouse. An alternative strategy is to combine the Cre-*loxP* system with the Flp-*FRT* system; the selection cassette is FLRTed (flanked by *FRT* sites) and the target gene floxed. Transient expression of Flp in targeted ES cells, or crossing targeted animals to Flp expressing animals is used to remove the selection cassette before crossing to a Cre expressing mouse line.

2.1.3. Nociceptor specific proteins

In order to generate a nociceptor specific Cre expressing mouse a gene that is expressed exclusively in this cell population must be identified. Here, several potential candidate genes will be discussed.

2.1.3.1. Transient Receptor Potential channels

In 1997, Caterina *et al.*, (Caterina et al., 1997) cloned the vallinoid receptor VR1, now known as TRPV1, that is activated by moderate noxious heat (threshold of activation ~43°C), protons, capsaicin and other vallinoid compounds. TRPV1 is a transient receptor potential (TRP) non-selective cation channel that comprises six transmembrane domains with a 'P loop' between the fifth and sixth domains. It is expressed in 30-40% DRG neurons, primarily in both the peptidergic and non-peptidergic population of nociceptors (Amaya et al., 2003). However, recent studies have revealed that it is also present at much lower levels in several areas of the brain and in the liver and kidney (Mezey et al., 2000; Sanchez et al., 2001).

Another TRP channel, TRPV2, that shares ~50% homology with TRPV1, and is activated by noxious thermal stimuli with a higher threshold, ~52°C, but is not activated by vallinoid compounds, is also predominantly expressed in DRG neurons (Caterina et al., 1999). This channel is found in ~20% of DRG neurons, most of

which are myelinated. It is also present in the spleen, lung, brain and gastrointestinal tract.

Two TRP channels that are activated at low temperatures are expressed exclusively in a subset of nociceptors. TRPM8, a channel whose threshold for activation is ~23°C, and that is also activated by menthol, is found in only 5-10% of adult DRG neurons. The distribution pattern does not co-localise with IB_4, CGRP or TRPV1, but appears to belong to a subset that expresses TrkA, the receptor for NGF during development (Peier et al., 2002). ANKTM1 is a TRP-like channel that has a threshold of ~17°C. It is found in ~3.6% DRG neurons, all of which also express CGRP and TRPV1 (Story et al., 2003).

2.1.3.2. $P2X_3$ receptors

P2X receptors comprise ionotrophic ligand-gated ion channels, of which seven subtypes have been cloned (reviewed in Burnstock, 2002).The receptors form two transmembrane domains joined by a large extracellular loop, with intracellular N- and C- termini. Functional channels are formed by homo- and hetero-multimers of the various subtypes. The channels are activated by ATP and adenosine diphosphate (ADP). A nociceptor specific P2X channel, $P2X_3$, was cloned in 1995 (Chen et al., 1995), that is expressed on non-peptidergic IB_4 positive C-fibre neurons, a subset of nociceptors. It is now known that the channel is also present at low levels in sympathetic and parasympathetic ganglia (Xiang et al., 1998).

2.1.3.3. Acid sensing ion channels

Acid sensing ion channels (ASICs) are voltage insensitive cation channels that are activated by protons. There is also evidence to suggest that they play a role in the transduction of mechanical stimuli (reviewed in Waldmann and Lazdunski, 1998; Welsh et al., 2002). The channels are formed as heteromultimers, each subunit comprising two transmembrane domains, with intracellular N- and C- termini and a large extracellular loop. Six ASIC subunits have been cloned, of which two, ASIC1b and ASIC3, are found exclusively in mouse sensory neurons. ASIC1b (Chen et al., 1998) is found in 20-25% of DRG neurons, 70% of which are myelinated. ASIC3 is

expressed on most large and small diameter neurons and is not specific to nociceptors (Price et al., 2001).

2.1.3.4. Tetrodotoxin-resistant voltage gated sodium channels

Voltage-gated sodium channels (VGSCs) are large channels, comprising an α (260kD), a β1 (36kD) and a β2 (33kD) subunit (Catterall, 2000). The α subunit forms the ion-conducting pore and the β subunits are responsible for the localisation of the channel, its inactivation kinetics and the level of channel expression (Malhotra et al., 2000; Smith et al., 1998). The α subunit has four domains, each with six transmembrane segments linked intracellularly. The positively charged fourth transmembrane segment (S4) serves as the voltage sensor, the 'P loop' between the fifth and sixth segments forms the narrow outer lining of the pore and the sixth segment forms the wide inner lining of the pore. The intracellular loop connecting domains III and IV has a hydrophobic motif (isoleucine, phenylanaline, methionine, threonine) that inactivates the channel by folding into and blocking the inner mouth of the pore.

Ten voltage-gated sodium channel α subunits ($Na_V1.1$-1.9, Na_x) (Goldin et al., 2000) have been cloned - see Table 2.1 (Baker and Wood, 2001). One of the characteristics that differentiate between them is their sensitivity to the puffer fish poison tetrodotoxin (TTX). TTX resistance is mediated by amino acid residues within the P-loop of the first domain (Noda et al., 1989), the site of TTX binding. TTX sensitive channels have a hydrophobic residue in this region whereas TTX resistant channels have a hydrophilic serine residue.

The TTX-sensitive channels $Na_V1.1$, 1.2, 1.6, 1.7 and the TTX-resistant channels $Na_V1.8$ and 1.9 have all been shown to be present in sensory neurons. However, only $Na_V1.9$ and $Na_V1.8$ are exclusively in this location. $Na_V1.9$, previously known as NaN (Dib-Hajj et al., 1998), has been shown to be localised to unmyelinated DRG neurons (Amaya et al., 2000; Tate et al., 1998). More recently, Fang *et al.,* showed that it is also present in some myelinated nociceptive neurons (Fang et al., 2002).

Channel	Previous name	Gene symbol	Chromosome (human)	Pharmacology	Abundance in adult DRG
$Na_v1.1$	Type I	SCN1A	2q24	TTX-s	Present
$Na_v1.2$	Type II	*SCN2A*	2q23-24	TTX-s	Present
$Na_v1.3$	Type III	*SCN3A*	2q24	TTX-s	Upregulated in axotomy
$Na_v1.4$	SkM	*SCN4A*	17q23-25	TTX-s	Absent
$Na_v1.5$	Cardiac	*SCN5A*	3p21	TTX-r	Absent
$Na_v1.6$	NaCh6	*SCN8A*	12q13	TTX-s	Abundant
$Na_v1.7$	PN1	*SCN9A*	2q24	TTX-s	Abundant
$Na_v1.8$	SNS/PN3	*SCN10A*	3p21-24	TTX-r	Abundant
$Na_v1.9$	NaN	*SCN11A*	3p21-24	TTX-r	Abundant
Na_x	NaG	*SCN6A/7A*	2q21-23	?	Present

Table 2.1: Voltage-gated sodium channel α subunits in sensory neurons. Abbreviations: DRG, dorsal root ganglion; TTX-s, tetrodotoxin-sensitive; TTX-r, tetrodotoxin resistant (Baker and Wood, 2001).

Others have detected both the transcript and protein in myenteric neurons (Rugiero et al., 2003).

Several groups have examined the pattern of expression of $Na_V1.8$ (Akopian et al., 1996; Amaya et al., 2000; Novakovic et al., 1998; Sangameswaran et al., 1996) and shown that it is present in the majority of unmyelinated DRG neurons, but also in some myelinated Aδ and Aα/β neurons. It is also present in the trigeminal and nodose ganglia. Djouhri *et al.,* (Djouhri et al., 2003a) recently examined the $Na_V1.8$ expression pattern in lumbar DRGs and correlated it with neuronal function in 104 neurons. They found a significant negative correlation between the intensity of immunoreactivity for $Na_V1.8$ and cell size both within the whole DRG and in the neurons examined in detail. 83% of C, 93% of Aδ, and 25% of Aα/β neurons showed positive staining. Over 80% of nociceptive neurons and less that 20% of non-nociceptive neurons contained $Na_V1.8$, and all nociceptive neurons showed intense immunoreactivity whereas all non-nociceptive neurons showed weak immunoreactivity.

The $Na_V1.8$ gene was cloned in 1996 (Akopian et al., 1996; Sangameswaran et al., 1996) and was the first channel to be shown to mediate the TTX resistant current that was originally recorded in 1978 (Matsuda et al., 1978). The detailed structure of the murine $Na_V1.8$ gene was described in 1997 (Souslova et al., 1997) and shows a 95.3% overall amino acid homology with rat $Na_V1.8$. The gene consists of 27 exons spanning approximately 90kb and is located on chromosome 9.

2.2. Materials and Methods

2.2.1. Chemicals and enzymes

Chemical reagents and bacterial media were purchased from BDH, Invitrogen, Pharmacia and Sigma. Restriction endonucleases, modifying enzymes and DNA polymerases were purchased from New England Biolabs and Promega.

2.2.2. Plasmids and DNA fragments

The plasmid pBluescript® II SK- phagemid was purchased from Stratagene (Figure 2.3). The pBS500 vector, encoding Cre, was a gift from Professor Brian Sauer (Gagneten et al., 1997).

The plasmid encoding the neomycin cassette, pYR6.1, was obtained from Y. Rudhard & R. Schoepfer.

The plasmids encoding the polyadenylation signals were pUHD15-1, from R. Schoepfer, obtained from Bujard, ZMBH, Heidelberg (Gossen and Bujard, 1992), and TNR1/CII/S5c-Stop, originally from pGL3Basic (Promega), obtained from M. Nassar.

The vector containing a HSV-TK cassette (1.85kb) (Mansour et al., 1988) was obtained from R. Schoepfer, originally from K. Thomas and M. Capecchi.

2.2.3. DNA Digestion with Restriction Enzymes

Plasmid digestions were typically carried out in a volume of 10µl, including 5U of each enzyme, the appropriate buffer and up to 3µl of DNA. Digestion reactions were incubated for one hour at the optimal temperature for the enzyme(s) used.

2.2.4. Analysis of DNA Digests

Analysis of the products of DNA digestions was performed using electrophoresis on agarose gels.

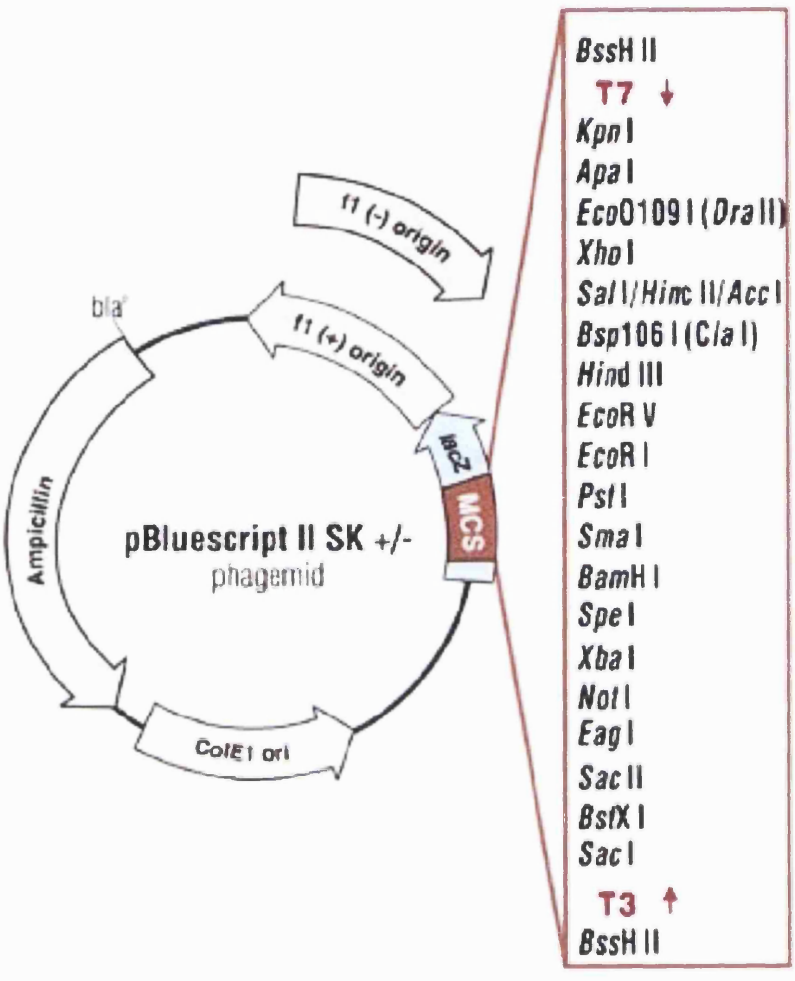

Figure 2.3: Map of pBluescript II SK+/-.
The phagemid contains a polylinker with 21 unique restriction enzyme recognition sites. T7 and T3 RNA polymerase promoters flank the polylinker. The polylinker is in the N-terminal portion of a lacZ gene fragment. Without inserts the lacZ gene is transcribed.
(Reproduced from http//www.stratagene.com/displayProduct.asp?productId=267)

Gels were prepared from electrophoresis grade agarose (Invitrogen) in Tris-acetate EDTA (TAE) buffer (40mM tris-acetate and 1mM EDTA, pH 8.0) and contained 0.1μg/ml ethidium bromide (BDH). 0.8% agarose was used to resolve fragments more than 1.5kb in size and 1.2% for fragments less than 1.5kb in size. Prior to loading, the DNA digests were mixed in a ration of 10:1 with DNA loading buffer (0.25% Bromophenol blue, 0.25% xylene cyanol FF and 15% Ficoll). The Hyperladder I (Bioline) and 100 base pair DNA ladder (Invitrogen) were used as molecular weight markers. Electrophoresis of gels was performed in TAE buffer at 2.0 – 5.0 V/cm. Electrophoresis was carried out until the bromophenol blue dye migrated 3/4 of the gel length. DNA was visualised and results were documented using a 3UV™ Transilluminator and Mitsubishi video copy processor.

2.2.5. Purification of DNA fragments

DNA fragments were purified from DNA restriction digests or PCR after they were resolved using low melting point agarose (Gibco BRL). The band containing the desired fragment was identified by size. The band was then excised and the gel slice stored in a 1.5ml microfuge tube at –20°C. DNA was then purified using the JETsorb® gel extraction kit (Genomed). 3μl/mg of high salt buffer and 0.1μl/mg JETSORB beads were added to the gel slice, vortexed and incubated at 50°C for 15mins to adsorb the DNA onto the beads. The tube was then centrifuged at maximum speed for 30secs and the supernatant discarded. The pellet was washed in 300μl high salt buffer, centrifuged again and the supernatant discarded. The pellet was then washed twice with 300μl low salt buffer, and air-dried for 10mins at 50°C. The DNA was resuspended in 20μl TE, incubated at 50°C, the tube centrifuged again, and the supernatant recovered.

2.2.6. Purification of Plasmid DNA

2.2.6.1 Mini-preps

Small-scale plasmid purifications were performed using alkaline lysis. Up to 25-30μg of high copy number DNA was obtained from a 2ml overnight bacterial culture in T-Broth (Gibco-BRL) containing 150μg/ml ampicillin. Each culture was inoculated from an individual bacterial colony. Cultures were grown overnight shaking at 37°C. Approximately 1.5mls of each culture was transferred to a 1.5ml microfuge tube. Cells were harvested by centrifugation at 8000g for 30secs. The supernatant was aspirated and the cells were resuspended in 150μl mini-prep solution I (50mM glucose, 25mM TrisCl, pH 8.0 and 10mM EDTA, pH 8.0). Cells were then lysed with the addition of 300μl of mini-prep solution II (0.2M NaOH and 1% SDS). Tubes were mixed by inverting and incubated on ice for 5mins. Cell debris and bacterial genomic DNA were pelleted by centrifugation at 12000g for 5mins. The supernatant was transferred to a new tube, 1μl RNAse A (NewEngland Biolabs) was added, and incubated at 37°C for 15mins. Plasmid DNA was precipitated by adding 800μl ethanol (BDH) and pelleted by centrifugation at 12000g for 5mins. DNA pellets were washed with 500μl of 70% ethanol, air-dried and resuspended in 50μl TE (10mM Tris-Cl, 1mM EDTA). DNA purified by this procedure was used in restriction enzyme analysis, DNA sequencing and PCR.

2.2.6.2. Midi-prep

High purity DNA suitable for transfection of cell lines was obtained using a plasmid DNA purification kit (Qiagen) according to the manufacturers protocol. Approximately 50μg of purified DNA was usually obtained from a 50ml overnight culture grown in T-broth and containing 150μg/ml ampicillin at 37°C with shaking.

2.2.7. DNA Ligations

DNA ligations were typically performed in a 10.0μl reaction containing 0.5U of T4 DNA ligase (New England Biolabs) and 50-100ng of each DNA fragment. Dephosphorylation of the plasmid backbone was performed in all cases. 0.5μl shrimp alkaline phosphatase (SAP) (Roche) and 1x buffer (50mM Tris-HCl pH7.5, 10mM $MgCl_2$, 10mM dithiothreitol, 1mM ATB, 25μg/ml bovine serum albumin) (New England Biolabs) was added to the prepared backbone and left at 37°C for

30mins and then at 70°C for 10mins. Ligation reactions were incubated at 14°C overnight.

2.2.8. Preparation of competent E. coli

Competent *E. coli* (DH5α) were prepared using a modified protocol of Dower et al (Dower et al., 1988). A 6ml overnight culture was diluted in 1litre of LB-broth (Gibco BRL) and grown at 37°C with vigorous shaking to a density of 0.5-0.7OD at 600nm. Cultures were then chilled on ice for 30-45 minutes and cell harvested by centrifugation at 4000g for 5mins. The pellet was resuspended in 1litre of ice-cold sterile water and spun at 4000g for 5mins. The pellet was the resuspended in 20mls ice cold sterile 10% glycerol and spun at 4000g for 5mins. The pellet was finally resuspended in 2mls of sterile ice cold 10% glycerol. 40µl aliquots were dispensed into chilled 0.5ml microfuge tubes. Aliquots of competent *E. coli* were stored at –70°C.

2.2.9. Bacterial Transformations

DNA plasmids were introduced into competent *E. coli* (DH5α) by electroporation. Typically, 20µl of competent *E. coli* were thawed on ice and mixed with 10-25% of the ligation reactions. Electroporation was carried out using a Biorad Gene Pulser® II. Resistance was set to 600 Ohms and voltage set to 1.8kV for 1mm cuvettes.
500µl SOC medium (2.0% w/v bacto-tryptone, 0.5%w/v bacto-yeast extract, 8.5mM NaCl, 0.24mM KCl, 10mM $MgCl_2$ and 20mM Glucose) (Sigma) at 37°C was added to the cuvette immediately after the electroporation pulse was delivered. The fluid was then transferred into 15ml tubes and shaken at 37°C for 30-45mins. The electroporated bacteria were then plated out onto 90mm Luria Broth (LB) agar plates (Gibco-BRL) containing 150µg/ml ampicillin (Sigma). Colonies of transformed bacteria were visible after 12-14 hours of incubation at 37°C.

2.2.10. Polymerase chain reaction

Polymerase chain reactions (PCR) were prepared in sterile 0.5ml eppendorf tubes using sterile pipette tips. 1.0ng of template DNA, 0.2μM of each primer, 0.2mM dNTP (Sigma), 2.5mM $MgCl_2$ (Promega), 1x Mg^{2+} free Taq buffer (Promega) and 1u Taq DNA polymerase were used in a 50μl reaction volume. PCR conditions used were: initial denaturing - 94°C x 2mins, cycling denaturing - 94°C x 30secs, cycling annealing - 55-65°C, cycling extension - 72°C 20secs. The cycling steps were repeated 29 times. The reactions were carried out in a PCT-220 DNA Dyad (MJ research) machine.

PCR was used to amplify several DNA fragments used in the cloning and screening process. Two components of the targeting vectors were amplified using PCR. To ensure that the translational start site of $Na_V1.8$ was replaced by the translational start site of Cre, a small fragment, the ATG-chimera, encoding the area immediately upstream of the $Na_V1.8$ translational start site and the beginning of the Cre sequence, was derived using PCR. The sense primer, mSNS seq7s, encoded bp –445 to bp –422 of $Na_v1.8$, ending 36 bps upstream of an XmaI restriction enzyme site, and the antisense primer, mSNSCre seq1a, encoded bp –20 to bp –1 of $Na_v1.8$ and bp 1-49 of the Cre sequence to just downstream of an AgeI restriction enzyme site. The $Na_v1.8$ 3'UTR was also derived by PCR; the sense primer, mSNS pcr8s, included bps 6013-6037 and the antisense primer, mSNS pcr9a, bps 6426-6448 of mouse $Na_v1.8$ cDNA. BamHI and XhoI restriction enzyme site sequences used for cloning were also included in these primer sequences. Several probes used for screening were also derived using PCR. The probe - SNS6 - used to screen the mouse BAC library for genomic DNA containing exon 1 of $Na_V1.8$, encoded bps 165 to 587 of rat $Na_v1.8$ cDNA (this includes part of the 5'UTR, exon 1 and most of exon 2) and was amplified from rat $Na_v1.8$ cDNA. Three probes used for screening of embryonic stem cell lines - Cre probe, neoR probe and HSV-TK probe, were also amplified from the final $Na_V1.8$Cre2 targeting vector. The sense primer for the Cre probe encoded Cre bps35-58 and the antisense primer encoded Cre bps 985-1008 of the Cre coding sequence. The sense primer for the neoR probe encoded bps 13-36 and antisense primer encoded bps 985-1008 of the coding sequence. The sense primer

for the HSV-TK probe encoded bps 85-108 and antisense primer bps 1065-1088 of the thymidine kinase coding sequence.

Primers used for each product are shown below:

ATG chimera: mSNS seq7s: 5' - AGCAAGAGGCAAATCATAGTCAGC – 3'

mSNSCre seq1a: 5' –TCGACCGGTAATGCAGGCAAATTTTGGT GTACGGTCAGTAAATTGGA**CAT**CTTCTCATTCTTCTTGGGG AAGGATTTACA – 3'.

Letters in bold face indicate the translational start of Cre. The AgeI site is underlined.

$Na_v1.8$ 3' UTR: mSNSpcr8s: 5'– AG**GGATCC**AACTCGAGAGACACTCCAGCA TGCACGGGGCG – 3'

mSNSpcr9a: 5' – CGC**GGATCC**GGCCGACCCTCAGGTATTGT CCGG – 3'.

BamHI sites are indicated in boldface, and the XhoI site is underlined. This fragment was amplified using Vent polymerase to ensure that blunt ends were produced. 1u Vent polymerase, 1x Vent polymerase buffer and 10μM $MgSO_4$ were used in the reaction.

SNS6 probe:	rSNSseq1s: 5' – AGCAAAGAGTGTAAATTCTTCCCC – 3'
	rSNSseq3a: 5' – GGACAGACACTTTGATGGCTGTTC – 3'
Internal Cre probe:	Cre seq2s: 5' – CTGCATTACCGGTCGATGCAA CGA – 3'
	Cre seq3a: 5' – GCACCATTGCCCCTG TTTCACTAT – 3'
Internal neoR probe:	neo seq2s: 5' – ATTGAACAAGATGGATTGCA CGCA – 3'
	neo seq3a: 5'–TCAGAAGAACTCGTCAAGAAGGGCGA– 3'
HSV-TK probe:	HSV-TK seq2s: 5'–TTGCGCCCTCGCGGCAGCAAGAA– 3'
	HSV-TK seq3a: 5'–TCGCAGATCGTCGGTATGGAGCCT– 3'

2.2.11. Phenol-Chloroform extraction

50µl phenol/chloroform/isoamylalcohol (ratio=50:48:2) was added to the 50µl PCR reaction after its completion. The mixture was briefly vortexed and centrifuged at 15 000g for 2mins. The PCR reaction (aqueous phase) was removed and transferred to a new eppendorf tube. 5µl 3M sodium acetate was added and then 110µl 100% ethanol. The mixture was mixed and centrifuged at 15 000g for 5mins. The PCR product was washed with 70% ethanol, allowed to air-dry for 5-10mins and resuspended in 20µl distilled water.

2.2.12. DNA Sequencing

Sequencing reactions were prepared using the BigDye DNA Sequencing Kit (ABI Prisms) that is based on the Sanger dideoxynucleotide chain termination method. Approximately 0.5µg of plasmid DNA was used as a template, prepared by midi-prep. 1µl reaction mixture, 3µl reaction buffer and 1µl 3.2pM primer was used in a 10µl sequencing reaction. The primers used for sequencing included T3, T7 (Promega), and mSNSseq1a (5' – CTCCTGTCCATCACCCCTACTTG A – 3'). Thermal cycling was carried out in a PCT-220 DNA Dyad machine (MJ Research). PCR conditions were 25x denaturation - 20secs at 96°C, primer annealing - 15secs at 49°C, primer extension - 4mins at 60°C. The PCR product was then precipitated; 50µl chloroform added and the tubes vortexed and spun briefly. The supernatant was then transferred to a 1.5ml Eppendorf tube. 80µl 75% isopropanol was added to each tube, they were then vortexed briefly, left at room temperature for 1hr and centrifuged at maximum speed for 20mins. The supernatant was discarded, 250µl 75% isopropanol added, the tubes vortexed and centrifuged again for 5mins at maximum speed. The supernatant was discarded and the pellet dried in a vacuum centrifuge for 10-15mins. Colleagues in the Biology department carried out the sequencing.

2.2.13. Labelling DNA probes by Random Priming

The DNA fragment to be used as a probe was obtained and resolved in a 0.6% low melting point agarose (Gibco BRL). The desired band was excised from the gel and placed in a 1.5ml microfuge tube. 3mls of water was added for each gram of agarose excised. The DNA fragment was denatured at 96°C for 3mins, vortexed and stored at –20°C. The DNA was labelled with ^{32}P ATP (3000Ci/mMol) (Amersham) using the Megaprime DNA labelling kit (Amersham). ~25ng of DNA was placed in a 1.5ml Eppendorf tube and 4µl dCTP, 4µl dGTP, 4µl dTTP (each in Tris/HCl pH 8.0, 0.5mM EDTA), 5µl random nonamer primers and 5µl reaction buffer (10x concentrated buffer containing Tris/HCl pH7.5, 2-mercaptoethanol, $MgCl_2$) added. 5µl ^{32}P ATP was then added followed by the Klenow. The mixture was vortexed briefly, spun and left to incubate at 37°C for 10mins for labelling to occur. The labelled DNA was purified from the non-incorporated nucleotides using the QIAquick nucleotide removal kit (Qiagen). 500µl PN binding buffer was added and the solution applied to a QIAquick spin column tube placed in a 1.5ml Eppendorf tube. The sample was spun at 600rpm for 5mins to bind the DNA to the column. The flow-through solution was discarded, 500µl PE buffer added, the tube centrifuged for 1min at 6000rpm and the flow-through discarded. This step was repeated. The column was then centrifuged again at maximum speed for 1min. The DNA was eluted by adding 50µl TE to the spin column membrane, leaving it to stand at room temperature for 1min and then centrifuging at maximum speed for 1min.

2.2.14. Southern Blotting

About 20-30µg of genomic DNA (1-2µg plasmid DNA) was digested with 100U (10U for plasmid DNA) of the desired restriction enzyme in a 50µl (10-15µl for plasmid DNA) reaction volume. Digestion reactions were incubated at the appropriate temperature overnight (1hr for plasmid DNA). Digested DNA was loaded in a 0.6% gel in TAE and electrophoresed in TAE buffer for a few hours.
After electrophoresis was complete, the DNA was denatured by incubating the gel in denaturing solution (1.5M NaCl and 0.5M NaOH) for about 60mins with gentle

shaking. The gel was then incubated in neutralisation solution (1.5M NaCl, 0.5M Tris-Cl, pH 7.2 and 1mM EDTA, pH 8.0) for 30mins with gentle shaking. DNA was transferred to a nylon membrane (Hybond-N+) by capillary action using 10x SSPE (1.5M NaCl, 100mM NaH_2PO4-H_2O, 10mM EDTA and pH adjusted to 7.4 with 10M NaOH) as the transfer buffer. DNA was fixed to the nylon membrane using the 'auto cross link' setting of a UV Stratalinker-2400 (Stratagene) which delivered 1200mJ.

2.2.15. Hybridisation and washing of Southern Blots

Southern blot membranes were placed in hybridisation tubes and incubated in hybridisation solution (5x Denhardt's reagent (Sigma), 6x SSPE, 0.5% SDS, 50% formamide (BDH)), containing 100µg/ml tRNA at 42°C overnight. Labelled DNA probes were denatured by placing at 100°C for 5mins and then on ice for 5mins before being added to the hybridisation tube. Hybridisation was carried out at 42°C overnight in a hybridisation oven. A Geiger counter was used to check that the membrane had been labelled. Thereafter, the membranes labelled with the DNA probes were washed twice at 65°C with 4x SSPE plus 1% SDS for 8mins and a third time for 5mins. The washed membranes were exposed to Kodak X-R autoradiography films at –70°C.

2.2.16. Shotgun cloning of plasmid colonies

Shotgun cloning was used to isolate subclones from the BAC clone that contained exon 1 that had been identified by Southern blotting with SNS6. 150mm LB-agar master plates (Gibco-BRL) containing 150µg/ml ampicillin (Sigma) were prepared with X-gal (5-Bromo 4 chloro-3-indolyl-β-D-galactoside)/IPTG (isopropylthio-β–D-galactoside): 80µl X-gal (20mg/ml in dimethylformamide) and 8µl IPTG (200mg/ml) were mixed in 500µl LB, spread evenly over each plate and left to dry at room temperature. The BAC clone was digested with BamHI or ApaI and ligated into pBluescript® II SK- that was prepared by digestion with the same restriction

enzyme and dephosphorylation. The ligation reactions were electroporated into competent DH5α *E.Coli* that were then spread evenly over each master plate and incubated at 37°C for 14 hours when the colonies were of reasonable size. The plates were stored at 4°C.

2.2.17. Replica Blotting of plasmid DNA

Hybond N+ nylon membrane pieces were cut so that they would fit snugly inside the master plates. Each one was lowered onto the colonies and left for 1-2mins to transfer part of each colony to the membrane. Needlepoints were used to mark the membrane and the plate for orientation. The plates were stored at 4°C. The membranes were then incubated in the following solutions by placing them on Whatman paper soaked in each solution: 10% SDS for 5mins, denaturing solution for 10mins, neutralising solution for 5mins twice and finally 2x SSPE for 5mins. The denatured DNA was then fixed to the nylon membrane using the 'auto cross link' setting of a UV Stratalinker-2400 (Stratagene) which delivered 1200mJ.
Membranes were transferred to a dish containing 2x SSPE and washed for 10mins at room temperature. They were then pre-hybridised in 100mls hybridisation solution containing 100μg/ml tRNA at 42°C overnight. The radiolabelled probe, SNS6, was denatured and added and left to hybridise at 42°C overnight. The membranes were washed at 42°C with 4x SSPE and 1% SDS for 10mins, 4x SSPE and 1% SDS for 5mins and then with 0.1x SSPE and 1% SDS for 2mins. The washed membranes were exposed to Kodak X-R autoradiography films at -70°C for 48hrs. The films were then orientated with the master plates using the needlepoints, and the colonies that corresponded to positive signals on the films were picked and each one grown in 2mls TB/Amp. DNA was extracted by mini-prep, digested with BamHI or ApaI and the fragments resolved in a 0.8% agarose gel. Southern blotting with SNS6 was then used to select subclones that contained a single insert of the size corresponding to those obtained in the BAC blots.

2.2.18. Modification of pBluescript® II SK- multiple cloning site

The targeting vectors were cloned into pBluescript® II SK-. However, because of the nature of the restriction enzyme sites within the component fragments of the vectors, the multiple cloning site of pBluescript® II SK- was modified so that appropriate restriction enzyme sites were present. Oligonucleotides encoding these restriction enzyme sites needed for cloning were designed.

The following oligonucleotides were used to make a polylinker, pLCS2 that was used in the cloning of the 5'arm of homology/Cre construct:

5' – GCGGCCGCAGGTGACCCTGCAGCCCGGGTGATCAACCGGTTCTA GAACG CGTCTCGAGGTAC – 3'

5' – CTCGAGACGCGTTCTAGAACCGGTTGATCACCCGGGCTGCAGGGTC ACC TGCGGCCGCAGCT – 3'.

This polylinker contained the following sites: SacI overhang / NotI / BstEII / PstI / XmaI / BclI / AgeI / XbaI / MluI / XhoI / KpnI overhang.

The following oligonucleotides were used to make a polylinker, pLCS1 that was used in the cloning of $Na_V1.8Cre1$ and $Na_V1.8Cre2$:

5' – ATCGATCTGCAGGGATCCATGCATGGTACCGAGCTCAAGCTTCTCG AGAGATCTTGATCACCCGGGCCGCGGGTAC – 3'

5' – CCGCGGCCCGGGTGATCAAGATCTCTCGAGAAGCTTGAGCTCGGTA CCATGCATGGATCCCTGCAGATCGATAGCT – 3'.

This polylinker contained the following sites: SacI overhang / ClaI / PstI / BamHI / NsiI / KpnI / SacI / HindIII / XhoI / BglII / BclI / XmaI / SacII / KpnI overhang

To prepare pLCS1 and pLCS2 for introduction into pBluescript® II SK- (Stratagene), 10μM solutions of each were prepared, mixed and incubated at 95°C for 10mins and left to cool slowly. They were then ligated into the SacI and KpnI sites of the pBluescript® II SK- polylinker.

2.3. Results

2.3.1. Targeting vector strategy and design

Of the DRG specific proteins examined, $Na_V1.8$ is the only one that is found exclusively in sensory neurons, and that, within the DRG, has an expression pattern that includes almost all nociceptors and few non-nociceptors. It was therefore decided to use the promoter for $Na_V1.8$ to drive Cre expression.

The primary objective of the targeting vector strategy was therefore to 'knock-in' the translational start of Cre to the translational start of $Na_V1.8$, to maximise the chances of an expression pattern that mimicked that of $Na_V1.8$. Two targeting vectors, $Na_V1.8$Cre1 and $Na_V1.8$Cre2, were designed to achieve this – see Figure 2.4. The vectors designed shared several features:

- Arms of homology flanking the exogenous elements. These were to be at least 5kb in size to increase the likelihood of homologous recombination.
- The Cre sequence. To ensure absolutely precise positioning of the Cre ATG at the $Na_V1.8$ translational start, it was decided to use PCR to produce a small DNA fragment comprising the last bases of the 5' untranslated region (UTR) of $Na_V1.8$ and the first bases of the Cre sequence. This fragment, the ATG chimera, was to be flanked by a restriction enzyme site at its 5' end that could be used to clone the rest of the 5' arm of homology, and by a restriction site at its 3' end that could be used to clone the rest of the Cre fragment. The first exon of $Na_V1.8$ is 305 base pairs in size. The initiator methionine is at bp 36 and a BamHI site, used to clone the 3' arm of homology, is at bp 281. The cloning strategy would result in loss of the intervening part of the first exon.
- The positive selection marker. A neomycin cassette (neoR) that was flanked by *FRT* sites was to be used. The inclusion of *FRT* sites would provide a means to excise the cassette using FLPe expressing mice (Buchholz et al., 1998) that were available in the laboratory. The cassette was to be inverted to prevent cessation of transcription at its' polyA tail.

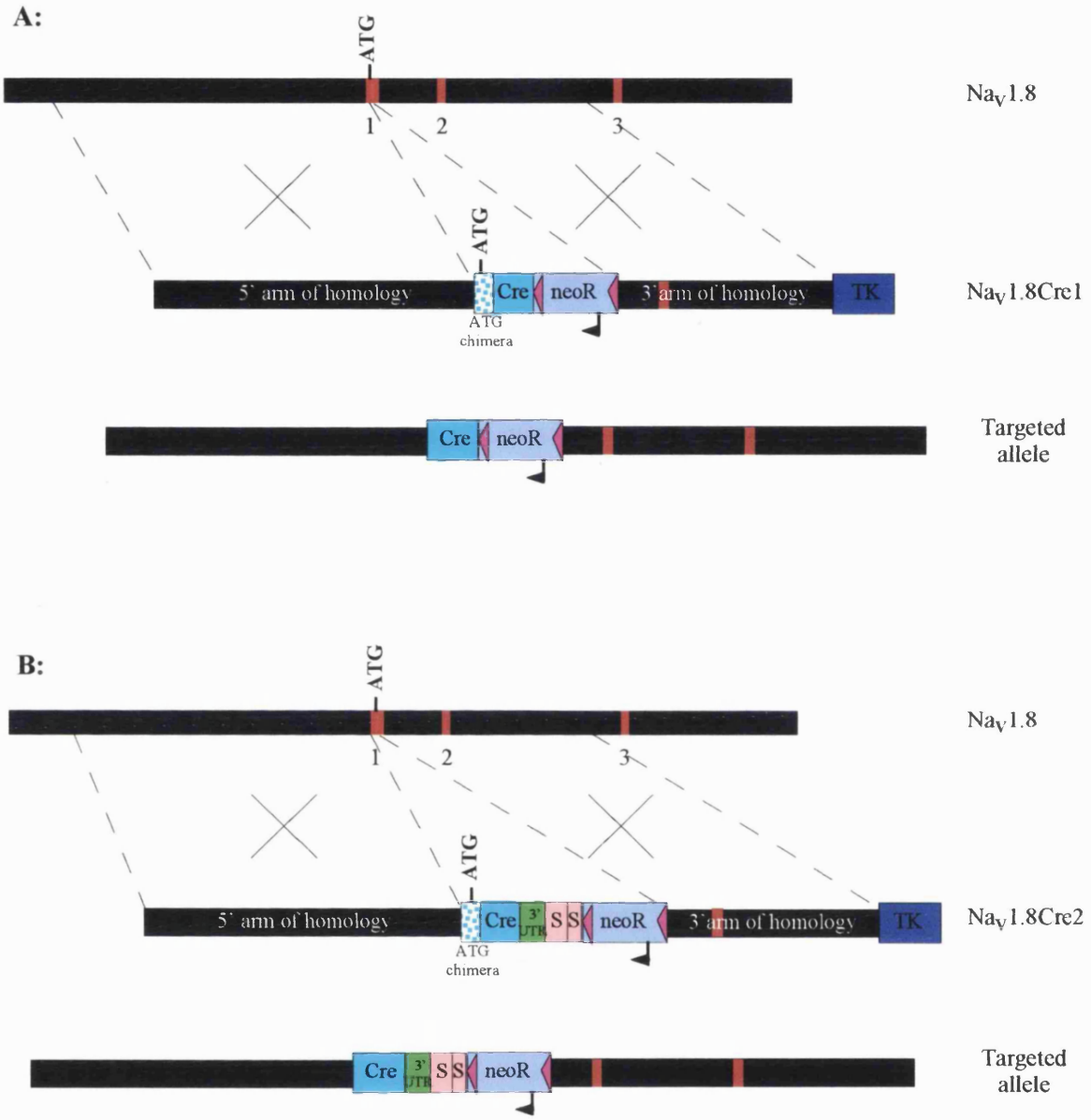

Figure 2.4: Diagram of targeting vectors. A: Nav1.8Cre1 **B:** Nav1.8Cre2.

Solid black lines indicate genomic DNA, red boxes indicate exons, pink triangles indicate *FRT* sites, and the arrow indicates the direction of transcription of the neoR gene. Cre refers to the Cre cassette, neoR to the neomycin cassette, S to polyadenylation signal, and TK to the Herpes Simplex thymidine kinase cassette. Crosses indicate areas of homologous recombination. Diagram not to scale.

- The negative selection marker. A Herpes Simplex virus Thymidine Kinase (HSV-TK) was to be used.

$Na_V1.8$Cre was designed to comprise the two arms of homology, the Cre cassette positioned at the $Na_V1.8$ translational start site, an inverted neoR cassette downstream of Cre, and the HSV-TK cassette downstream of the 3' arm of homology. The whole of $Na_V1.8$ would be transcribed, including any regulators of translation in the 3' UTR or elsewhere within the gene, but the presence of the exogenous components was expected to disrupt the open reading frame resulting in a non-functional $Na_V1.8$ protein.

The strategy for $Na_V1.8$Cre2 was developed in the light of the knowledge that there is an exon encoding the 5' UTR approximately 30kb upstream of the first coding exon of $Na_V1.8$ (Souslova et al., 1997). This raised the potential risk of splicing out of the manipulated Cre-containing exon since the splicing machinery may not recognise a modified exon. For this reason, it was decided to use two polyadenylation signals to terminate transcription after the Cre gene. These would prevent transcription of the rest of the $Na_V1.8$ gene, and therefore eliminate the chance of splicing out of the Cre-containing exon. Two signals were used to reduce the chances of transcriptional read-through. It was also decided to include the 3' part of exon 27 of $Na_V1.8$ that encodes the 3'UTR (Souslova et al., 1997) in the targeting vector as there was a possibility that it may encode important regulators of translation. It was positioned to be downstream of the Cre gene.

Since the two targeting vectors shared some components, the cloning strategy involved the generation of three intermediate constructs – see Figure 2.5. The 5' arm of homology, the ATG chimera and the rest of the Cre cassette were to be cloned to produce the 5' arm of homology/Cre construct that contributed to both targeting vectors. The other components of each vector downstream of the Cre cassette, except the HSV-TK cassette, were to be cloned separately. The 5' arm of homology/Cre construct was then to be cloned with each of the other constructs into a HSV-TK containing vector to produce $Na_V1.8$Cre1 and $Na_V1.8$Cre2.

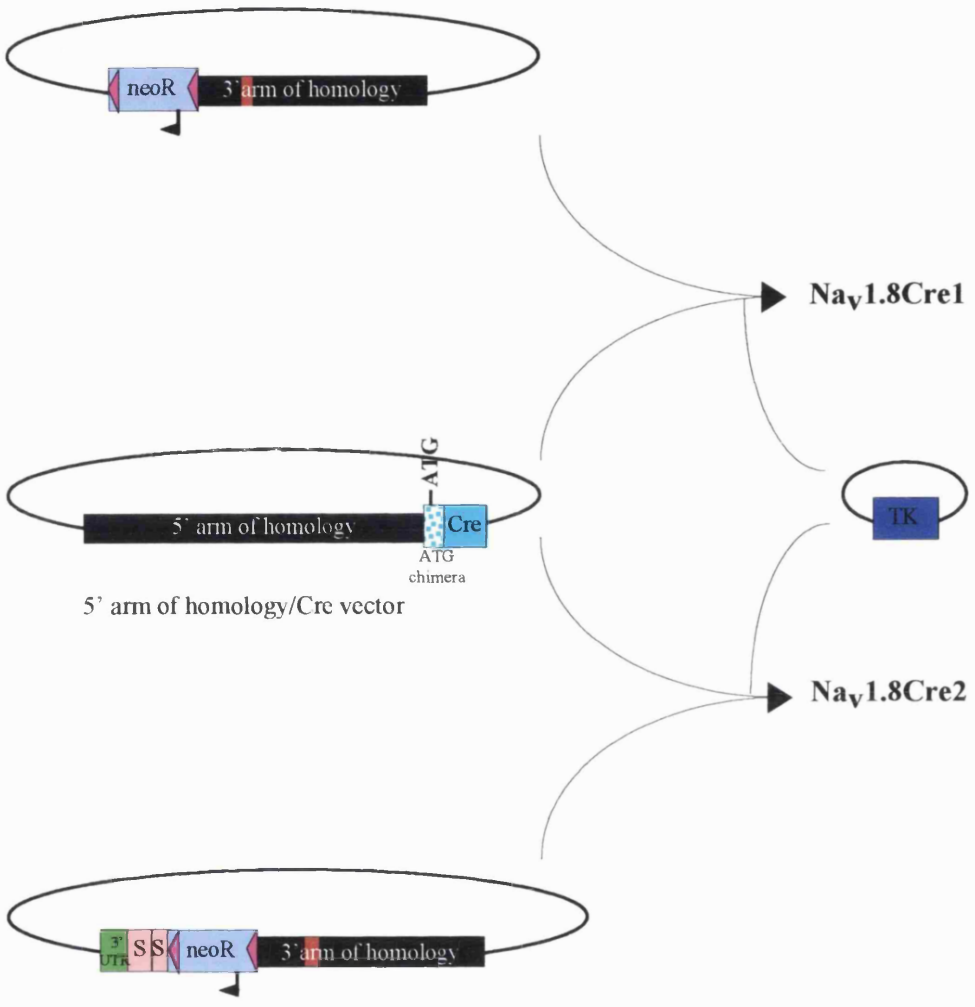

Figure 2.5: Strategy for cloning the targeting vectors.
The 5' arm of homology/Cre vector contributes to Na$_V$1.8Cre1 and Na$_V$1.8Cre2. The other components of each vector, except the HSV-TK cassette, were to be cloned separately. Three fragmennt ligations into the HSV-TK containing vector were to be used to produce Na$_V$1.8Cre1 and Na$_V$1.8Cre2.

2.3.2. Cloning of ES cell Targeting vectors

2.3.2.1. Isolation of mouse genomic DNA containing exon 1 of $Na_V1.8$

To isolate a bacterial artificial chromosome (BAC) clone containing genomic sequences of $Na_V1.8$, a ^{32}P labelled probe for exon 10-12 of $Na_V1.8$, derived from rat $Na_V1.8$ cDNA (Souslova et al., 1997) was used to screen the RCPI-22 129S6/SvEvTac mouse BAC library (Roswell Park Cancer Institute, Buffalo NY 14263) (Osoegawa et al., 2000). This screening was carried out by Dr. Mohammed Nassar.

Southern blotting was then used to identify fragments within this BAC clone that included the translational start site of $Na_V1.8$. A 0.4kb probe, SNS6, encoding part of the5'UTR, exon 1 and most of exon 2, was amplified from rat $Na_V1.8$ cDNA using the primers rSNSseq1s and rSNSseq3a. The BAC clone was digested with ApaI, BamHI, HindIII and KpnI and hybridised to SNS6. Several fragments were identified - see Figure 2.6. The probe hybridised strongly to a 12.5kb ApaI flanked fragment, and weakly to 4.5kb and 8kb fragments. It was thought that a poorly digesting ApaI site within the 12.5kb fragment accounted for the two smaller fragments. Two BamHI flanked fragments, 6.5kb and 8.5kb in size, were also identified. The HindIII flanked fragment was over 15kb and the KpnI fragment 5kb in size – these two were not analysed further.

Shotgun cloning was then used to subclone both the BamHI and the 12.5kb ApaI flanked fragments. The individual subclones were isolated using replica blotting followed by hybridisation to SNS6. Thirty-six positive colonies containing BamHI flanked subclones and 54 positive colonies containing ApaI flanked subclones were picked and processed. Of these, four 6.5kb and two 8.5kb BamHI flanked subclones, and three 12.5kb ApaI flanked subclones that hybridised to SNS6, were processed (Figure 2.7).

2.3.2.2. Mapping of the genomic $Na_V1.8$ subclones

A variety of restriction enzymes were used to map the subclones and compared with published data (Souslova et al., 1997). They were found to cover an area (18kb) of $Na_V1.8$ starting 8.0kb upstream of exon 1 and ending 3.0kb downstream of exon 3 –

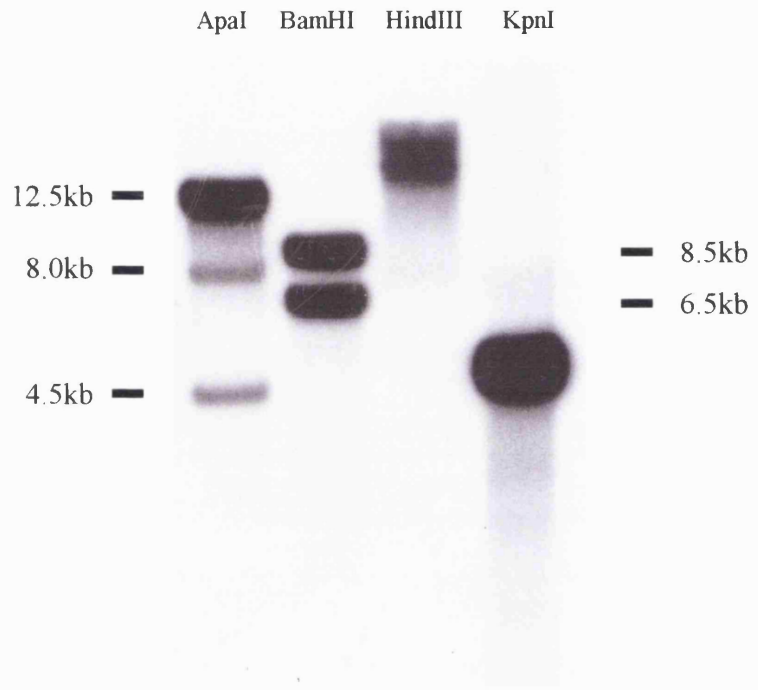

Figure 2.6: Southern blot of the mouse BAC clone containing $Na_V1.8$ to select fragments containing its translational start site.
To select fragments containing the $Na_v1.8$ translational start site, the BAC clone was digested with ApaI, BamHI, HindIII and KpnI, and hybridised with an oligonucleotide probe SNS6, encoding part of the 5'UTR, exon 1 and most of exon 2. SNS6 hybridised to 8.5kb and 6.5kb BamHI flanked fragments, 12.5kb, 8.0kb and 4.5kb ApaI flanked fragments, a 15kb HindIII flanked fragment and a 5kb KpnI flanked fragment. The BamHI and ApaI flanked fragments were analysed further

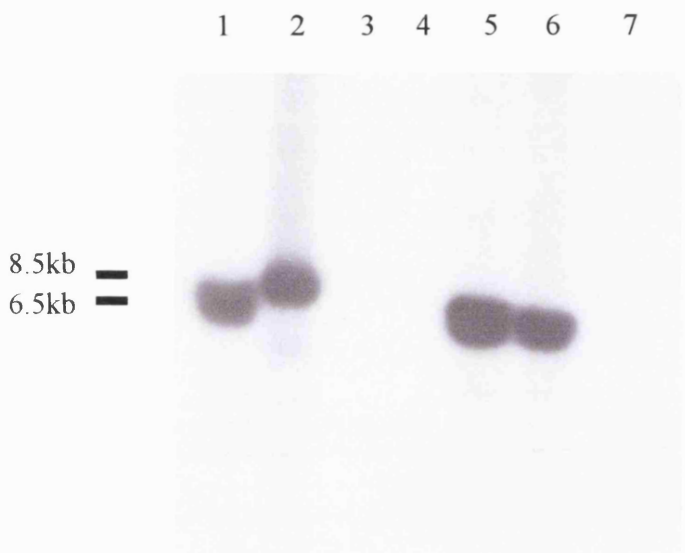

Figure 2.7: Southern blot of genomic subclones selected by shotgun cloning and digested with BamHI.
Hybridisation of the subclones selected by shotgun cloning with SNS6 allowed identification of subclones containing the 8.5kb fragment (seen in lane 2) and the 6.5kb fragment (seen in lanes 1, 5, and 6).

see Figure 2.8. The data confirmed that the BamHI site dividing the 8.5kb and 6.5kb subclones was within exon 1, and that the 12.5kb ApaI fragment contained an ApaI site within it, as had been suggested by the Southern blot data.

To clone the Cre coding sequence into the translational start site of $Na_V1.8$, the sequence of the 5' UTR upstream of exon 1 was required. The promoter regions for T3 and T7 flank the polylinker of pBluescript® II SK- and these were exploited for sequencing purposes. T3 was used to sequence the 3' end of the 8.5kb fragment and T7 was used to sequence the 5' end of the 6.5kb fragment. These data confirmed the exact sequence of exon 1 and determined the sequence of an antisense primer, mSNSseq1a, which started 64bps upstream of exon 1. mSNSseq1a was then used to sequence the 5'UTR further upstream of exon 1. In all, the sequence from bp –558 to +670 of $Na_V1.8$ was determined in the BAC subclones.

2.3.2.3. Cloning of the Targeting vectors

As mentioned above, to simplify cloning of the targeting vectors $Na_V1.8$Cre1 and $Na_V1.8$Cre2, three intermediate constructs were made. The 5' arm of homology and the Cre cassette were cloned to produce the 5' arm of homology/Cre construct that contributed to both targeting vectors and the other components contributing to each vector were cloned separately. Drs. Mohammed Nassar and Greta Forlani performed some of these steps.

2.3.2.3.1. Cloning of the 5' arm of homology / Cre construct Figure 2.9.

1. The pBluescript® II SK- polylinker was modified using pLCS2. This polylinker encoded the following restriction enzyme sites that were needed for cloning: NotI / BstEII / XmaI / AgeI / MluI / XhoI.

2. The ATG chimera (0.4kb) was obtained by PCR using the 8.5kb BamHI genomic subclone as a template. The primers mSNSseq7s and mSNSCreseq1a were used. The resulting fragment encoded the area upstream of the $Na_V1.8$ translational start site including an XmaI site at its 5' end, and the start of the Cre sequence, including an AgeI site at its 3' end. The PCR product was digested with XmaI and AgeI and

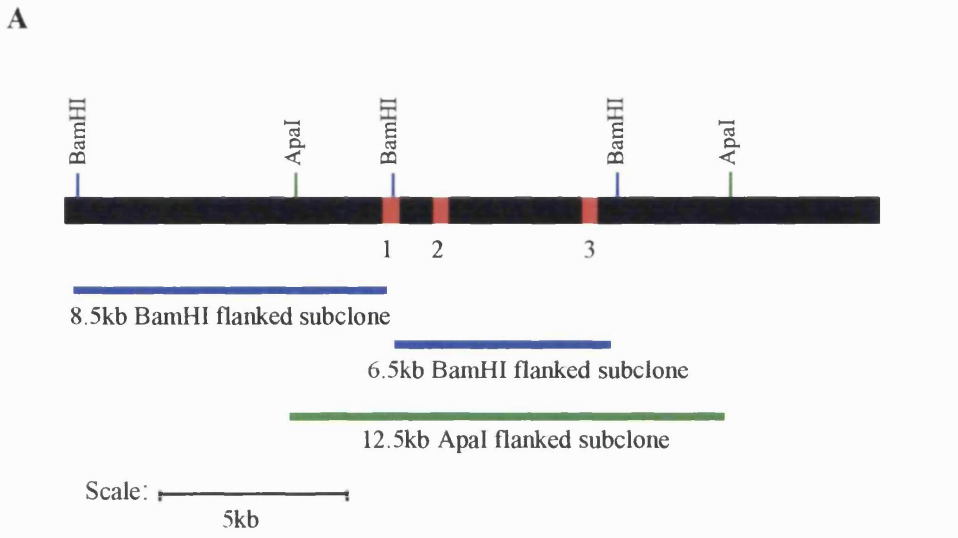

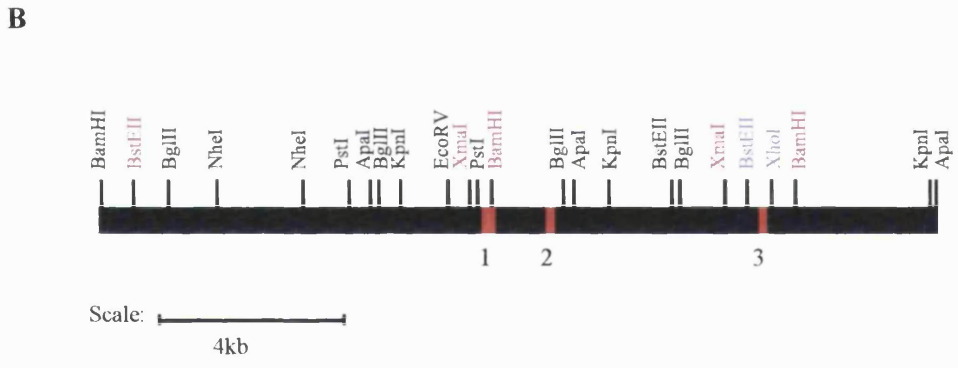

Figure 2.8: Schematic representation of the $Na_V1.8$ BAC clone.

Solid black lines indicate introns, red boxes indicate exons.

A: Area of the $Na_V1.8$ BAC clone covered by the three subclones isolated using shotgun cloning.

B: Positions of restriction enzyme cutting sites in DNA covered by the subclones. Sites used for cloning the targeting vectors are indicated in magenta, and sites used to clone the 3' probe in purple.

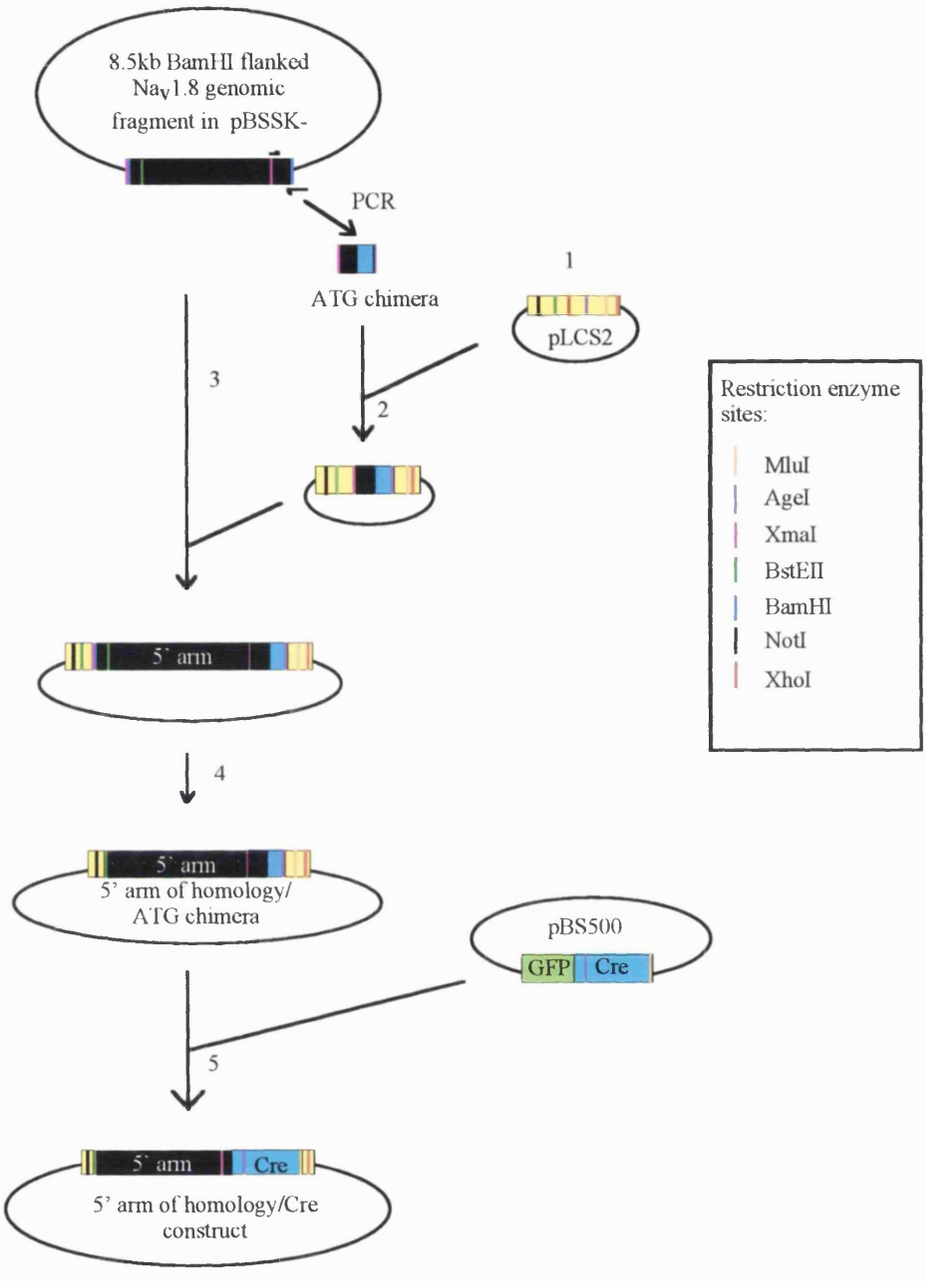

Figure 2.9: **Schematic representation of the cloning of the 5' arm of homology/Cre construct.**

See text for details of individual steps. pLCS2 refers to the pBluescript SK- plasmid, modified with the polylinker pLCS2, into which the component fragments were cloned. pBS500 refers to the Cre containing plasmid, 5' arm to the 5' arm of homology. Single headed arrows denote the sites of the primers used to synthesise the ATG chimera. The NotI and XhoI sites at the ends of the polylinker were used to clone Nav1.8Cre1 and Nav1.8Cre2.

ligated into the corresponding sites in the modified pBluescript® II SK-, pLCS2. Restriction enzyme digestion followed by sequencing was used to confirm that the fragment had been correctly inserted.

The rest of the 5' arm of homology was cloned in two steps:

3. A 8.0kb fragment was excised from the 8.5kb $Na_v1.8$ genomic subclone and cloned using XmaI into the end product of 2.

4. A 0.7kb fragment at its' 5' end was then excised using BstEII digestion and religation. Restriction enzyme digestion was used to confirm these steps had been performed correctly.

5. The remainder of the Cre sequence (1.0kb) was excised from pBS500 using AgeI and MluI and cloned using the same sites in the product of 4. Restriction enzyme digestion was used to confirm this step.

2.3.2.3.2. Cloning of $Na_v1.8$Cre 1 Figure 2.10.

1. The pBluescript® II SK- polylinker was modified using pLCS1. This polylinker encoded the following restriction enzyme sites that were needed for cloning: SacII / SacI / XhoI / BglII / XmaI / BamHI.

2. The neomycin cassette (neoR) (neomycin coding sequence flanked by *FRT* sites) (1.29kb) was excised from pYR6.1 using SacI and SalI sites and then ligated into SacI and XhoI sites of the product of 1. Since SalI and XhoI have compatible cohesive ends they were destroyed in this step.

3. The 3' arm of homology (5.5kb) was excised from the 6.5kb $Na_v1.8$ genomic subclone using BamHI and XmaI. It was ligated into the BglII and XmaI sites of the endproduct of 2. Since BamHI and BglII restriction enzyme sites have compatible cohesive ends they were destroyed in this step.

4. This fragment was cloned into pBluescript® II SK– using SacII and BamHI.

5. The final $Na_v1.8$Cre1 targeting vector was prepared using a three-fragment ligation. The 5' arm of homology/Cre construct was obtained as a 8.7kb NotI and XhoI fragment, and the neoR – 3' arm of homology construct was obtained as a 6.9kb XhoI and SacII fragment. These two fragments were ligated into the NotI and SacII sites of a vector containing a HSV-TK cassette (1.85kb). Extensive restriction

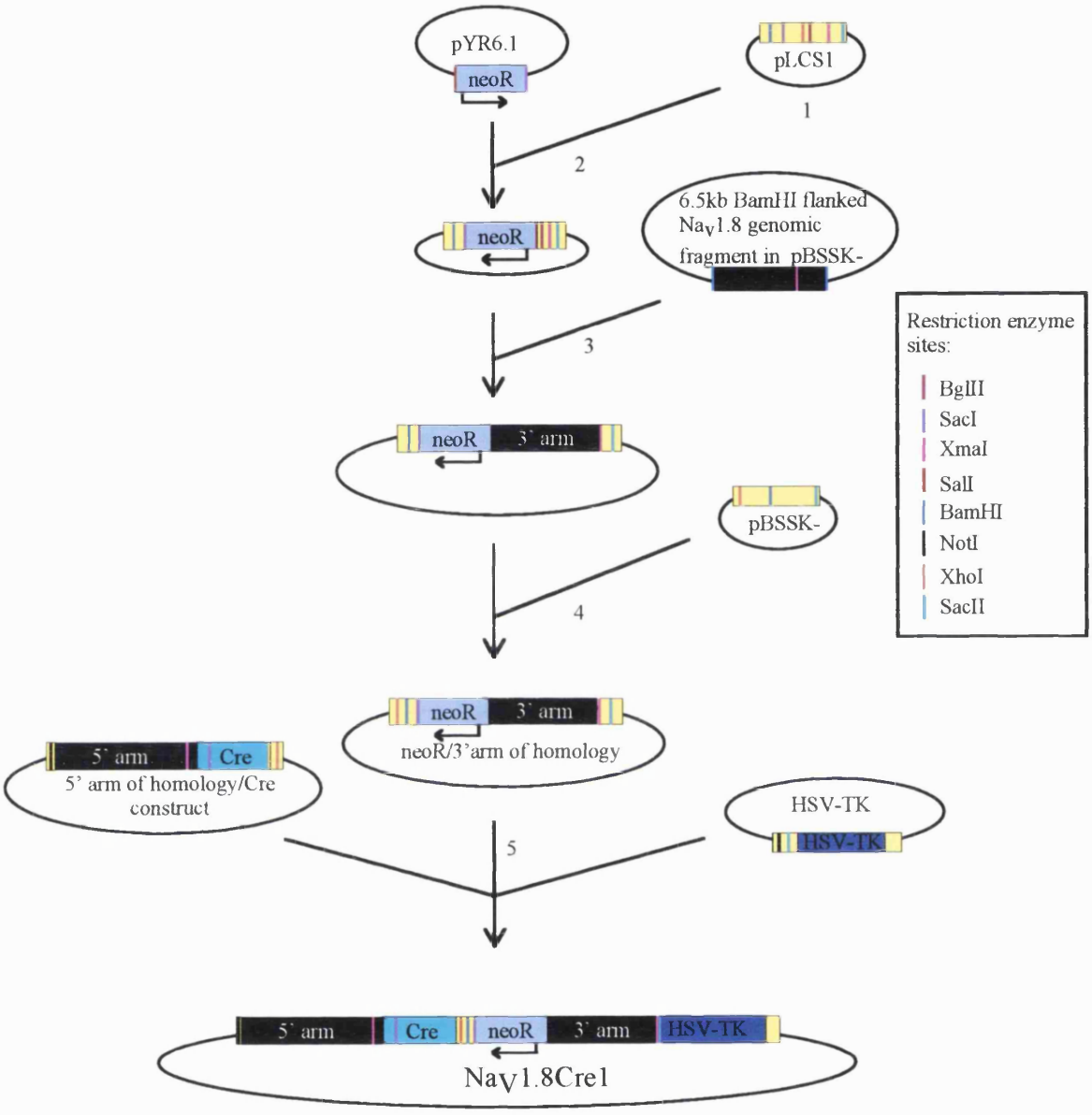

Figure 2.10: Schematic representation of the cloning of Nav1.8Cre1.

See text for details of individual steps. pLCS1 refers to the pBluescript SK- plasmid, modified with the polylinker pLCS1, into which component fragments were cloned, neoR to the neomycin cassette, pBSSK- to pBluescript SK- plasmid, 3' arm and 5' arm to the 3' and 5' arm of homology respectively, and HSV-TK to the Herpes Simplex Virus thymidine kinase cassette.

enzyme digestions confirmed the structure of the vector. The vector was linearised at the Not I site.

2.3.2.3.3. Cloning of $Na_V1.8Cre2$ Figure 2.11.

1. A SV40 polyadenylation signal (0.4kb) was excised from pUHD15-1 using BamHI/HindIII sites. A synthetic polyadenylation signal (0.2kb) was excised from TNR1/CII/S5c-Stop using HindIII and PstI sites. The two fragments were then ligated simultaneously into BamHI and NsiI sites of the modified pBluescript® II SK- containing the neomycin cassette (see *Cloning of $Na_V1.8Cre$ 1*, step 2.). Since PstI and NsiI have compatible cohesive ends these sites were destroyed during this step. Restriction digestion and sequencing were used to ensure that these fragments had been correctly inserted.

An XhoI site within the multiple cloning site that flanked the 0.2kb polyadenylation signal was killed using XhoI digestion and Klenow fill-in followed by religation. It was necessary to kill this site since an XhoI site flanking the 3'UTR was to be used in the final three-fragment ligation to join all the components of $Na_V1.8Cre2$ together. Restriction digestion was used to confirm that the site had been killed.

2. The $Na_v1.8$ 3' UTR (0.4kb) was obtained by PCR using the $Na_v1.8$ BAC clone as the template and the primers mSNSpcr8s and mSNSpcr9a. The resulting PCR product was digested with BamHI and ligated into the BamHI site of the endproduct of 1. Correct orientation was confirmed by restriction digests and sequencing.

3. The 3' arm of homology (5.5kb) was excised from the 6.5kb $Na_v1.8$ genomic subclone using BamHI and XmaI. It was ligated into the BamHI and XmaI sites of the endproduct of 2. Since BamHI and BglII restriction enzyme sites have compatible cohesive ends they were destroyed in this step.

4. The final targeting vector was prepared using a three-fragment ligation. The 5' arm of homology/Cre construct was obtained as a 8.7kb NotI and XhoI fragment, and the 3' UTR – 3' arm of homology construct was obtained as a 8.3kb XhoI and SacII fragment. These two fragments were ligated into the NotI and SacII sites of the HSV-TK cassette.

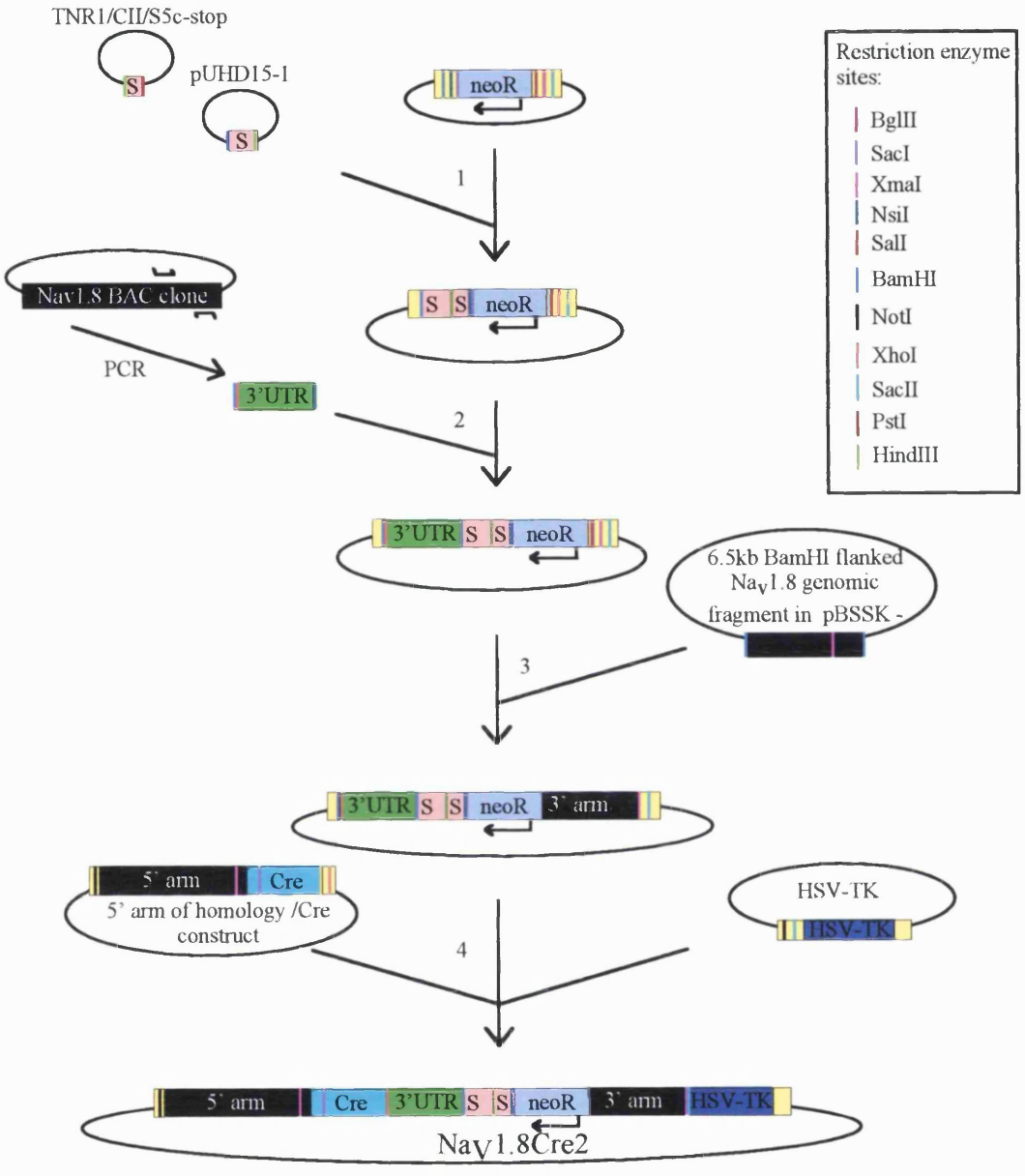

Figure 2.11: Schematic representation of the cloning of Na$_V$1.8Cre2.

See text for details of individual steps. Single headed arrows denote the sites of primers used to synthesise the 3' UTR. S refers to the polyadenylation sequences, neoR to the neomycin cassette, 3' arm and 5' arm to the 3' and 5' arm of homology respectively, and HSV-TK to the Herpes Simplex Virus thymidine kinase cassette.

Extensive restriction enzyme digestions confirmed the structure of the vector. The vector was linearised at the Not I site.

2.3.3. Transfection of Targeting vectors into 129 ES cells

This was carried out by Monica Mendelsohn, Howard Hughes Medical Institute, Columbia University, USA. Transfected 129/SvEvTac derived ES cells were plated for drug selection; Geneticin (G418) was used for positive selection. For $Na_V1.8$Cre1 and $Na_V1.8$Cre2, genomic DNA was isolated from 185 and 184 ES cell clones respectively that survived selection and sent to the laboratory for screening.

2.3.4. Screening of ES cell clones

Selection of the ES cell clones in which homologous recombination of the targeting vectors had occurred was performed using Southern blot analysis. The strategy for screening was developed to exploit BamHI restriction enzyme sites. As discussed, there are three BamHI sites in wild type alleles, one in the 5' UTR, 8.5kb upstream of the second BamHI site that is 245bp after the ATG in exon 1. The third site is in intron 3, 6.5kb downstream of the site in exon 1. The BamHI sites present in the targeting vector components or used in the cloning process were as follows – see Figure 2.12:

- The Cre sequence has a BamHI site at bp356.
- The polylinker pLCS1 was designed to include a BamHI site.
- The BamHI site within exon 1 was used to excise the 3' arm of homology from the BAC clone but it was destroyed in the cloning of both targeting vectors because it was ligated into a BglII site of pLCS1 – these restriction enzyme sites have compatible cohesive ends.

During the cloning of $Na_V1.8$Cre1, the BamHI site in pLCS1 was not utilised. It was therefore located between the neoR cassette and the Cre cassette, 0.7kb from the site within the Cre sequence.

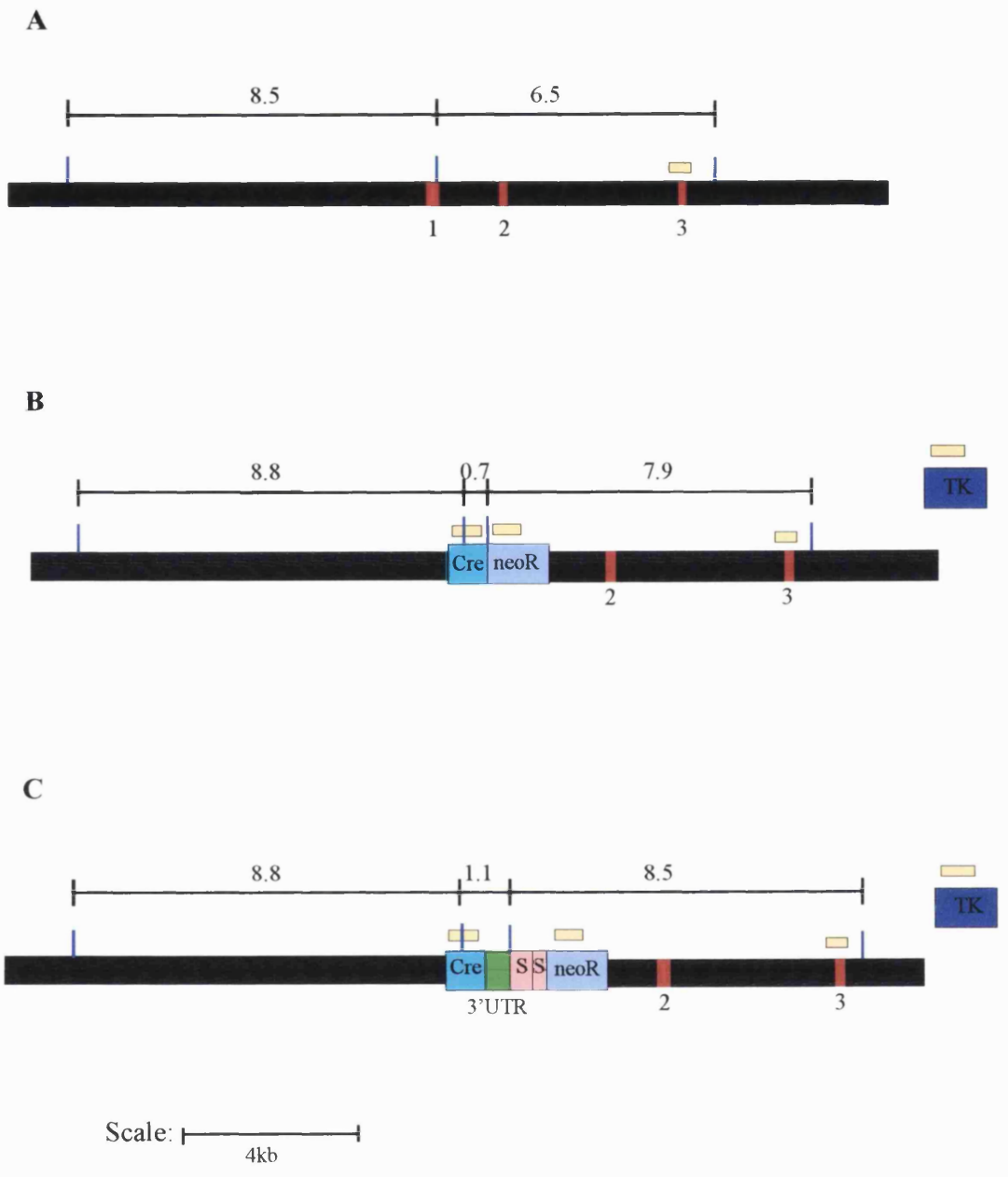

Figure 2.12: Diagram of strategy used to screen the ES cell clones.
Solid black lines indicate genomic DNA, with exons in red. Positions of BamHI sites are shown in blue **A** in wildtype DNA, **B**, after targeting of Na$_V$1.8Cre1, and **C**, after targeting with Na$_V$1.8Cre2. Distances between the BamHI sites, in kb, are shown. The probes used for screening are shown in yellow.

During the cloning of $Na_V1.8$Cre2, the BamHI site in pLCS1 was used to clone the stop signals. Thus it was located between the $Na_V1.8$ 3' UTR and the stop signals, at a position 1.1kb downstream of the BamHI site in the Cre sequence.

For each screen the clones were digested with BamHI and screened using the following probes:

1. External 3' probe: This probe comprised a 0.5kb genomic sequence located immediately 3' to the 3' arm of homology. The probe allowed confirmation that the 3' end of the targeting vectors was present. It was used to screen all ES cell clones received, and the positive clones from this screen were then analysed further. In wild type alleles the probe was expected to hybridise to the 6.5kb fragment flanked by the BamHI sites in exon 1 and intron 3. Correct targeting of $Na_V1.8$Cre1 would result in a 7.9kb BamHI fragment hybridising to this probe, flanked by the BamHI site in pLCS1 upstream of the neomycin cassette and by the site in intron 3. Correct targeting of $Na_V1.8$Cre2 would result in hybridisation to a 8.5kb fragment, flanked by the BamHI site between the 3' UTR and the stops signals and the site in intron 3.

To prepare the probe, a 1.5kb fragment was excised from the 6.5kb $Na_V1.8$ genomic subclone using XmaI sites, and ligated into the XmaI sites of pBluescript® II SK-. Restriction enzyme digestion confirmed correct orientation of the fragment. This small fragment was then digested with BstEII, XhoI and NsiI, and the probe, flanked by BstEII and XhoI, prepared.

Four positive clones were isolated from ES cells transfected with $Na_V1.8$Cre1 and seven from ES cells transfected with $Na_V1.8$Cre2. Figure 2.13 shows the results using this probe.

2. Internal Cre probe: This 0.9kb probe included most of the Cre coding sequence including the BamHI site within it. This probe allowed confirmation that the 5' end of each of the vectors was correctly integrated, and the detection of vectors that had been randomly integrated into the ES cell genome. In wild type alleles no hybridisation was expected. In alleles targeted with $Na_V1.8$Cre1, the probe was expected to hybridise to two fragments - a 8.8kb fragment, flanked by the BamHI site within the 5' UTR and the site within the Cre sequence, and a 0.7kb fragment flanked by the BamHI site within the Cre sequence and the site in pLCS1 located in

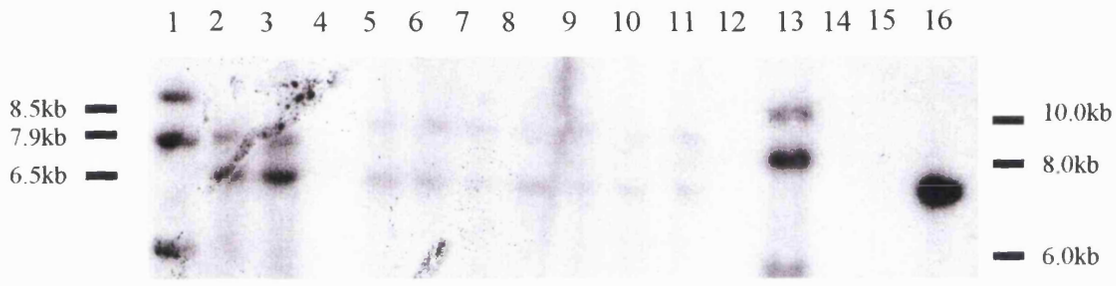

Figure 2.13: Southern blot of ES cell clones digested with BamHI and hybridised to the external 3' probe.
Lanes 2 and 3 were loaded with DNA from the positive $Na_V1.8Cre1$ clones, lanes 5-11 with DNA from the positive $Na_V1.8Cre2$ clones, and lane 16 with wild type DNA. The Hyperladder marker was loaded into lanes 1 and 13. The wild type 6.5kb band can be seen in all ES cell clones, the 7.9kb band in the $Na_V1.8Cre1$ containing clones and the 8.5kb band in the $Na_V1.8Cre2$ containing clones.

this case at the 3' end of the Cre sequence. In alleles targeted with $Na_V1.8$Cre2, the same 8.8kb fragment was expected. The second fragment was expected to be 1.1kb in size, since the BamHI site within pLCS1 would be downstream of the 3' UTR. The probe was derived by PCR using the final $Na_V1.8$Cre2 Targeting vector as the template. The expected results were seen in all cases. Figure 2.14 shows the data for two of the $Na_V1.8$Cre1 containing ES cells and all the $Na_V1.8$Cre2 containing clones. A second randomly integrated copy of $Na_V1.8$Cre1 was detected in one of the $Na_V1.8$Cre1 containing clones (Lane 1). In one of the $Na_V1.8$Cre2 containing clones, (Lane 6) the 8.8kb band was weak but visible.

3. Internal neoR probe: This 0.8kb probe confirmed that the 3' ends of the vectors had been correctly integrated and allowed detection of randomly integrated vectors. In wild type alleles no hybridisation was expected. In alleles targeted with $Na_V1.8$Cre1, the probe was expected to hybridise to a 7.9kb fragment, flanked by the BamHI site just 5' to the neomycin cassette and the site in intron 3. In alleles targeted with $Na_V1.8$Cre2, a 8.5kb fragment was expected; the size of the fragment would be increased by the size of the two stop signals.

The probe was derived by PCR using the $Na_V1.8$Cre2 targeting vector as the template. Figure 2.15 shows the results using this probe. The expected results were seen. As with the Cre probe, the randomly integrated copy of $Na_V1.8$Cre1 (Lane 1) and a weak band in one of the $Na_V1.8$Cre2 containing clones (Lane 6) are seen.

4. HSV-TK probe: This 1.0kb probe was used to confirm the absence of the HSV-TK cassette in the targeted alleles. It was derived by PCR using $Na_V1.8$Cre2 targeting vector as the template. The expected results were seen in all cases – see Figure 2.16.

2.3.5. Production of Chimeras by blastocyst injection

This was carried out by Monica Mendelsohn, Howard Hughes Medical Institute, Columbia University, USA. C57BL/6J mice were used as hosts. For each transfer, blastocysts were recovered on day four from the uterine lumen of a pregnant mouse. ES cells were then injected into the blastocyst and the embryo transferred to the

uterus of a pseudopregnant mouse. Two chimeras were produced following blastocyst injection of ES cells positive for $Na_V1.8Cre2$. They were bred and germ line chimeric mice generated. These animals were sent to the laboratory. $Na_V1.8Cre1$ chimeras were not produced.

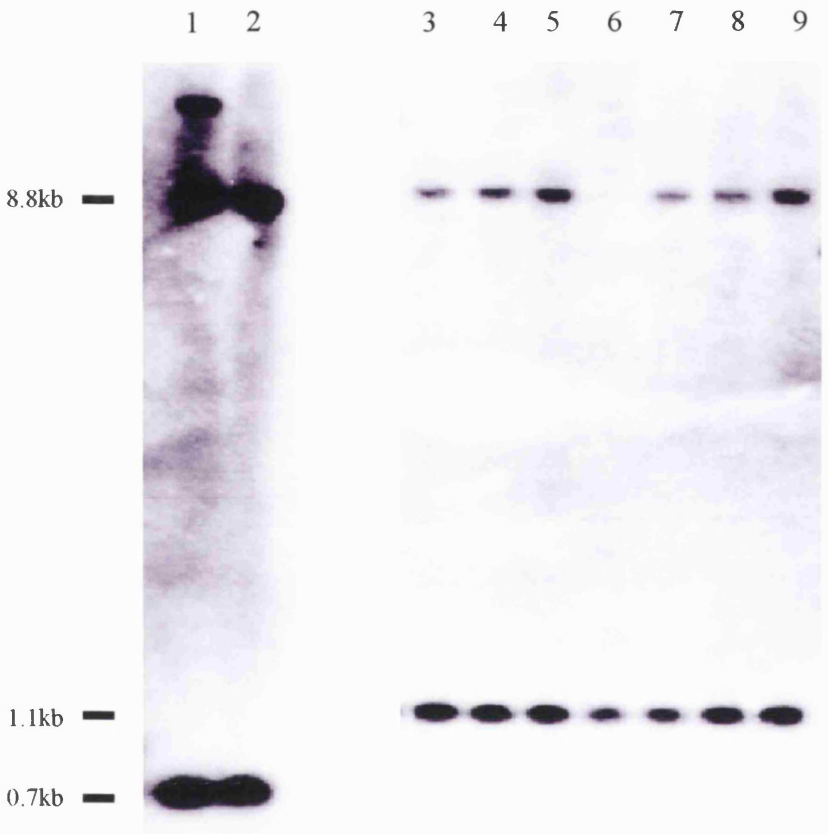

Figure 2.14: Southern blot of ES cell clones digested with BamHI and hybridised to the internal Cre probe.
Lanes 1 and 2 were loaded with DNA from the positive $Na_V1.8Cre1$ clones and lanes 3-9 with DNA from the positive $Na_V1.8Cre2$ clones. A 8.7kb band can be seen in all ES cell clones, a 0.7kb band in the $Na_V1.8Cre1$ containing clones and a 1.1kb band in the $Na_V1.8Cre2$ containing clones. (Data provided by M. Nassar).

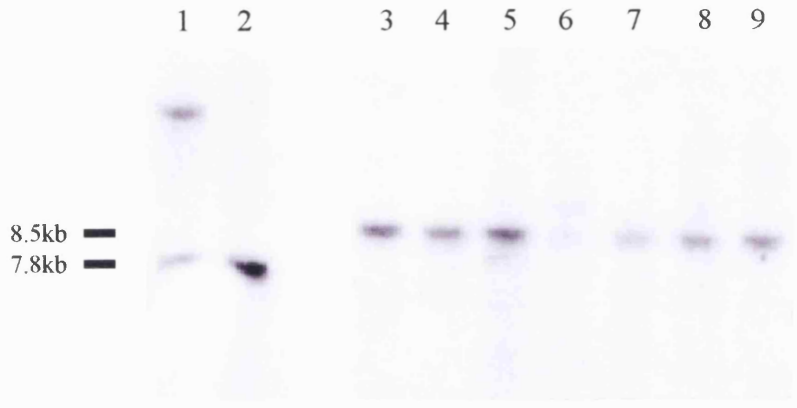

Figure 2.15: Southern blot of ES cell clones digested with BamHI and hybridised to the internal neoR probe.
Lanes 1 and 2 were loaded with DNA from the positive $Na_V1.8Cre1$ clones and lanes 3-9 with DNA from the positive $Na_V1.8Cre2$ clones. A 8.5kb band can be seen in the $Na_V1.8Cre1$ containing clones and a 7.8kb band in the $Na_V1.8Cre2$ containing clones. (Data provided by M. Nassar).

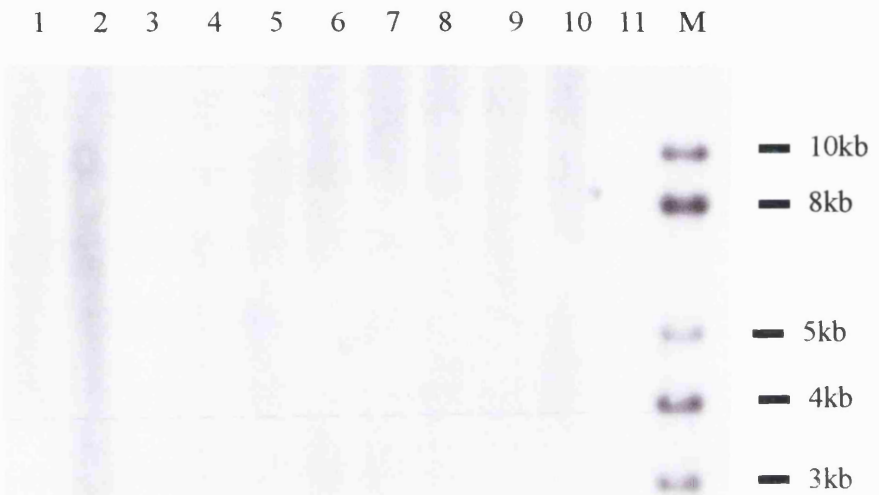

Figure 2.16: Southern blot of ES cell clones digested with BamHI and hybridised to the HSV-TK.
Lanes 1 and 2 were loaded with DNA from the positive $Na_V1.8Cre1$ clones, lanes 4-10 with DNA from the positive $Na_V1.8Cre2$ clones. Lane 12 has the Hyperladder marker. There is no hybridisation to the probe.

2.4. Discussion

This chapter describes the strategy for and generation of two targeting vectors in which the Cre gene is knocked-in to the translational start of the TTX-resistant voltage-gated sodium channel $Na_V1.8$ that is almost exclusively expressed in nociceptive afferent sensory neurons. Both targeting vectors, $Na_V1.8Cre1$ and $Na_V1.8Cre2$, were successfully cloned and transfected into 129 ES cells. One hundred and ninety two ES cell clones that survived positive selection were screened for homologous recombination, and of these 2.1% (4/185) and 3.8% (7/184) showed correct targeting of $Na_V1.8Cre1$ and $Na_V1.8Cre2$ respectively.

Correctly targeted ES cells were transferred into C57BL/6J blastocysts and two germ line chimeras were produced from $Na_V1.8Cre2$ ES cells.

In the first of the targeting vectors, $Na_V1.8Cre1$, the Cre gene was inserted into the translational start site of $Na_V1.8$. The presence of a non-coding exon ~30kb upstream of the first coding exon raised the potential for splicing out of an exogenously modified exon, and this led to the strategy for the second targeting vector, $Na_V1.8Cre2$. In this vector, the Cre gene followed by the $Na_V1.8$ 3' UTR were inserted into the translational start site of $Na_V1.8$, and two polyadenylation signals were placed downstream of the 3' UTR to stop transcription thereafter.

Both targeting vectors underwent homologous recombination in 129/SvEvTac derived ES cells, and injection of $Na_V1.8Cre2$ expressing ES cells into C57BL/6J blastocysts resulted in the production of germ line transmitting $Na_V1.8Cre2$ chimeras. Because germ line transmitting chimeras were not produced from $Na_V1.8Cre1$ expressing ES cells, we were unable to determine whether there would have been interference with the transcription of $Na_V1.8Cre1$ targeted alleles.

The majority of animals produced to date with tissue-specific Cre expression have been generated using the transgenic approach. This approach takes advantage of the promoter and regulatory sequences of genes with tissue-specific expression patterns. The isolated promoter/regulatory sequences are assembled in genetic construct

designed to direct the expression of Cre coding sequences. The advantages of using this approach are that mice in which there is germ line transmission are generated quickly and relatively easily. However, although a gene with the desired expression pattern can often be identified with ease, the transgenic approach depends on the identification and isolation of all the promoter/enhancer and regulatory sequences, which may be spread over large distances in the genome. Transgenic constructs containing all regulatory sequences can faithfully replicate tissue-specific gene expression independent of the integration site within the genome. However, often they are not fully identified and incorporated in transgenic constructs. The integration site can therefore influence the promoter activity and affect the expression pattern of Cre. Mistimed gene expression, expression of the gene in extraneous tissues and/or mosaic expression within the target tissue often occur. For these reasons it is very important to screen the founder lines generated carefully and select those with the appropriate expression pattern (de Boer et al., 2003).

An alternative transgenic approach is to use BACs to generate tissue specific Cre expressing mice. This method shares the practical advantages outlined above and, in most cases, because the BAC containing the target gene is so large, knowledge of the promoter/regulatory sequences is not required and positional effects are rare. However 10-15% of genes have regulatory elements that are positioned far away from their coding region, and if they are used, positional effects may be encountered. In addition, for very large genes the BAC approach has a low probability of success (Gong et al., 2003).

Use of gene targeting to generate a target vector in which Cre is 'knocked in' to the translational start site of a gene with a desired expression pattern (Rickert et al., 1997) provides an alternative strategy that obviates these problems. The endogenous promoters and all other regulatory sequences remain unchanged and are utilised to control Cre expression in a site-specific manner. The resulting expression pattern reflects that of the target gene and there are rarely positional effects. However this method is more time consuming than transgenesis, and usually results in loss of the target gene. The Cre expressing animals are therefore often maintained as heterozygotes.

An example of the utility of the knock-in approach was shown by Guo *et al.,* (Guo et al., 2000) who initially used the transgenic approach with the aim of generating animals in which Cre expression was restricted to the cerebral cortex. They used 11kb of the genomic sequence upstream of the putative ATG translational start site of Exm1, a gene expressed exclusively in the cerebral cortex, to drive Cre expression. None of the resulting lines displayed an expression pattern similar to that of Exm1. The same group then went on to knock-in Cre to the translational start site of the Exm1 gene and successfully generated a line with the expected expression pattern (Jin et al., 2000).

The knock-in approach was used in this strategy since we were aware that heterozygous $Na_V1.8$ knock-out animals have no detectable phenotype (Akopian et al., 1999). The precise size and location of the $Na_V1.8$ promoter and regulatory sequences is not known, making it difficult to assemble a transgenic construct capable of directing $Na_V1.8$-specific gene expression independent of transgene integration. In contrast, the knock-in approach provides a method to generate animals in which Cre mimics $Na_V1.8$ expression in nociceptors. Animals that are homozygous for the $Na_V1.8$Cre2 allele and a floxed target gene would have this genotype and potentially provide further insights into gene function and interaction in nociception.

The Cre sequence used in this project (Gagneten et al., 1997) has an optimised translational start site (Kozak, 1986) and a neutral mutation in the coding region. Several groups have included a nuclear localisation signal (NLS) in their construct design (Gu et al., 1993), but Le *et al.,* (Le et al., 1999) have shown that the Cre sequence itself, although prokaryotic in origin, carries determinants that direct it to the nucleus. Shimshek *et al.,* (Shimshek et al., 2002) recently described the development of an improved Cre sequence, iCre, in which, as well as including a Kozak sequence and NLS, the prokaryotic Cre sequence was altered make it more like a eukaryotic sequence; silent base mutations corresponding to human codon use preferences were made, putative cryptic splice sites were eliminated and the CpG content minimised. They showed that iCre activity and expression levels were approximately 2-fold higher than native Cre *in vitro*, and that in transgenic mice in

which a gonadotrophin-releasing hormone promoter was used to drive iCre, there was significant Cre mediated recombination.

The strategy used in the generation of the two targeting vectors was dependent on the insertion of the Cre ATG into that of $Na_V1.8$. Another strategy that could have been employed was to use a viral internal ribosomal entry site (IRES) sequence that mediates cap-independent entry of the ribosome. mRNAs in eukaryotic cells are translated after the ribosomes associate with the 5' cap structure, whereas viruses produce uncapped mRNAs whose translation is dependent on IRES sequences in their 5' UTRs. In 1988 Pelletier and Sonenberg (Pelletier and Sonenberg, 1988) demonstrated that mRNAs for a selectable marker and reporter gene separated by an IRES expressed both proteins efficiently. Since then IRESs have been widely used to place genes under the control of an endogenous locus without disturbing its function. The exogenous gene is cloned downstream to the IRES and the whole complex is targeted to the 3' UTR of the endogenous locus. When an IRES followed by a selection marker is placed within the endogenous gene sequence, a loss-of function mutation is produced. IRESs are mostly employed when the function of the target gene is to be retained. Their major disadvantage is that the level of translation of the exogenous gene is often compromised. This strategy was not employed in this project to maximise the amount of Cre protein produced.

The use of a FLRTed positive selection marker in the vector design in this project ensures that the potential negative effect of the promoter driving the neomycin phosphotransferase is avoided.

In summary, the exclusive expression pattern of $Na_V1.8$ has been exploited and two targeting vectors designed in which Cre is knocked-in to the translational start of $Na_V1.8$. Germ line expressing F1 chimeric mice have been produced for one of the vectors, $Na_V1.8$Cre2.

Chapter 3

The $Na_V1.8Cre2$ mouse: characterisation and analysis of Cre expression

3.1. Introduction

This chapter describes the characterisation and analysis of the onset and pattern of Cre expression in $Na_V1.8$Cre2 mice. A detailed examination of the expression pattern within DRGs was performed. In the introduction I will describe the use of reporter mice to detect Cre activity, the morphological classification of DRG neurons that was exploited to examine the pattern of expression in this tissue and the reported expression pattern of the target gene, $Na_V1.8$.

3.1.1. ROSA26 Reporter mice

Careful evaluation of the pattern of Cre expression is vital before using it to delete floxed genes. This can be done *in vivo* using reporter mice in which a ubiquitously active promoter drives the expression of a reporter gene that is preceded by a floxed polyadenylation sequence. Cre-mediated excision of the polyadenylation sequence allows expression of the reporter. One of the most widely used reporter strains - R26R - was engineered by Soriano (Soriano, 1999). He exploited the ROSAβgeo26 mouse line, in which retroviral sequences and a β-galactosidase-neomycin resistance fusion gene (βgeo) were randomly integrated into the genome to produce a promoter trap. The resulting animals showed ubiquitous expression of β-galactosidase detectable at E7 (Friedrich and Soriano, 1991). Zambrowicz *et al.,* went on to define the locus of integration of the construct (Zambrowicz et al., 1997), and Soriano then used gene targeting to insert a floxed neomycin cassette and triple polyadenylation signal, followed by a *lacZ* gene and a polyadenylation signal, ~250bp upstream of the original gene-trap integration site of the ROSA26 locus (Soriano, 1999) (see Figure 3.1). Cre mediated excision of the neomycin cassette and triple polyadenylation signal results in transcription of *lacZ.*

The E.coli *lacZ* gene encoding β-galactosidase is a classical histochemical reporter gene. β-galactosidase can be detected using a variety of substrates, the most

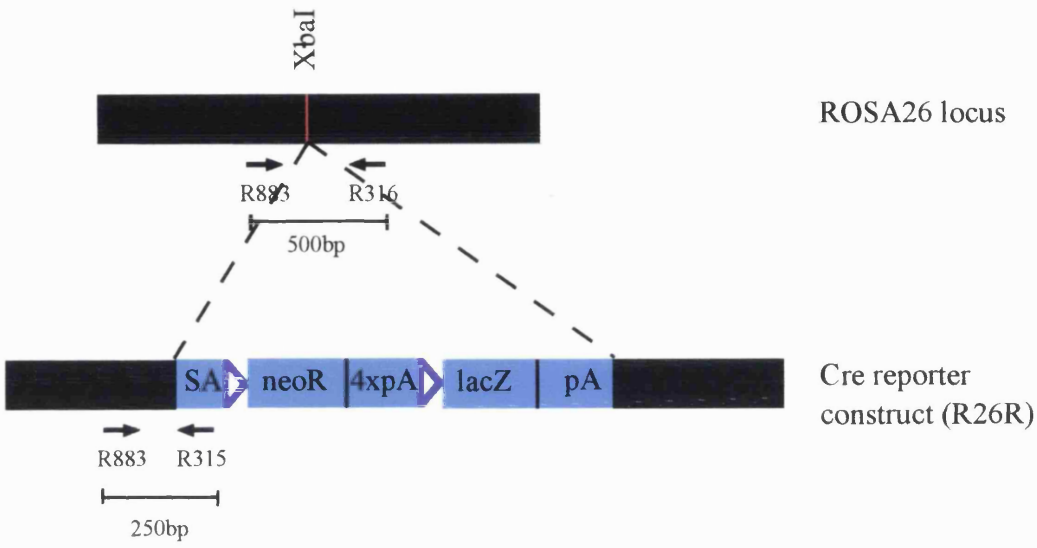

Figure 3.1: Diagram of the ROSA26 locus (Soriano 1999).
The site of insertion of Cre reporter construct, and location of PCR primers used are shown.
SA= splice acceptor site, neoR=PGK neomycin cassette,
pA= polyadenylation signal. Purple triangles indicate *loxP* sites.

commonly used of which is 5-bromo-4-chloro-3-indolyl-β-D-galactoside, known as X-gal (Holt and Sadler, 1958). β-galactosidase cleaves X-gal to produce a soluble colourless indoxyl monomer that, after dimerisation, is oxidised into a stable insoluble blue compound easily detected under light microscopy. Alternatively, antibodies directed against β-galactosidase can be used to detect the protein.

3.1.2. Morphological classification of DRG neurons

DRGs contain the cell bodies of afferent sensory neurons. These were originally classified into two groups by the morphological appearance of their soma – large light cells (due to an abundance of neurofilaments) and small dark cells (due to an abundance of ribosomes). Lawson and Waddell then showed that the large light cells included all myelinated Aδ and Aαβ neurons, and that they could be labelled by an antibody directed against the 200kb neurofilament protein, RT97 (Lawson and Waddell, 1991). They showed that RT97-positive neurons comprised ~40% of lumbar DRG neurons.

Neurofilaments are members of the intermediate filament (IF) family of cytoskeletal proteins, found in most eukaryotic cell types (Steinert and Roop, 1988; Strelkov et al., 2003). IF proteins constitute a large heterogeneous group of proteins that have been subdivided into 5 groups, I-V, depending on their localisation. They have a central α-helical rod that is remarkably conserved between the subgroups. The individual proteins form a two chain coiled-coil molecule that polymerises, and these in turn assemble into 10nm intermediate filaments.

Neurofilaments comprise group IV of the IFs and consist of three protein subunits, NF-H (200kDa) (also known as NF200), NF-M (145kDa), and NF-L (65kDa). Shaw *et al.,* (Shaw et al., 1986) showed that several antibodies directed against NF-H react only to the phosphorylated form of the protein. They generated an anti-NF-H monoclonal antibody, N52, which was insensitive to the phosphorylation state.

Another IF, peripherin, was first described in 1982 (Greene, 1989) as a 52kDa protein present in cultured neuronal cells. Peripherin was then classified as a group III IF that appears at E9 *in utero*, and is present throughout the peripheral nervous

system in motor, sensory, autonomic and enteric neurons, as well as in the central nervous system (ventral horn motor neurons, cranial nerve nuclei, olfactory epithelium, retinal ganglion cells and brain stem nuclei) (Troy et al., 1990). Ferri *et al.,* (Ferri et al., 1990) examined the differential distribution of NF-positive and peripherin-positive neurons in the lumbar DRGs of rats, and showed that they defined two distinct populations of neurons. Peripherin positive neurons comprised 66% of the neurons that had a mean diameter of 23.6μm, whereas the NF-positive neurons comprised 26% of the neurons with a mean diameter of 39.5μm. In addition, 8% neurons that were intermediate in diameter (mean=31.2μm) were immunopositive for both proteins. Antibodies directed against peripherin are now widely used to identify unmyelinated DRG neurons. Therefore, using a combination of antibodies directed against neurofilament and peripherin, DRG neurons can be classified into myelinated and unmyelinated neurons.

As outlined in chapter 1, the plant lectin IB_4 that binds to α-D-galactose residues present in the carbohydrate chains of membrane-associated glycoconjugates, defines a non-peptidergic subpopulation of nociceptors that express the GDNF receptor complex, c-ret, and the purinergic receptor $P2X_3$. These nociceptors do not express TrkA.

3.1.3. Expression pattern of $Na_V1.8$

In the original descriptions of $Na_V1.8$ in rats, Akopian *et al.,* and Sangameswaran *et al.,* (Akopian et al., 1996; Sangameswaran et al., 1996) confirmed that the channel was confined to sensory neurons. Akopian *et al.,* using PCR and Northern Blot analysis, found the transcript in DRGs and trigeminal ganglia. Within the DRG and trigeminal ganglion, there was little overlap between immunostaining for NF200, and *in situ* hybridisation signal for the $Na_V1.8$ transcript. Sangameswaran *et al.,* found that the transcript was present in DRGs, nodose ganglia and in low levels in the sciatic nerve. Within the DRG, $Na_V1.8$ mRNA was found in 76% of small diameter cells and 33% of large diameter cells.

Since then, several other groups have examined the expression pattern of $Na_V1.8$ in DRGs. Amaya *et al.,* (Amaya et al., 2000) found, using an antibody directed against the C-terminus of rat $Na_V1.8$, that the channel protein was expressed in 49.8% of peripherin positive DRG neurons and 9.5% NF200 positive neurons in rats. Positive $Na_V1.8$ immunostaining was also seen in the superficial layers of the dorsal horn at the central terminals of primary sensory afferent neurons. In another study, the same group found positive $Na_V1.8$ immunostaining in 49% of rat L4 DRG neurons (Decosterd et al., 2002).

Novakovic *et al.,* (Novakovic et al., 1998) showed, using *in situ* hybridisation, that $Na_V1.8$ mRNA was present in 77% of small and medium cells and 44% of large cells. Using immunohistochemistry, positive staining was seen in 78% of all small and medium cells, but not in large cells.

Since myelinated, NF200-positive neurons and unmyelinated, peripherin-positive neurons comprise approximately 26-30% and 66-70% of DRG neurons respectively (Ferri et al., 1990), one can calculate from some of these data an estimate of the percentage of the total DRG neurons that expressed $Na_V1.8$. Thus, the data presented by Sagameswararan *et al.,* Amaya *et al.,* and Novakovic *et al.,* suggests that approximately 63% (53% unmyelinated and 10% myelinated neurons), 37% (35% unmyelinated and 2% myelinated neurons) and 67% (54% unmyelinated and 13% myelinated neurons) of DRG neurons respectively were positive for $Na_V1.8$.

As outlined in Chapter 2 (see Section 2.1.3.4), Djouhri *et al.,* have conducted a detailed analysis of $Na_V1.8$ in rat lumbar DRG neurons (Djouhri et al., 2003a) and correlated it with neuronal function in 104 neurons. Using a polyclonal antibody directed against residues 1892 to 1956 of $Na_V1.8$, they found that 83% of C, 93% of Aδ, and 25% of Aαβ neurons showed positive immunoreactivity for $Na_V1.8$.

Recently $Na_V1.8$ transcript and protein has been detected in cerebellar Purkinje cells both in a mouse model of multiple sclerosis (chronic relapsing experimental allergic encephalomyelitis), and in post mortem tissue of patients with multiple sclerosis (Black et al., 2000). In addition, abnormal expression of $Na_V1.8$ has been detected in Purkinje cells of the *taiep* rat, in which there is degeneration of oligodendrocytes after myelin has formed (Black et al., 1999b). Transfection of $Na_V1.8$ into mouse

Purkinje cells results in functional channel expression and an alteration of firing patterns in these cells (Renganathan et al., 2003). These findings suggest that in demyelinating conditions expression of $Na_V1.8$ can occur.

3.2. Methods

3.2.1. Animal Breeding

Animals were bred in the University College London animal house facility and conditions complied with United Kingdom Home Office guidelines. They were housed in filter cages, with a 12hour light/dark cycle and were fed standard chow and water *ad libitum*.

3.2.2. Isolation of genomic DNA from tail samples

After weaning, animals were identified using coat colour and earmarking, and approximately 1cm of tail was removed and placed in a 1.5ml eppendorf tube. 500µl tail lysis buffer (100mM Tris-HCl pH8.5, 5mM EDTA, 0.2% SDS, 200mM NaCl) containing 100µg/ml Proteinase K (Roche) was added to each sample and they were incubated at 55°C overnight. Samples were vortexed vigorously and centrifuged at 15 000g for 10mins. The aqueous supernatant was transferred to a clean eppendorf tube and 500µl isopropanol added. The tubes were inverted until a white cloudy DNA precipitate was seen, and then were centrifuged at 15 000g for 2mins to pellet the DNA. The supernatant was removed and the pellet washed twice with 70% ethanol and dried before resuspending in 200µl TE.

3.2.3. Polymerase chain reaction

Polymerase chain reaction (PCR) was used for genotyping transgenic animals. Reactions were prepared in sterile 0.5ml eppendorf tubes using sterile pipette tips. 0.5-1ng of template DNA, 0.4µM of each primer, 0.2mM dNTP (Sigma), 2-2.5mM $MgCl_2$ (Promega), 1x Mg^{2+} free Taq buffer (Promega) and 0.3u Taq DNA polymerase were used in a 25µl reaction volume. Touch down PCR was used for primers pairs marked with an asterisk. Touch down PCR conditions used were: initial denaturing: 94°C x 2mins, cycling denaturating: 94°C x 30secs, cycling annealing: 65°C x 15secs, cycling extension: 72°C x 1min; these cycling conditions

were repeated 10 times reducing the annealing temperature by 0.5°C on each cycle. This was followed by 30 cycles of denaturating: 94°C x 30secs, annealing: 55 or 60°C x 15secs, extension: 72°C x 1min. For all other primer pairs, the following conditions were used - initial denaturing: 94°C x 2mins, cycling denaturing: 94°C x 30secs, cycling annealing: 55°C x 30secs, cycling extension: 72°C x 1min; the cycling conditions were repeated 34 times. Reactions were carried out in a PCT-220 DNA Dyad (MJ research) machine and resolved on a 1.2% agarose (Invitrogen) gel. The sequences of the primers used are as follows:

*mSNS seq13s (24bps starting 151bps upstream of the start of exon 1):

5'- TGTAGATGGACTGCAGAGGATGGA – 3'.

*Cre seq5a (bps 251-275 of the Cre coding sequence):

5' – AAATGTTGCTGGATAGTTTTTACTGCC – 3'.

*smstop seq1s (bps 20-43 of the stop sequence):

5' – TCATGCATAATAAAATATCTTTATTTTCAT – 3'.

*mSNS seq12a (bps 284-307 of $Na_V1.8$ exon 1):

5' – TTACCCGGTGTGTGCTGTAGAAAG – 3'.

*neo seq1a: (bps 296-320 of the neomycin sequence):

5' – GCGTCACCTTAATATGCGAAGTGG – 3'.

R315 (located in the splice acceptor sequence of the reporter (Soriano, 1999)):

5' – GCGAAGAGTTTGTCCTCAACC – 3'.

R316 (located 124bp downstream of the provirus integration site (Soriano, 1999)):

5' – GGAGCGGGAGAAATGGATATG – 3'.

R883 (located ~400bps upstream of the provirus integration site (Soriano, 1999)):

5' - AAAGTCGCTCTGAGTTGTTAT – 3'.

3.2.4. Southern Blotting

The protocol outlined in chapter 2 was used.

3.2.5. Extraction of tissues for X-gal staining

Adult animals were stunned with CO_2 and then terminally anaesthetised using intraperitoneal sodium pentobarbitone (Rhône Mérieux) – 150mg/kg. Once anaesthetised the thoracic cavity was opened, the right atrium nicked, and the animal perfused, via the left ventricle, with 20mls of ice cold phosphate buffered saline (PBS) (0.14M NaCl, 2.7mM KCl, 10mM Na_2HPO_4, 1.7mMKH_2PO_4) followed by 20mls of ice cold 4% paraformaldehyde (BDH) in PBS.

3.2.5.1. Dorsal root ganglia

The skin covering the dorsal surface of the spinal column was divided and the spinal column removed. Using a dissecting microscope (Leica), a saggital incision was made through the vertebral bodies and spinal cord, along the whole length of the spinal column. The two halves were then separated. To extract the DRGs, the spinal cord was displaced to expose the vertebral foramina and each DRG removed using size 5 forceps. They were placed in PBS and then fixed for 10mins in ice cold 4% paraformaldehyde in PBS for 10mins.

3.2.5.2. Brain, liver, kidney, heart, adrenal gland, thymus and lung

These organs were removed from their surrounding tissue, rinsed in PBS, and fixed in ice cold 4% paraformaldehyde in PBS for 20-60mins.

3.2.5.3. Olfactory epithelium

The skin covering the dorsal aspect of the face was removed. Under a dissecting microscope, a saggital incision was made through the nasal bones. These were gently lifted to expose the olfactory mucosa, which was then eased away from the turbinates and nasal septum by blunt dissection, and removed. The mucosa was rinsed in PBS and fixed for 10mins in ice cold 4% paraformaldehyde in PBS.

3.2.5.4. Myenteric plexus

The myenteric plexus lies between the longitudinal and circular muscle layer of the gastrointestinal tract. To obtain a laminar preparation of intestine, the whole gastrointestinal tract was removed from the abdominal cavity and placed in PBS.

The gut was freed from its mesentery, the small intestine located, and 1cm lengths, proximal to the terminal ileum, were cut. The lumen of each length was cleaned with PBS and a 100µl pipette tip passed through it until the wall was stretched around the pipette tip. Using a size 11 blade, the intestinal wall was lightly scored in a longitudinal direction, close to the mesenteric attachment, cutting through the longitudinal and circular muscle layers to the connective tissue outside the submucosa. A cotton wool bud was then used to tease the outer layers away from the submucosa around the circumference of the gut length. The laminar preparation of the outer part of the intestinal wall was then rinsed in PBS, laid out flat and fixed for 10mins in ice cold 4% paraformaldehyde in PBS.

3.2.5.5. Superior cervical ganglia

The superior cervical ganglia (SCGs) are located posterior to the carotid bifurcation. The carotid bundle was exposed on either side of the trachea. Using a dissecting microscope the bundle was ligated at its root for orientation, and blunt dissection used to expose the carotid bifurcation. A block of tissue including the common carotid artery and carotid bifurcation was removed and placed in a petri dish containing Sylgard (Sylgard 184 Elastomer Kit, BDH). The tissue was kept wet with PBS. The superior cervical ganglion was located and carefully dissected away from the surrounding tissues. It was rinsed in PBS and fixed for 10mins in ice cold 4% paraformaldehyde in PBS.

3.2.5.6. Trigeminal ganglia

Skin covering the dorsal aspect of the skull removed. The cranial bones were removed to expose the brain and the anterior end of the brain lifted to expose the cranial nerves. The optic nerves were divided and the trigeminal nerves divided at their site of entry into the brain. The brain was removed, and the trigeminal ganglia exposed in the grooves of the petrous temporal bone using careful dissection. The ganglia were carefully removed, rinsed in PBS, and fixed for 10mins in ice cold 4% paraformaldehyde in PBS.

3.2.5.7. Nodose ganglia:

The nodose ganglia are located at the root of the vagus nerve, just inferior to the jugular foramen. The carotid bundle was exposed on either side of the trachea. The vagus nerve was located and, under a dissecting microscope, its path followed to the brain stem using blunt dissection. The ganglion was located and excised. It was rinsed in PBS and then fixed in 4% paraformaldehyde in PBS for 10mins.

3.2.6. Sectioning of tissues for X-gal analysis

All tissues were stored in 30% sucrose (BDH) + 0.02% sodium azide (BDH) at 4°C until they were sectioned.

3.2.6.1. Brain

The brain was left in X-gal solution (5mM potassium ferricyanide, 5mM potassium ferrocyanide, 2mM $MgCl_2$, 0.5mg/ml X-gal in dimethyl formamide (BDH), 1x PBS) at 35°C overnight and 40μm sagittal sections taken using a freezing microtome. Sections were floated in PBS and mounted onto electrostatically charged slides (Superfrost Plus, BDH).

3.2.6.2. Other tissues

All other organs were sectioned using a Cryostat (Bright). Prior to sectioning, they were mounted in optimal cutting temperature (O.C.T.) compound (BDH), frozen on dry ice and stored at –70°C if necessary. O.C.T. blocks were left to equilibrate at –20°C in the cryostat for at least 1hr before sectioning. Sections were mounted on electrostatically charged slides (Superfrost Plus, BDH). After sectioning, slides were left to dry at room temperature for at least 30mins, and then stored at –20°C. For X-gal staining of DRGs and SCGs, serial 10μm sections were mounted on sequential slides, such that sections on an individual slide were separated by 80μm. 10-15μm sections of all other tissues were taken at approximately 30-50μm intervals.

3.2.7. X-gal staining

Slides were left to equilibrate at room temperature for at least 30mins. They were then washed in 1x PBS twice for 10mins each and then left in X-gal solution (5mM potassium ferricyanide, 5mM potassium ferrocyanide, 2mM $MgCl_2$, 0.5mg/ml X-gal in dimethyl formamide (BDH), 1x PBS) for 2hours at 35°C. They were washed three times in 1x PBS for 10mins each.

3.2.8. Neutral red counterstaining

Slides were left in 0.5% Neutral red (plus 1ml glacial acetic acid) for 2mins. They were rinsed in distilled water for 10secs, and dehydrated sequentially in 70% ethanol (10secs), 95% ethanol (10secs), and twice in 100% ethanol (10secs and 2mins). They were cleared using Histo-Clear (National Diagnostics) for 2mins and mounted with DPX mountant (BDH).

3.2.8. Analysis of percentage X-gal staining in DRGs

Five lumbar DRGs were taken from two adult animals, sectioned serially and mounted as outlined above, and stained with X-gal. They were counterstained with neutral red. A single slide, for each DRG was then used for analysis. For each section on the slide, the number of cells stained with X-gal, and the number of negative cells were counted. This was repeated three times and the mean for each value calculated. The sum of positive and negative cells for each DRG was then calculated, and the positive cells expressed as a percentage of the total number of cells.

3.2.9. Extraction and sectioning of DRGs for immunocytochemical analysis

Two methods were used to extract DRGs for immunocytochemical analysis. This was because perfusion with 4% paraformaldehyde interfered with the binding of the anti-peripherin and anti-$Na_V1.8$ primary antibodies. When these antibodies were

used, fresh DRGs were excised from animals that were terminated with CO_2. They were rinsed in PBS and mounted in O.C.T. for sectioning. The slides were left in 4% paraformaldehyde for 5mins, and then washed three times in1x PBS for 10mins each.

When other antibodies were used, DRGs were excised from perfused animals, using the method outlined above (Section 3.2.5.). Serial 10μm sections were mounted on sequential slides.

3.2.10 Immunocytochemistry

Slides were washed twice in 1x PBS + 0.3% Triton-X (Triton) (BDH) for 10mins each. The slides were placed in an immunohistochemistry tray and 600μl 10% goat serum (GibcoBRL) in 1x PBS + 0.3% Triton applied to each. The slides were left at room temperature for 3hrs. The primary antibody was diluted in 10% goat serum, applied to the slide in a volume of 600μl overnight at 4°C. Slides were then washed three times 10mins in 1x PBS + 0.3% Triton. The secondary antibody was diluted in 10% goat serum, applied to the slide in a volume of 600μl, and left in the dark at room temperature for 3hrs. The slides were then washed twice in 1x PBS + 0.3% Triton for 30mins and then placed for a third wash of 1x PBS + 0.1% 0.3% Triton overnight at 4°C. Two drops of Aqueous Mounting solution (Sigma) were applied to one end of the slide and a coverslip applied (BDH).

The following primary antibodies were used:

- Anti $Na_v1.8$ polyclonal antibody SNS11 (Djouhri et al., 2003a), at a dilution of 1:500
- Monoclonal anti-neurofilament-H antibody, N52 (Sigma), at a dilution of 1:1000
- Monoclonal anti-peripherin antibody (Chemicon), at a dilution of 1:1000.
- Polyclonal anti-β-galactosidase antibody (5 prime to 3 prime), at a dilution of 1:400.

The following secondary antibodies were used:

- Anti-mouse (goat) $(Fab)_2$ FITC (Jackson) at a dilution of 1:1000.

- Alexa Fluor 594 goat anti-rabbit IgG (Molecular Laboratories) at a dilution of 1:1000.

IB_4 conjugated to Alex Fluor 488 (Molecular Laboratories) was also used (in 70mMNaCl, 1mM $CaCl_2$, 0.5mM $MgCl_2$, 5mM HEPES, pH7.4) at a dilution of 1:100. It was applied with the secondary antibody, i.e. at room temperature for 3hrs.

3.2.11. Preparation of embryos for analysis

When analysis of embryos was planned, timed matings were set up in the evening and the female checked each morning for evidence of plugging. The day of plugging was taken as day E0. On the desired day, the pregnant female was killed using CO_2 and cervical dislocation. The string of embryos was removed from the abdominal cavity and placed immediately into PBS. Individual embryos were then separated and removed from their amniotic sacs using blunt dissection. They were washed in PBS containing 1:40 dilution of sodium pentobarbitone (Rhône Mérieux) at room temperature for 5mins and then three times in PBS. E14 and E15 embryos were skinned to enable better penetration of staining fluids. Tail biopsies were taken for genotyping.

The embryos were fixed in cold *lacZ* fix (1% formaldehyde, 2mM MgCl, 0.2% glutaraldehyde, 5mM EGTA, 0.02% triton in PBS) at room temperature – 40mins for E12, 1hour for E13, 1.5hours for E14 and 2hours for E15 and E17. They were then washed three times in *lacZ* wash (1mM EGTA, 2mM MgCl, 0.02% Triton in PBS) at room temperature for 30mins each, and incubated overnight in *lacZ* staining solution (5mM potassium ferrocyanide, 5mM potassium ferrincyanide, 2mM MgCl, 0.01% sodium deoxycholate 0.02% Triton, X-gal 1mg/ml in PBS) at room temperature in the dark. The following day the embryos were washed three times in PBS at room temperature, in darkness.

To clear, embryos were left in darkness at 4°C for 24hours in each of the following solutions; 70% ethanol, 100% methanol, fresh 100% methanol, and benzyl benzoate:benzyl alcohol (ratio of 2:1).

3.3. Results

3.3.1. Animal Breeding Strategy

Heterozygous F1 $Na_V1.8$Cre2-neoR animals (i.e. those containing the neoR cassette) were initially crossed to heterozygous FLP deletor (FLPeR) animals (Farley et al., 2000) to produce animals in which the neomycin positive selection marker was excised (referred to hereafter as $Na_V1.8$Cre2). These FLPeR animals were bred on a C57Bl/6 background.

For characterisation of the expression pattern of β-galactosidase, homozygous F1 $Na_V1.8$Cre2-neoR (i.e. those containing the neoR cassette) and homozygous F2 $Na_V1.8$Cre2 animals (i.e. those without the neoR cassette) were crossed to ROSA26 reporter (R26R)-/- animals.

For behavioural analysis, $Na_V1.8$Cre2 animals were backcrossed to C57Bl/6 animals to generate heterozygous F3 or F4 animals.

Homozygous F3 $Na_V1.8$Cre2, heterozygous F3 $Na_V1.8$Cre2 and wild type littermates were used for electrophysiological analysis.

3.3.2. Confirmation of knock-in of $Na_V1.8$Cre2 in vivo

Southern blotting was used to confirm correct knock-in of $Na_V1.8$Cre2-neoR, and excision of the positive selection marker *in vivo,* in $Na_V1.8$Cre2 mice. DNA from wild type, heterozygous $Na_V1.8$Cre2-neoR and heterozygous $Na_V1.8$Cre2 animals was digested with BamHI. The 0.5kb external 3' probe, the 0.9kb internal Cre and the 0.8kb internal neoR probes described in Chapter 2 (Section 2.3.4.) were used. Figure 2.12, A and C show the localisation of BamHI restriction enzyme sites in wild type and $Na_V1.8$Cre2-neoR alleles respectively.

1. External 3' probe: In wild type alleles this probe was expected to hybridise to a 6.5kb fragment flanked by the BamHI sites in exon 1 and in intron 3. In alleles targeted with $Na_V1.8$Cre2-neoR, a 8.5kb fragment was expected, flanked by the BamHI site between the 3' UTR and neomycin cassette and the site in intron 3. Excision of the neomycin cassette, seen in $Na_V1.8$Cre2 alleles, was expected to

reduce this fragment by 1.3kb resulting in a 7.2kb fragment – see Figure 3.2. These data shows that the targeting vector had been correctly inserted into the genome and that the neomycin cassette had been correctly excised in $Na_V1.8$Cre2 animals.

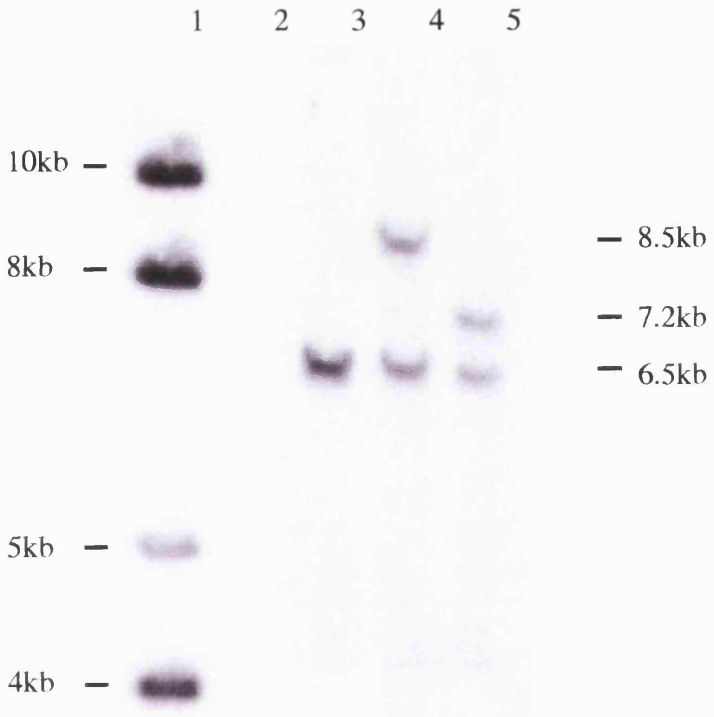

Figure 3.2: Southern blot of genomic DNA hybridised to the 3' probe.
DNA from wild type (lane 3), $Na_V1.8$Cre2-neoR +/- (lane 4) and $Na_V1.8$Cre2+/- (lane 5) animals are loaded. Lane 1 contains DNA size marker. See text for details.

2. Internal Cre probe: In both $Na_V1.8$Cre2-neoR and $Na_V1.8$Cre2 targeted alleles, this probe was expected to hybridise to two BamHI fragments, 1.1kb and 8.8kb in size, flanked by the sites in the 5' UTR, in the Cre cassette and between the 3' UTR and neomycin cassette. No hybridisation was expected in wild type alleles. Figure 3.3 confirms these results and that there were no randomly integrated copies of the targeting vector.

3. Internal neomycin probe: In $Na_V1.8$Cre2-neoR targeted alleles only, this probe was expected by hybridise to a single 8.5kb fragment flanked by the BamHI site between the 3' UTR and the neomycin cassette and the site in intron 3. Since in $Na_V1.8$Cre2 targeted alleles, the neomycin cassette has been excised, no hybridisation is expected. Figure 3.4 confirms this.

3.3.3. Genotyping

After confirmation of the genotype by Southern blotting, PCR was used to genotype all animals at 3-4 weeks of age. Figure 3.5 shows the location of the primers used to analyse modification of the $Na_v1.8$ locus. Primers outlined by Soriano (1999) were used to monitor inheritance of the R26R gene - their positions are shown in Figure 3.1. Figure 3.6 shows examples of PCR data using these primers.

mSNSseq13s and *mSNSseq12a*: This pair was used to detect the wild type $Na_v1.8$ allele and resulted in a 460bp product in wild type animals (seen in Figure 3.6A, lane 4). After knock-in of $Na_V1.8$Cre2-neoR, these primers would be 3.4kb apart, and after Flpe-mediated deletion of the neomycin cassette, 2.1kb apart so would not result in PCR products.

mSNS seq13s and *Cre seq5a*: This pair was used to detect knock-in of the Cre gene into the translational start of $Na_V1.8$, producing a 420bp product in both $Na_V1.8$Cre2-neoR and $Na_V1.8$Cre2 animals (seen in Figure 3.6A, lanes 5 and 6).

neo seq1a and *mSNS seq12a*: This pair was used to detect the presence of the neomycin cassette in $Na_V1.8$Cre2-neoR alleles, resulting in a 350bp product, which was absent in $Na_V1.8$Cre2 animals (seen in Figure 3.6A, lane 11).

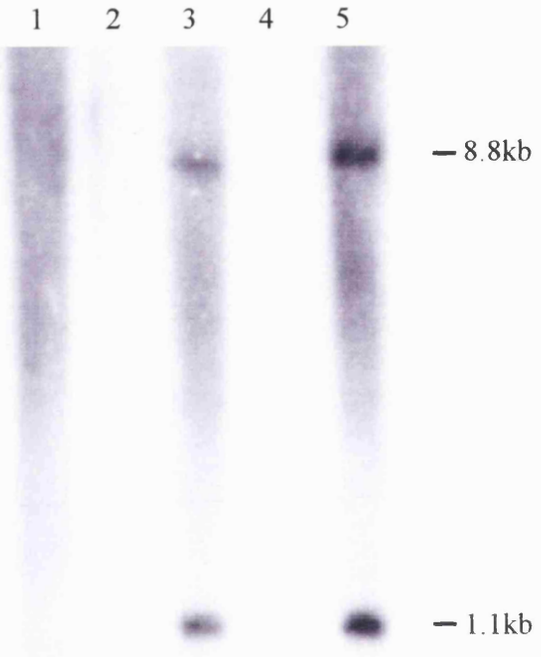

Figure 3.3: Southern blot of genomic DNA hybridised to the internal Cre probe. DNA from wild type (lane 1), $Na_V1.8$Cre2+/- (lane 3) and $Na_V1.8$Cre2-neoR+/- (lane 5) animals are loaded. See text for details.

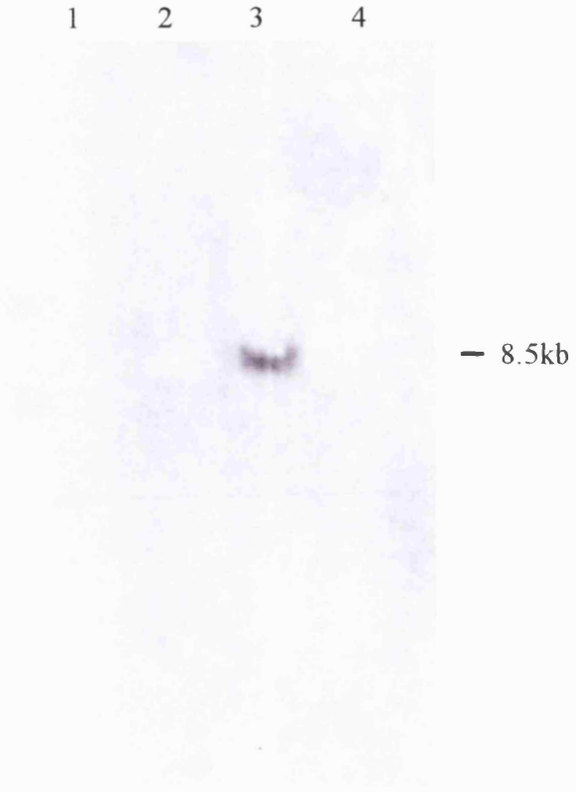

Figure 3.4: Southern blot of genomic DNA hybridised to the internal neoR probe. DNA from wild type (lane 2), +/-Na_V1.8Cre2-neoR (lane 3) and Na_V1.8Cre2 +/- (lane 4) animals are loaded. See text for details.

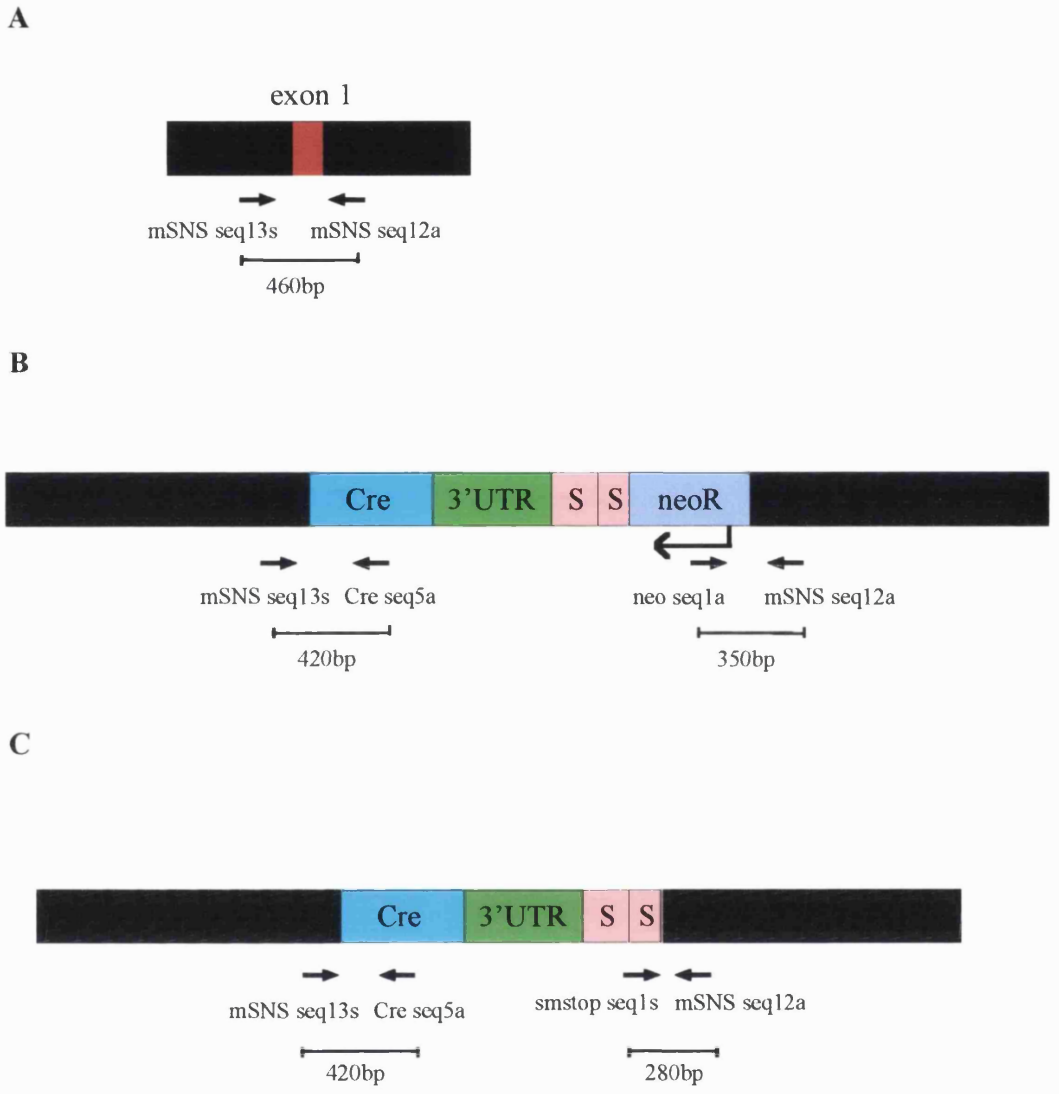

Figure 3.5: PCR scheme used to analyse modification of the $Na_V1.8$ locus.

Positions of the PCR primers and the expected product sizes are shown, **A:** when there is no modification of exon 1, **B:** after knock in of $Na_V1.8$Cre2-neoR, and **C:** after deletion of the neomycin cassette ($Na_V1.8$Cre2).

Diagram not to scale.

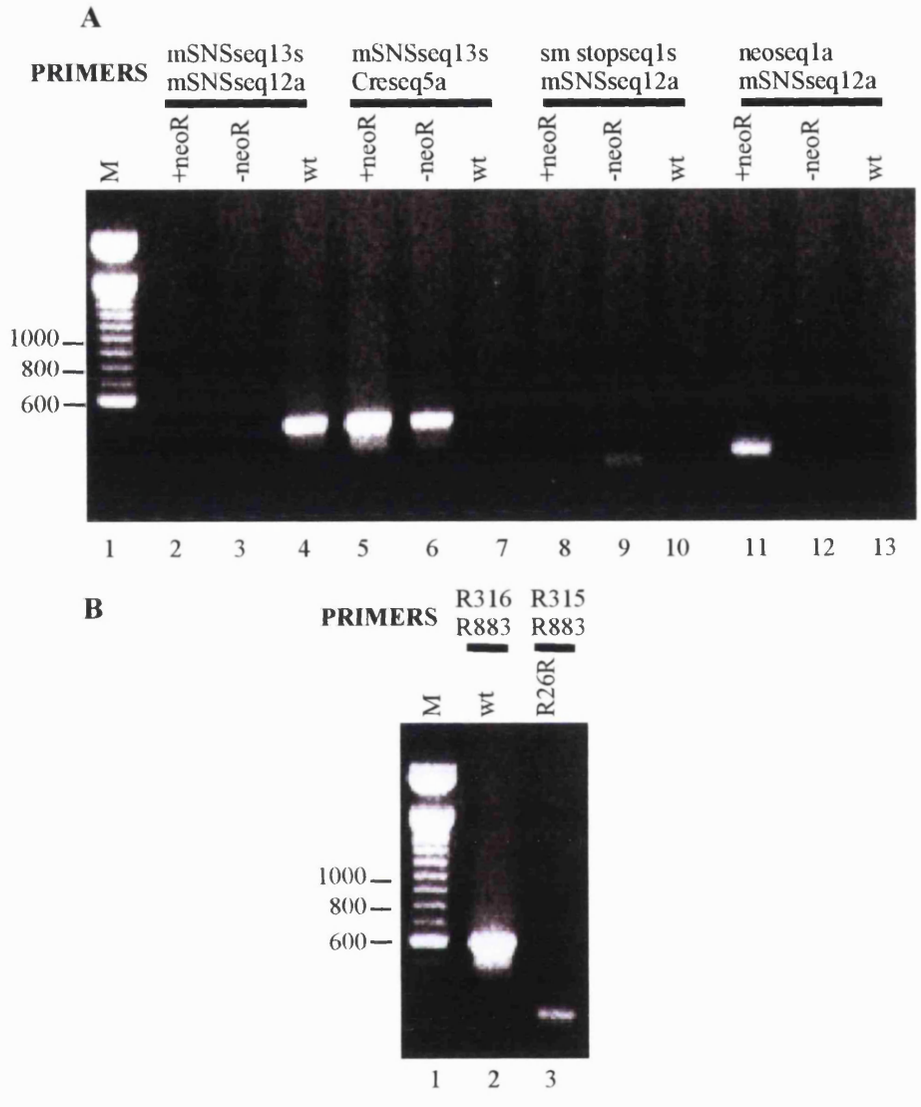

Figure 3.6: PCR used for genotyping
A: PCR used to detect modification of the Na$_V$1.8 locus.

Genomic DNA from homozygous Na$_V$1.8Cre2-neoR (+neoR), homozygous Na$_V$1.8Cre2 (-neoR) and wild type (wt) mice was used as template in this example.
Lane 1: 100bp marker (Invitrogen) (band sizes in bp). Lanes 2-4: A 460 bp band generated using mSNS seq13s and mSNS seq12a, was seen in wild type mice (lane 4). Lanes 5-7: mSNS seq13s and Cre seq5a were used to detect Na$_V$1.8Cre2-neoR and Na$_V$1.8Cre2 alleles, and resulted in a 420 bp band (lanes 5 and 6). Lanes 8-10: Flpe mediated deletion of the neomycin cassette was detected using smstop seq1s and mSNS seq12a and resulted in a 280bp band (lane 9). Lanes 11-13: Before removal of the neoR, a 350bp band was seen using neo seq1a and mSNS seq12a (lane 11).

B: PCR used to detect modification of the ROSA26 locus.

Genomic DNA from Na$_V$1.8Cre2/R26R animals was used as template in this example.

Lane 1: 100bp marker (Invitrogen) (band sizes in bp). Lane 2: R316 and R883 were used to detect wild type alleles (wt) resulting in a 500bp band. Lane 3: R315 and R883 were used to detect the R26R allele resulting in a 250bp band.

smstop seq1s and *mSNS seq12a*: The 280bp product produced by this pair confirmed that the neomycin cassette had been deleted (seen in Figure 3.6A, lane 9) and was seen in Na$_V$1.8Cre2 animals only. In Na$_V$1.8Cre2-neoR alleles, the primers would be 1.4kb apart and so would not result in a PCR product.

R883 and *R316*: This pair resulted in a 500bp product when a wild type allele was present (Figure 3.6B, lane2).

R883 and *R315*: This pair resulted in a 250bp product when the reporter allele was present (Figure 3.6B, lane3).

3.3.4. Pattern of lacZ expression in adult Na$_V$1.8Cre, R26R F1 animals

Homozygous R26R reporter mice were crossed to both Na$_V$1.8Cre2-neoR and Na$_V$1.8Cre2 animals to examine the pattern of Cre-mediated β-galactosidase activity before and after removal of the neomycin cassette respectively. In animals in which both alleles (R26R and Na$_V$1.8Cre2-neoR or Na$_V$1.8Cre2) were present, Cre mediated excision of the STOP signal upstream of lacZ in the R26 locus resulted in transcription of this gene, and so production of β-galactosidase. Activity of this enzyme was detected using two methods:

- X-gal staining. The chromogenic substrate X-gal, is converted by β-galactosidase into an insoluble dense blue compound, 5,5'-dibromo-4,4'-dichloroindigo, easily visualised by light microscopy.
- Anti-β-galactosidase antibody.

Na$_V$1.8Cre2-neoR and Na$_V$1.8Cre2 mediated β–galactosidase activity was studied in the DRGs of F1 animals. Na$_V$1.8Cre2 mediated β–galactosidase activity was studied in F1 mice in all major organs using X-gal. R26R+/- animals were used as controls to determine background *lacZ* expression.

3.3.4.1. Dorsal root ganglia: Figures 3.7 and 3.8

Positive X-gal staining was found in almost all small, some medium and a few large diameter DRG neurons from Na$_V$1.8Cre2/R26R and Na$_V$1.8Cre2-neoR/R26R F1 animals. There was no positive staining in DRGs from control R26R+/- animals.

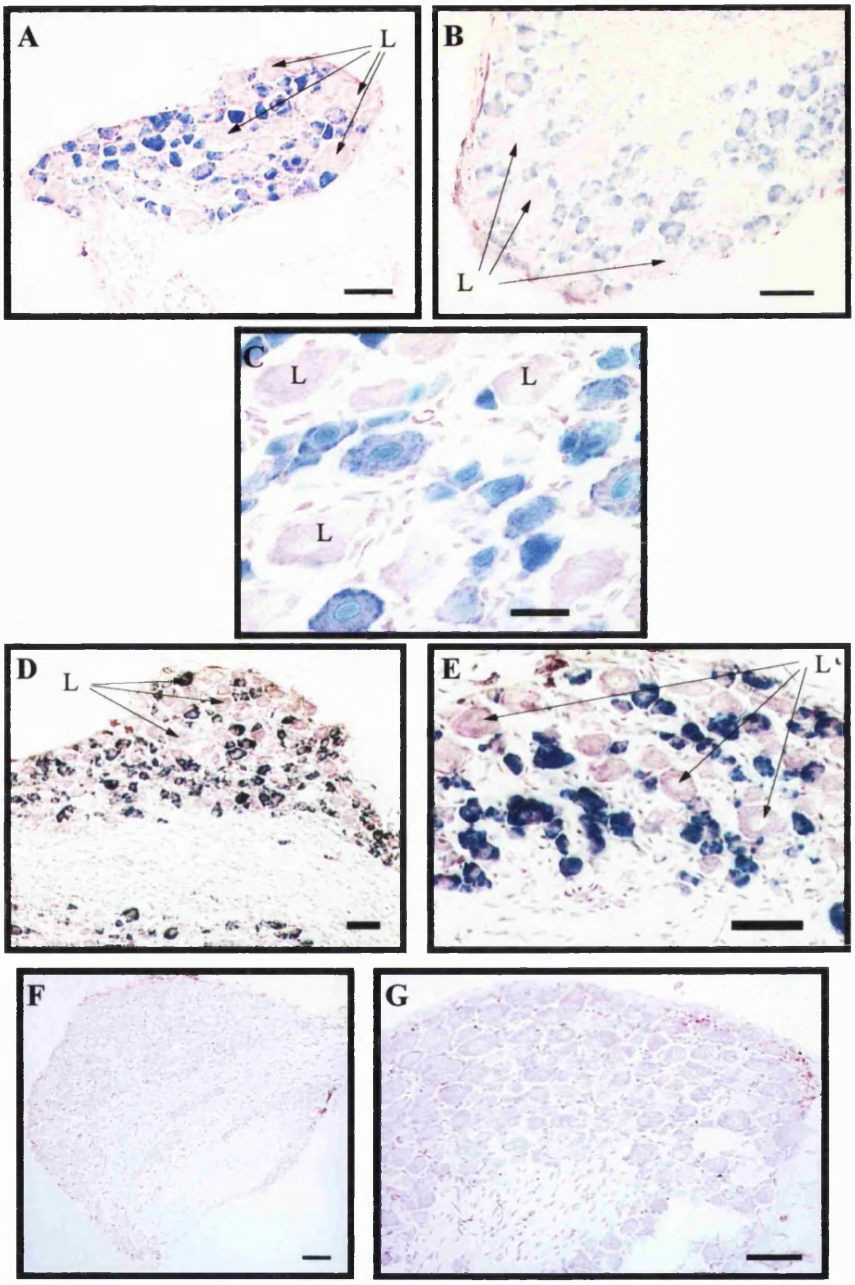

Figure 3.7: X-gal staining in DRGs from Nav1.8Cre2/R26R, Nav1.8Cre2-neoR/R26R and R26R+/- mice.
A: Section of a thoracic DRG from a Nav1.8Cre2/R26R animal. **B,C:** Sections of lumbar DRGs from a Nav1.8Cre2/R26R animal. **D, E:** Sections of lumbar DRGs from a Nav1.8Cre2-neoR/R26R animal. **F, G:** Sections of lumbar DRGs from a control R26R+/- animal. Sections were stained with X-gal and counterstained with neutral red. L indicates large diameter neurons.
Scale bar = 50μm

A

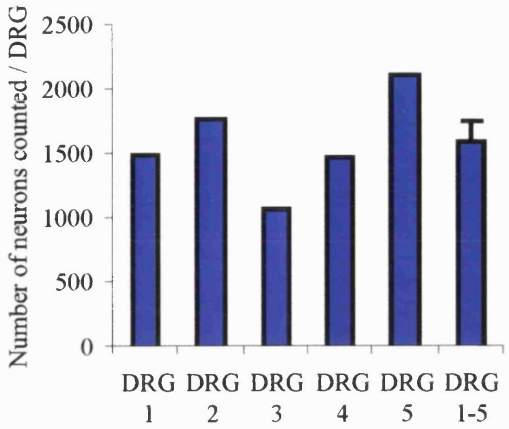

B

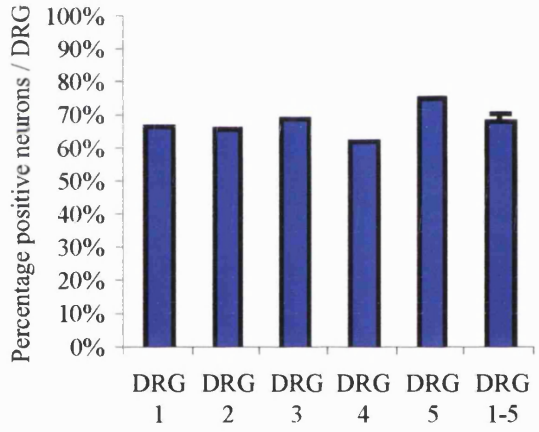

Figure 3.8: Analysis of X-gal staining in DRGs from Na$_V$1.8Cre2/R26R F1 mice.

A: Total number of DRG neurons analysed for Na$_V$1.8Cre2 mediated β-galactosidase activity in each DRG, and the mean for all DRGs (DRG1-5).

B: Percentage of DRG neurons showing Na$_V$1.8Cre2 mediated β-galactosidase activity in each DRG, and the mean for all DRGs (DRG1-5).

Positive staining was seen in almost all small, some medium and a few large diameter neurons. Since there was no difference in the staining between these two strains and since the positive selection marker can interfere with gene expression $Na_V1.8$Cre2-neoR/R26R F1 animals were not studied in further detail.

Detailed analysis of the staining of DRGs in $Na_V1.8$Cre2/R26R animals was performed. The percentage of DRG neurons with positive X-gal staining was assessed. Five lumbar DRGs taken from three animals were processed and the number of positive X-gal stained DRG neuronal cells on representative transverse sections, separated by 80μm, counted. Between 6 and 9 sections were analysed for each DRG. The total number of cells counted was 7960 - a mean of 1592±173 for each ganglion. Positive X-gal staining was found in 68.5±2.2% of neuronal cells. Figure 3.8 shows the results for individual DRGs and the mean for all five DRGs.

3.3.4.2. Trigeminal ganglia: Figure 3.9.

The pattern of positive X-gal staining seen in trigeminal ganglia from $Na_V1.8$Cre2/R26R animals was similar to that of the DRGs. Almost all small diameter and some medium and large diameter neurons were positive. There was no positive staining in trigeminal ganglia from R26R +/- animals.

3.3.4.3 Nodose ganglia: Figure 3.9.

A high percentage, approximately 75%, of neurons in the nodose ganglia from $Na_V1.8$Cre2/R26R F1 animals showed positive X-gal staining. Almost all positive neurons were small diameter. There was no staining in ganglia from control R26R+/- animals.

3.3.4.4. Superior cervical ganglia: Figure 3.9

Staining of SCGs from $Na_V1.8$Cre2/R26R F1 animals revealed a very small number of positive neurons. The ganglia from one animal were examined in detail. Both ganglia were sectioned serially and each section examined for positive staining. The total number of positive cells was counted for each ganglion, taking care not to count a cell that was seen in consecutive sections. 10 positive neurons were seen in

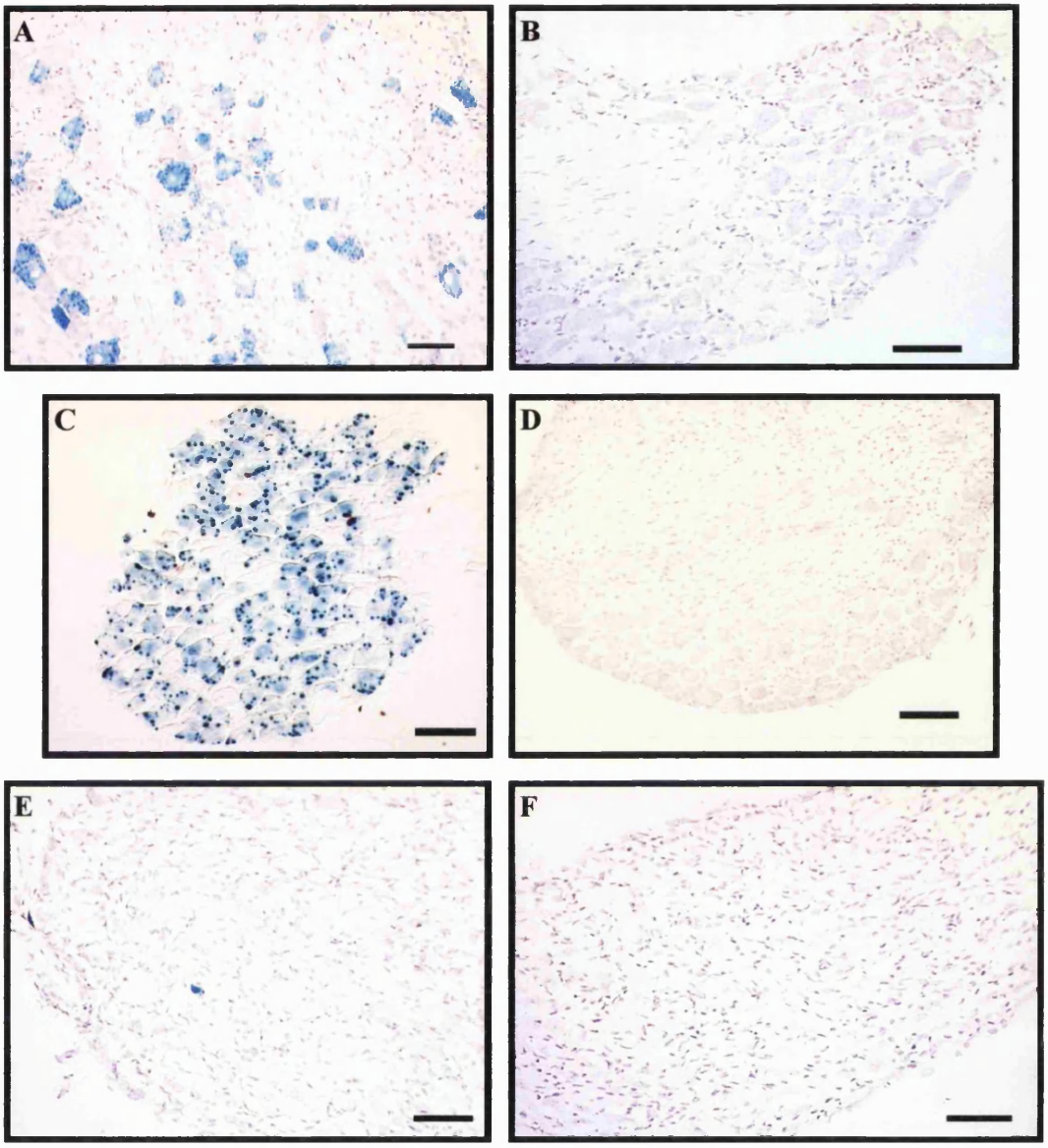

Figure 3.9: X-gal staining in the trigeminal, nodose and superior cervical ganglia from Na$_V$1.8Cre2/R26R mice.

A and **B:** trigeminal ganglion from Na$_V$1.8Cre2/R26R and R26R+/- animals respectively.

C and **D:** nodose ganglion from Na$_V$1.8Cre2/R26R and R26R+/- animals respectively.

E and **F:** SCGs from Na$_V$1.8Cre2/R26R and R26R+/- animals respectively .

Scale = 50μm.

one ganglion and 12 in the other. This represents approximately 0.2% each ganglion. There was no positive staining in SCGs from R26R +/- animals.

3.3.4.5. Negative tissues: Figures 3.10, 3.11 and 3.12

Detailed examination of the brain, including the cerebellum, and spinal cord from $Na_V1.8$Cre2/R26R F1 animals revealed no positive X-gal staining. The other major neuronal plexus, the myenteric plexus was examined, and revealed no staining. The heart, the site of the third TTX-resistant VGSC, $Na_V1.5$, was also negative. The olfactory epithelium, thymus, lung, liver, kidney, adrenal gland and skin were also negative.

3.3.5. Immunocytochemistry Figures 3.13-16

To examine the population of sensory neurons with β-galactosidase activity within the DRGs of $Na_V1.8$Cre2/R26R F1 animals, double labelling of DRG sections using an anti-β-galactosidase antibody in combination with cell type markers and an antibody directed against $Na_V1.8$ was performed.

DRG sections were double-labelled with anti-β-galactosidase and N52, an antibody directed against NF-200, a marker of myelinated neurons. As shown in Figure 3.13 the majority of β-galactosidase positive neurons were N52-negative. However a minority of neurons did co-express the two proteins, indicating that Cre is or has been active in some myelinated neurons.

In contrast, in sections double stained with anti-β-galactosidase and anti-peripherin antibodies, there was co-localisation between most of the peripherin-positive and β-galactosidase-positive neurons (Figure 3.14) indicating that Cre is or has been active in the majority of unmyelinated neurons. In addition β-galactosidase positive neurons that were peripherin-negative were also seen, representing myelinated neurons that express or have expressed Cre.

Double staining of sections with fluorescent labelled IB_4, used to identify the GDNF-dependent subgroup of nociceptors, and anti-β-galactosidase antibody revealed significant co-localisation of IB_4 and β-galactosidase-positive neurons (Figure 3.15). The IB_4 positive neurons represent approximately half of the

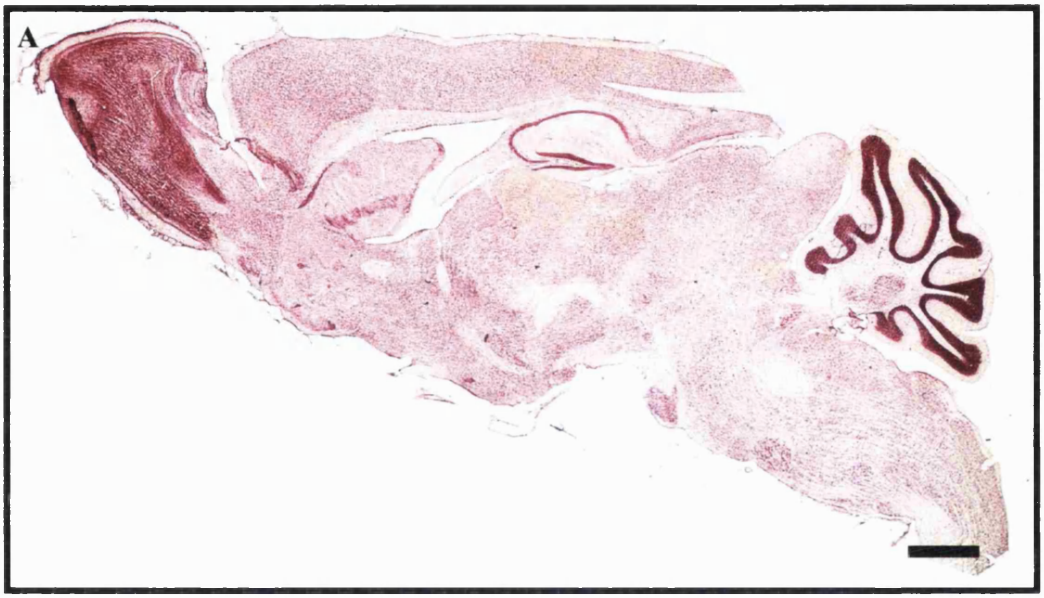

Figure 3.10: X-gal staining in the central nervous system of $Na_V1.8Cre2/R26R$ mice.
Parasaggital sections of
A: whole brain (scale=1mm)
B: cortex (scale=100μm)
C:hippocampus (scale=100μm) DG=dentate gyrus
D: thalamic region (scale= 300μm)
E: brain stem (scale=300μm) P=pons, M=medulla
F and **G:** cerebellum (scale=50μm) Mol=molecular layer, Gr=granular layer, Pkj=Purkinje cells
H: spinal corn (scale =100μm) DH=dorsal horn, VH=ventral horn.

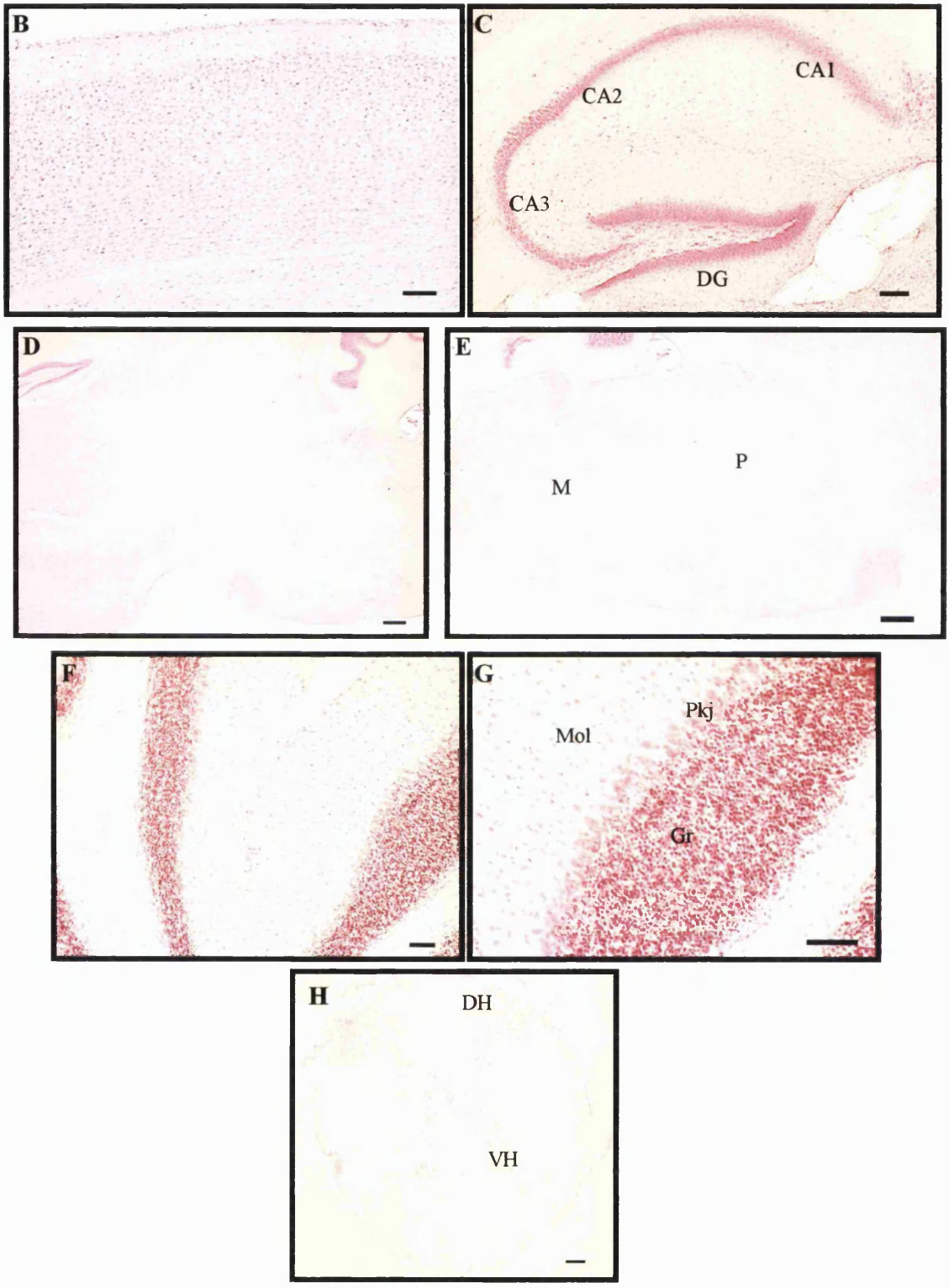

Figure 3.10 continued - see previous page for legend.

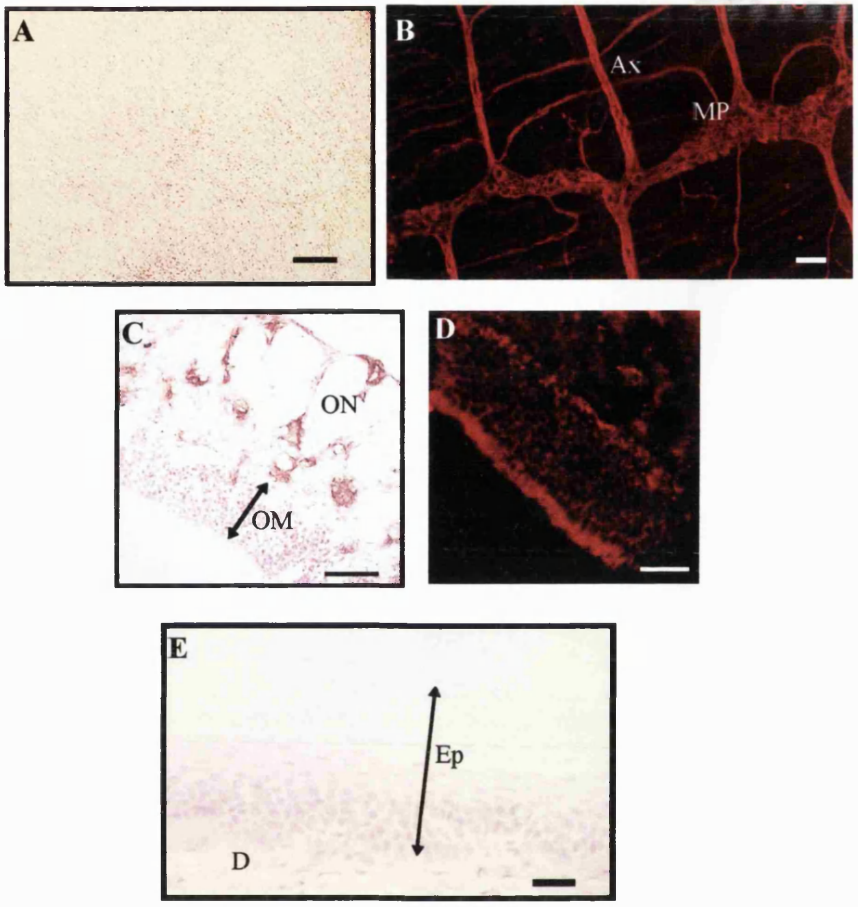

Figure 3.11: X-gal staining in the myenteric plexus, olfactory mucosa and skin from Nav1.8Cre2/R26R mice.

A-B: Laminar preparations of the muscle coat of the intestinal wall. **A:** This preparations was stained with X-gal and neutral red. The criss-cross pattern is due to the nuclei of the muscle cells of the longitudinal and circular muscle layers. **B:** The myenteric plexus, lying between the longitudinal and circular layers is visualised by staining with monoclonal anti-peripherin antibody and labelled with anti-mouse Rhodopsin red. Ax=axon, MP=Myenteric Plexus,
C-D: Transverse sections of olfactory mucosa. **C:** This section is stained with X-gal and neutral red. The olfactory epithelium is seen with olfactory nerves deep to the lamina propria. ON=Ofactory nerve, OM=Olfactory mucosa **D:** The neuroepithelium is visualised by staining with monoclonal anti-peripherin antibody and labelled with anti-mouse Rhodopsin red.
E: Transverse section of glabrous skin. Ep=epidermis with thick stratum corneum layer, D=dermis.
Scale bar=50μm.

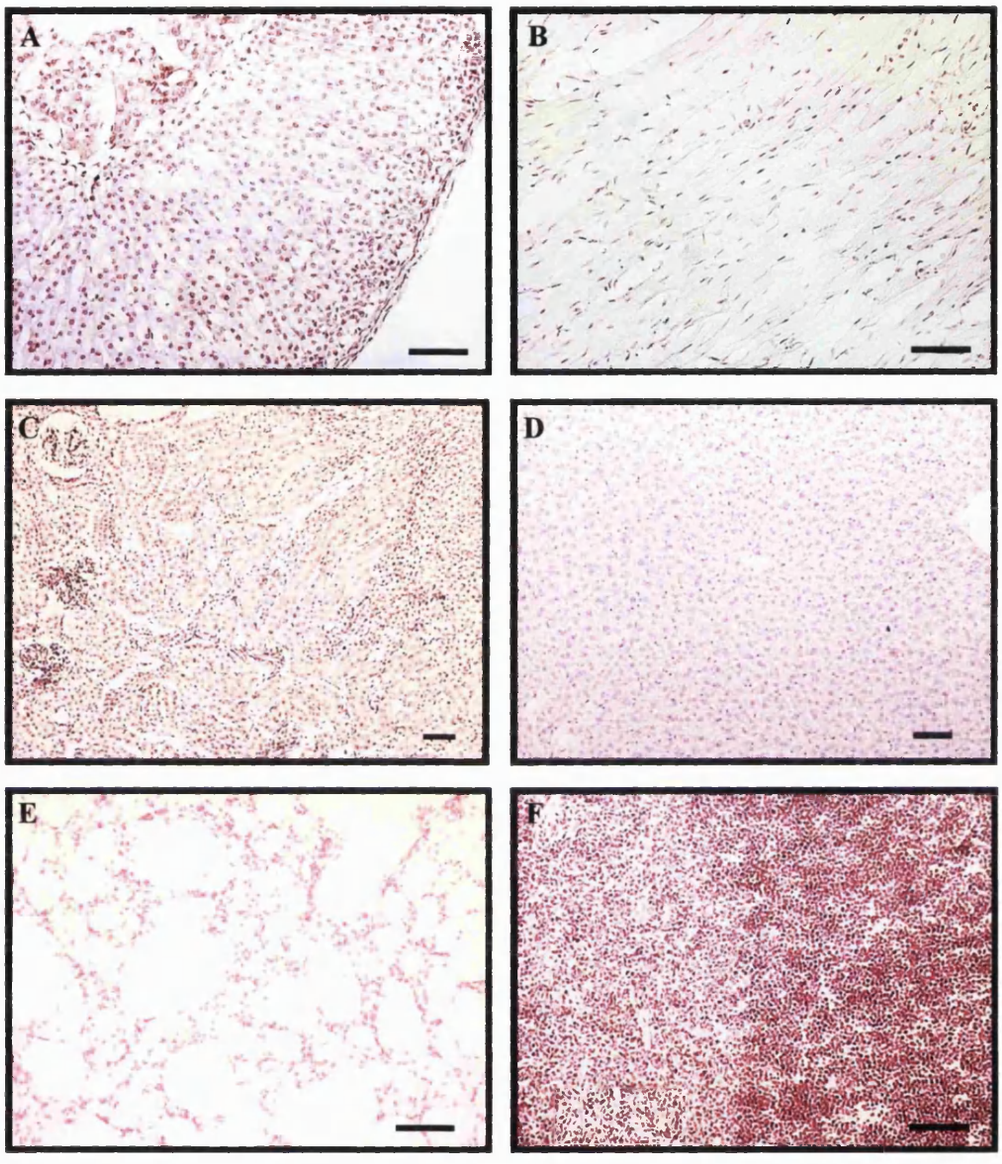

Figure 3.12: X-gal staining in the major viscera of Na$_V$1.8Cre2/R26R mice.

Transverse sections of **A:** adrenal (medulla is seen in the top left), **B:** cardiac muscle (left ventricle), **C:** kidney (glomeruli are seen on the left), **D:** liver, **E:** lung and **F:** thymus (medulla is seen on the left) taken from adult Na$_V$1.8Cre2/R26R animals. Sections were stained with X-gal and counterstained with neutral red.
Scale bar = 50μm.

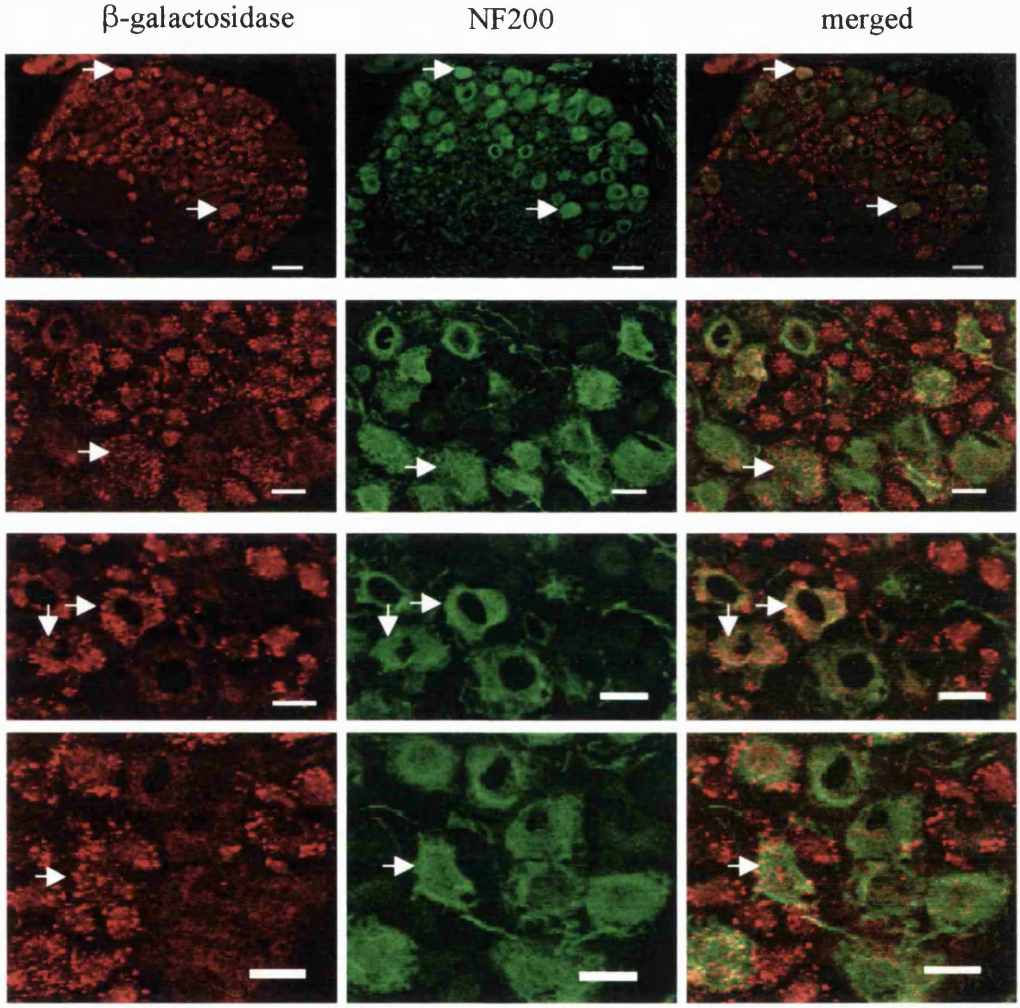

Figure 3.13: Co-localisation of β-galactosidase and NF200 in DRGs from $Na_V1.8$Cre2/R26R mice.
Sections were labelled with anti-β-galactosidase antibody conjugated to Alexa Fluor 594 (shown in the left panels) and anti-NF200 (N52) antibody conjugated to goat anti-mouse FITC (shown in the middle panels). The right panels are merged images of the left and middle panels.
Arrows indicate neurons that are immunopositive for β-galactosidase and NF200.
cale: top row=50μm, all others=20μm

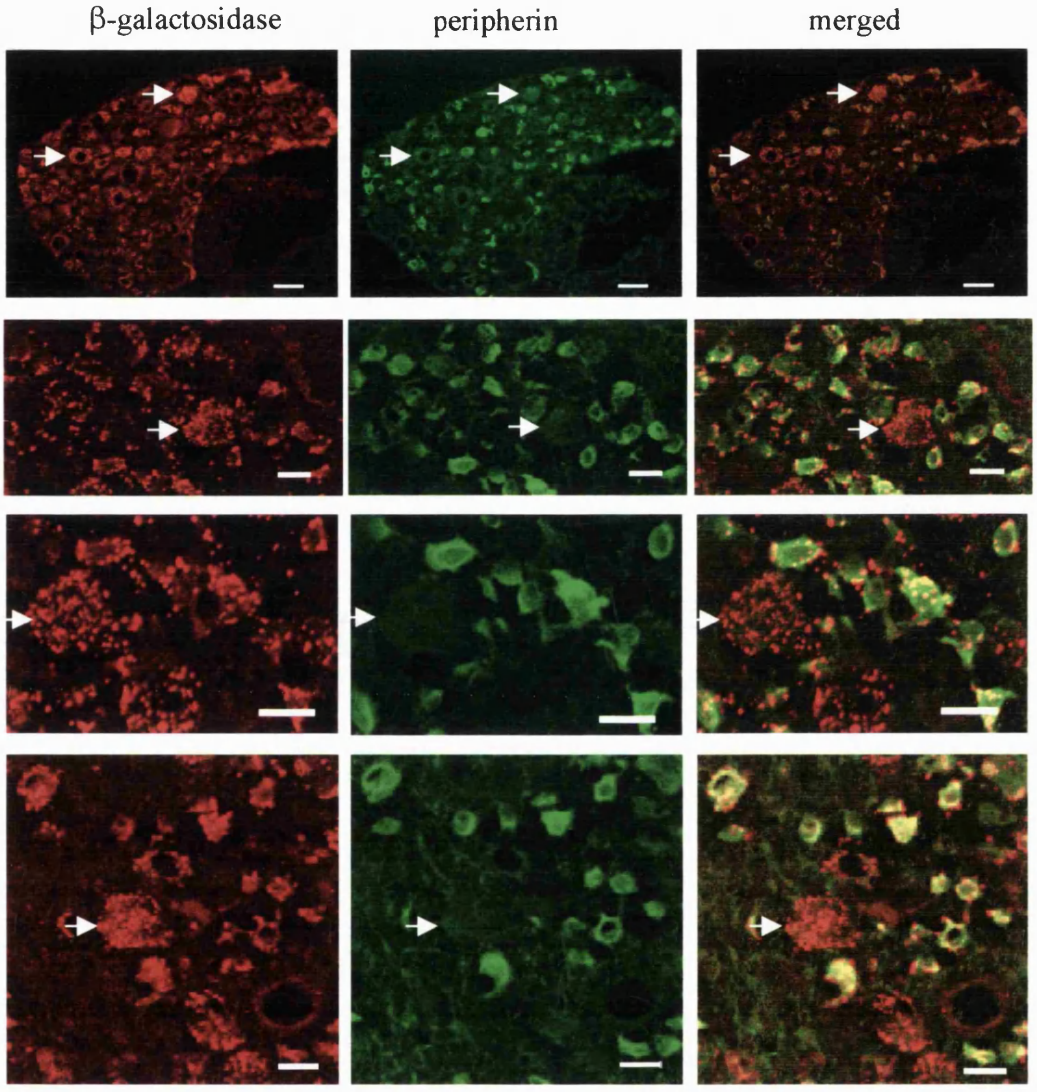

Figure 3.14: Co-localisation of β-galactosidase and peripherin in DRGs from $Na_V1.8$Cre2/R26R mice.
Sections were labelled with anti-β-galactosidase antibody conjugated to Alexa Fluor 594 (shown in the left panels) and anti-peripherin antibody conjugated to goat anti-mouse FITC (shown in the middle panels). The right panels are merged images of the left and middle panels.
Arrows indicate neurons that are immunopositive for β-galactosidase but showed no immunoreactivity for peripherin.
Scale: top row=50μm, all others=20μm.

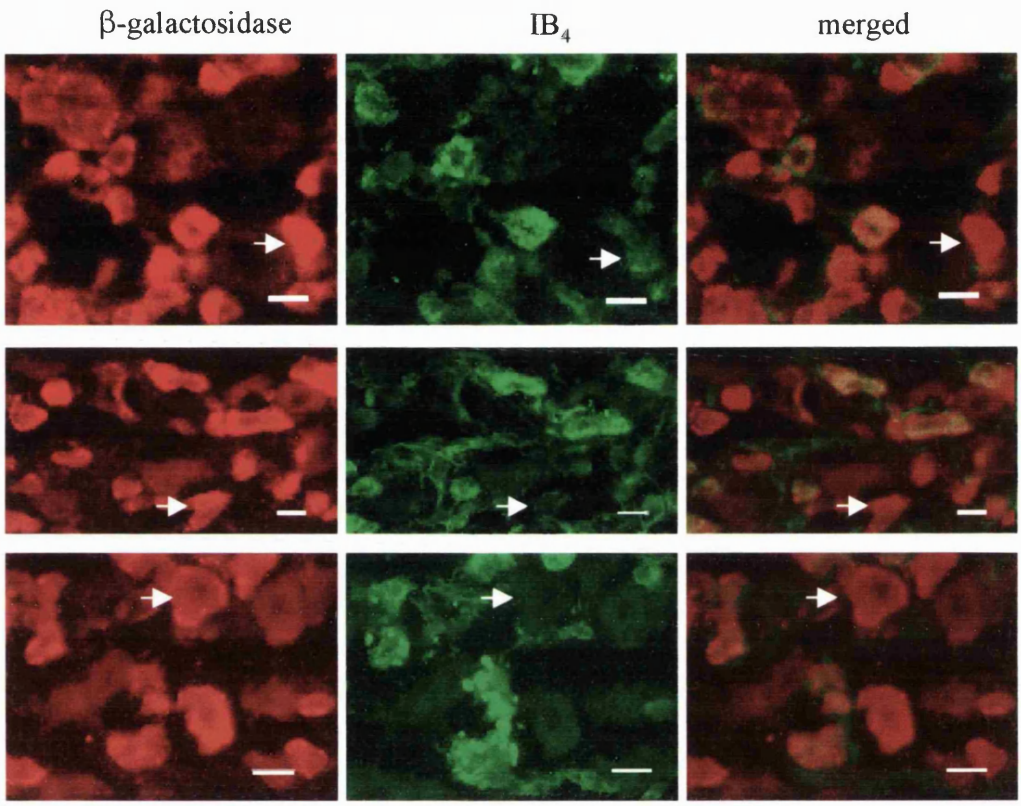

Figure 3.15: Co-localisation of β-galactosidase and IB_4 in DRGs from $Na_V1.8Cre2/R26R$ mice.
Sections were labelled with anti-β-galactosidase antibody conjugated to Alexa Fluor 594 (shown in the left panels) and IB_4 conjugated to Alexa Fluor 488 (shown in the middle panels). The right panels are merged images of the left and middle panels.
Arrows indicate neurons that are immunopositive for β-galactosidase but showed no IB_4 immunoreactivity.
Scale =20μm.

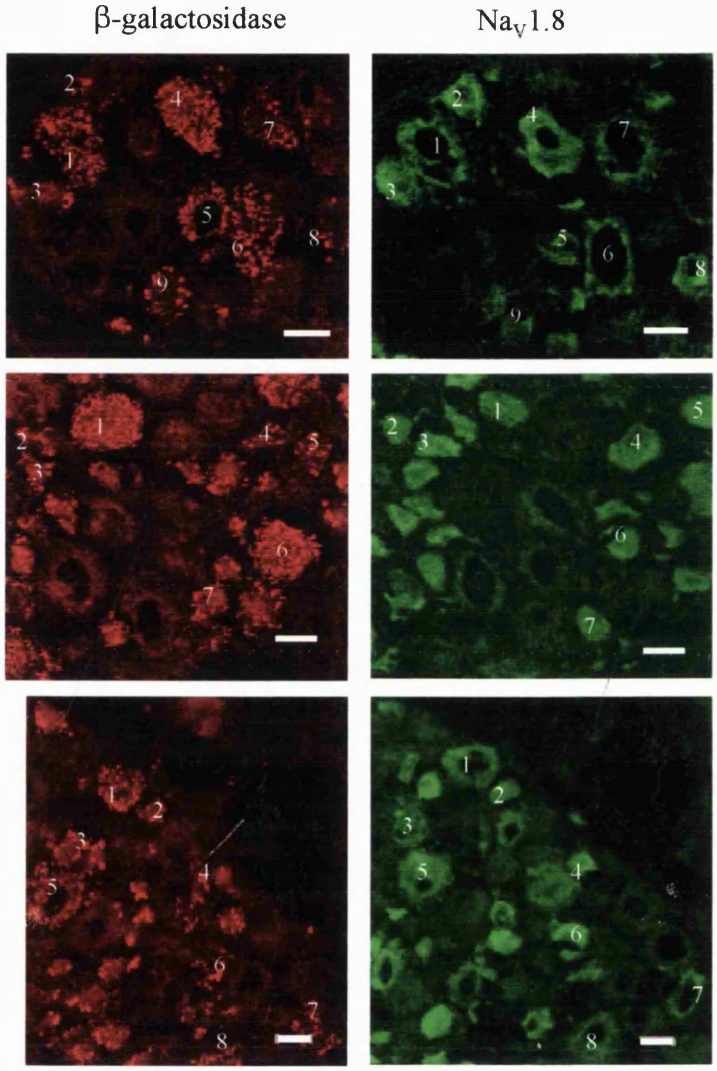

Figure 3.16: Co-localisation of β-galactosidase and $Na_V1.8$ in DRGs from $Na_V1.8$Cre2/R26R mice.
Serial sections were labelled with anti-β-galactosidase antibody conjugated to Alexa Fluor 594 (shown in the left panels), and anti-$Na_V1.8$ antibody conjugated to goat anti-rabbit FITC (shown in the middle panels).
Corresponding β-galactosidase positive, $Na_V1.8$ positive neurons are numbered in each panel.
Scale=20μm.

nociceptor population and almost all IB_4 all were β-galactosidase positive. The IB_4 negative small diameter neurons that were β-galactosidase positive represented the TrkA-positive nociceptors that express or have expressed Cre. In addition there were a few medium and large diameter IB_4 negative, β-galactosidase positive neurons representing myelinated neurons that express or have expressed Cre.

To compare the expression of lacZ with that of the target protein $Na_V1.8$, serial DRG sections were labelled with polyclonal anti-β-galactosidase and anti-$Na_V1.8$ antibodies. Serial sections were used because both antibodies available were polyclonal. Although comparing serial sections was technically more difficult than using double labelling on a single section, as shown in Figure 3.16, there was almost complete co-localisation between the staining patterns for the two antibodies.

These histological and immunocytochemistry data provide strong evidence that the pattern of Cre activity follows that of the target gene $Na_V1.8$.

3.3.6. Onset of Cre expression in utero Figures 3.17-20

Timed matings were set up between heterozygous Na $_V$1.8Cre2 and homozygous R26R animals and embryos obtained at E12, 13, 14 and 15. Each embryo was stained with X- gal and after genotyping, the staining pattern in $Na_V1.8$Cre2/R26R and control R26R+/- embryos was compared.

There was no positive X-gal staining in E12 $Na_V1.8$Cre2/R26R or control R26R+/- embryos - see Figure 3.17.

Positive X-gal staining was visible in E13 $Na_V1.8$Cre2/R26R embryos when compared with R26R+/- controls – see Figure 3.18. Staining was confined to the DRGs and the trigeminal ganglia. Staining of individual neurons within the ganglia could be distinguished, suggesting that a subpopulation of neurons express Cre (Figure 3.18E).

The pattern of staining in E14 $Na_V1.8$Cre2/R26R embryos was identical to that of the E13 embryos but was more intense – see Figure 3.19. There were no R26R+/- positive embryos amongst the progeny analysed (n=8), so comparison with control was not possible.

In E15 $Na_V1.8$Cre2/R26R embryos, the DRGs and trigeminal ganglia were positive, as before, and in addition, staining in the nodose ganglia was visible – see Figure 3.20. Background staining was visible in the vasculature of both $Na_V1.8$Cre2/R26R and control R26R+/- embryos.

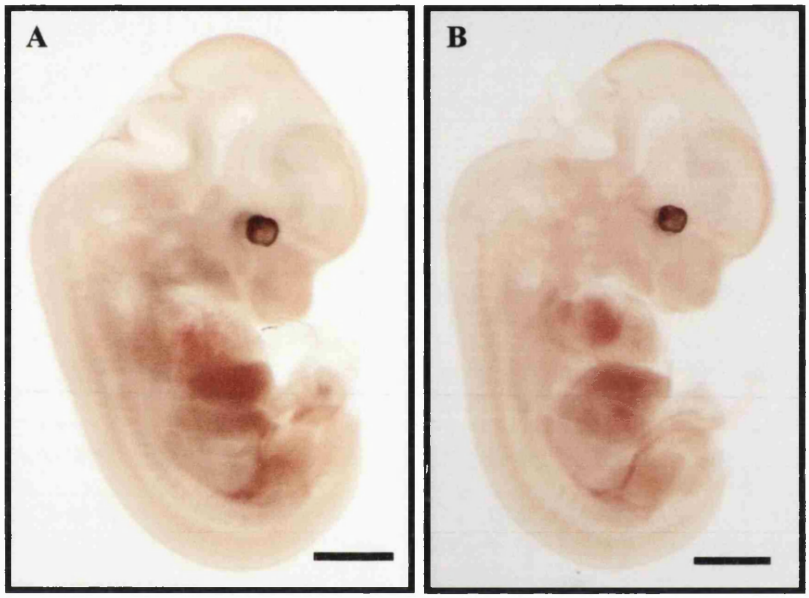

Figure 3.17: X-gal staining of E12 embryos.
No positive X-gal staining is seen in **A:** $Na_V1.8Cre2/,R26R$ or **B:** control R26R+/- embryos. Scale=1mm.

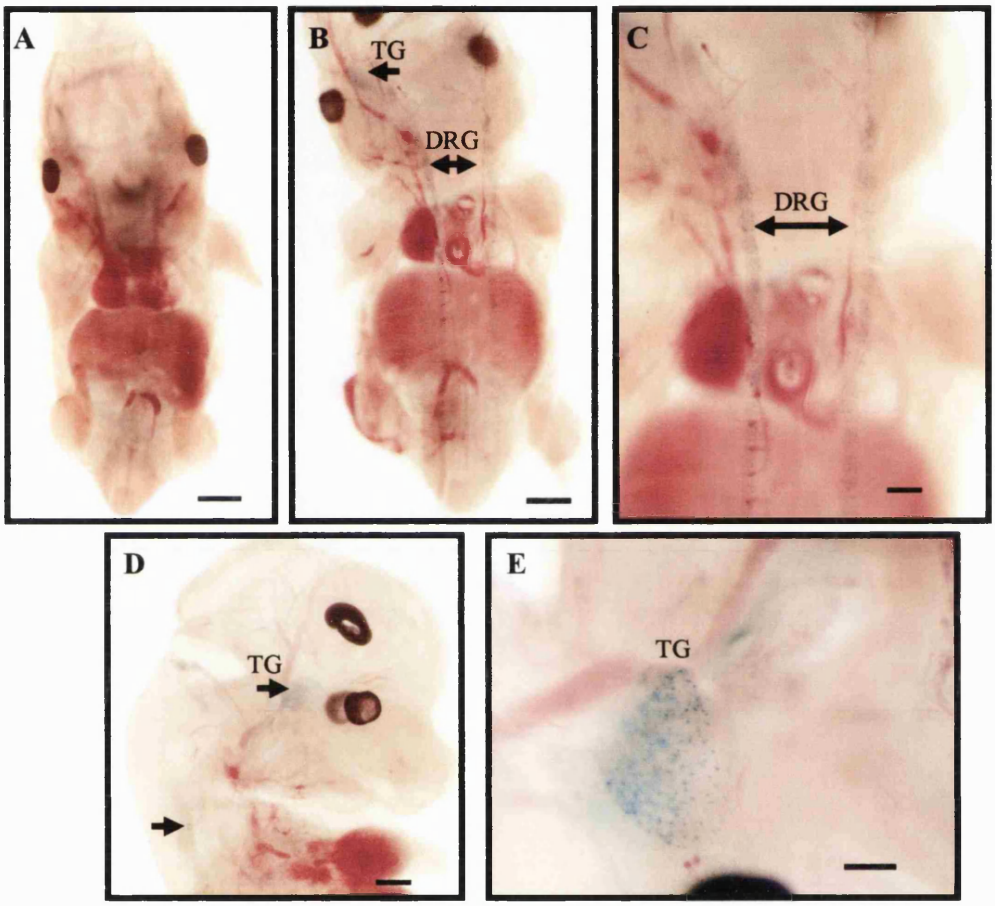

Figure 3.18: X-gal staining of E13 embryos.
A: No positive X-gal staining is seen in control R26R+/- embryos.
B-E: Faint discrete staining within the DRGs and trigeminal ganglia (TG) is seen in $Na_V1.8Cre2/R26R$ embryos.
Scale A,B=1mm, C=300μm, D=500μm, E=200μm.

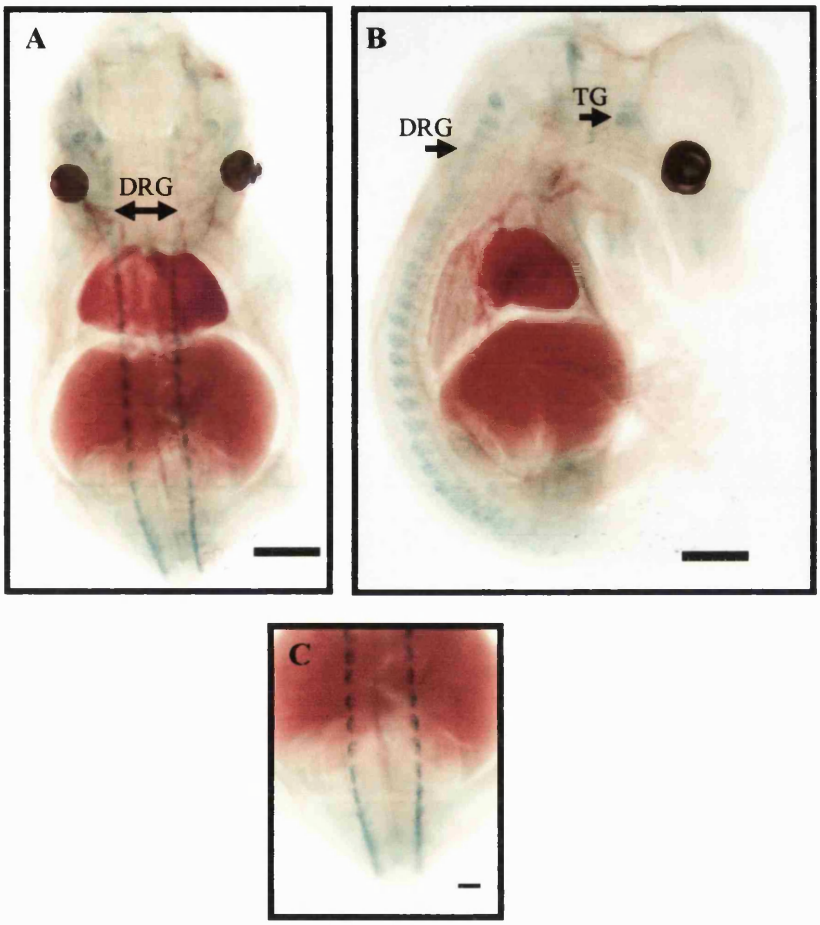

Figure 3.19: X-gal staining of E14 embryos.
A and **C:** Saggital, and **B:** lateral views of a $Na_V1.8Cre2/,R26R$ embryo stained with X-gal showing positive staining in the DRGs and trigeminal ganglia (TG). Scale : A, B=1mm, C=300μm.

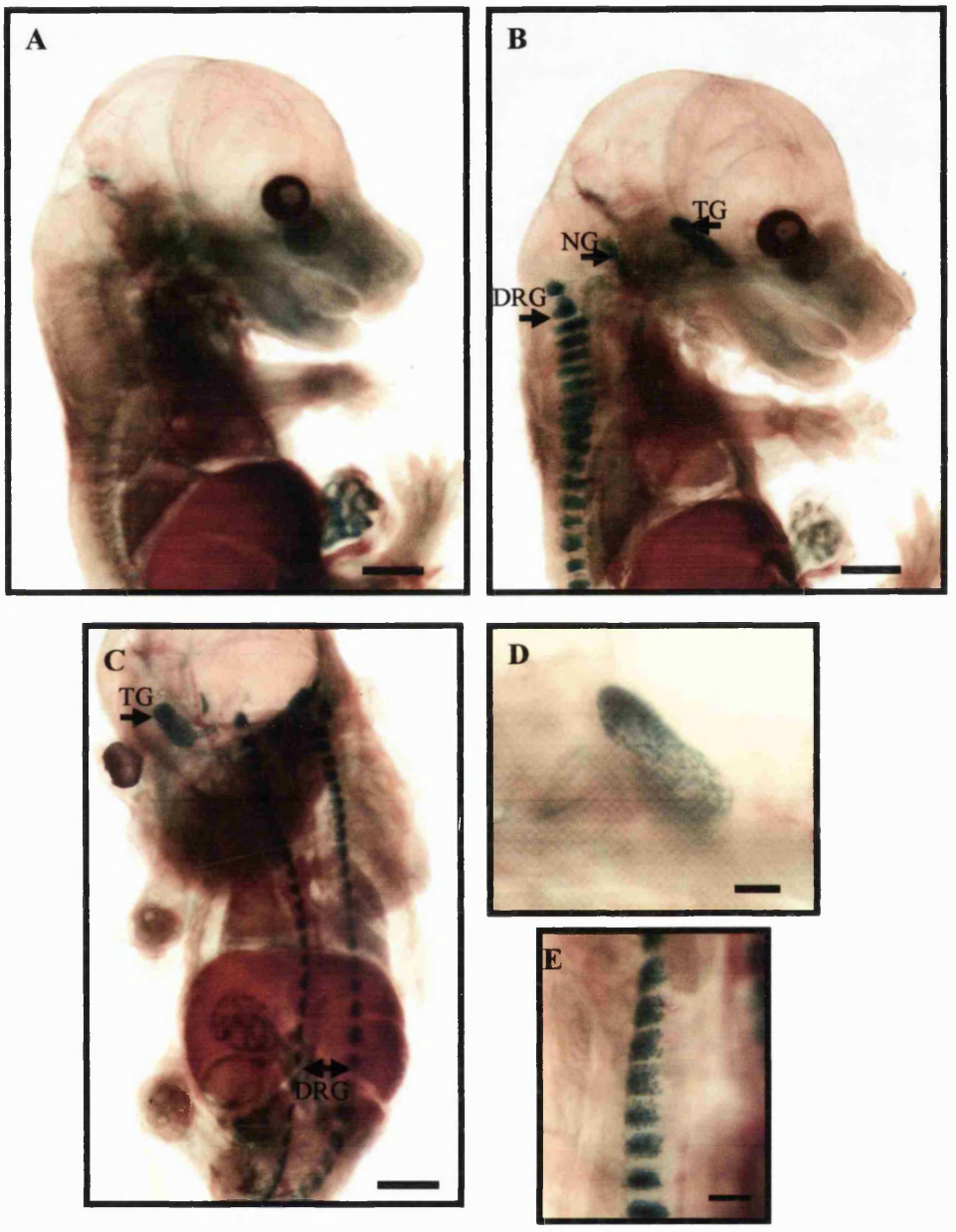

Figure 3.20: X-gal staining of E15 embryos.
A: X-gal staining of a R26R+/- embryo shows background staining in the vasculature. **B:** Lateral and **C:** saggital views of a $Na_V1.8Cre2/R26R$ embryo show intense staining in the DRGs, trigeminal ganglia (TG) and nodose ganglia (NG). **D** and **E:** high power images of a trigeminal ganglion and DRGs respectively, showing discrete neuronal staining.
Scale: A-C =1mm, D,E =300μm.

3.4. Discussion

This chapter presents data examining the tissue distribution of functional Cre in $Na_V1.8$Cre2/R26R animals and suggests that it follows that of the target protein, $Na_V1.8$. In adult animals, positive X-gal staining was seen in the DRGs, trigeminal and nodose ganglia, in line with the original descriptions of the distribution of $Na_V1.8$ (Akopian et al., 1996; Sangameswaran et al., 1996). Amaya *et al.,* (Amaya et al., 2000) also reported $Na_V1.8$ protein expression in the spinal cord, at the central terminals of sensory afferent neurons; this was not found in this study.

The small percentage (~0.2%) of SCG neurons with positive X-gal staining found in this study contrasts with data presented by Sangameswaran *et al.,* showing that no transcript was detected in SCGs using RT-PCR (Sangameswaran et al., 1996). This is not surprising because, even with RT-PCR, it would be difficult to detect such a small amount. The positive staining suggests that at some time in ontogeny there is transcription of $Na_V1.8$ in a few SCG neurons. The data do not indicate whether this transcription is transient or permanent or whether it results in translation. It is possible to transfect $Na_V1.8$ DNA into SCG neurons and record a slowly inactivating TTX-R current attributable to $Na_V1.8$ suggesting that the accessory proteins needed for functional channel expression are present in these neurons. The very small amount of β-galactosidase activity within the SCG indicated by this data is very unlikely to have a significant effect on a phenotype.

The absence of Cre mediated β-galactosidase activity in any other neuronal tissue or in non-neuronal tissue provides further evidence that the $Na_V1.8$ promoter is tightly controlling Cre expression.

The data examining the pattern of $Na_V1.8$Cre2 mediated β-galactosidase activity within DRGs concur with published data (Amaya et al., 2000; Djouhri et al., 2003a; Novakovic et al., 1998; Sangameswaran et al., 1996). A mean of 68% of lumbar DRG neurons from $Na_V1.8$Cre2/R26R animals were positive for X-gal, and almost all X-gal negative neurons were large in diameter. Of primary significance, the data indicate that the immunoreactivity for β-galactosidase is similar to that of $Na_V1.8$. In addition, there was significant co-localisation of β-galactosidase immunoreactivity

with peripherin and IB_4 suggesting that almost all unmyelinated neurons express Cre. The data examining the co-localisation of β-galactosidase with NF200 suggest that a maximum of 10% of myelinated neurons express Cre. These data concur with that presented by Djouhri *et al.,* (Djouhri et al., 2003a) and provide strong evidence that Cre expression is primarily confined to nociceptors and mimics that of $Na_V1.8$.

Positive X-gal staining was also seen in the trigeminal ganglia and although detailed analysis of the percentage of positive neurons was not made, the staining pattern was similar to that in the DRGs. In the nodose ganglia, however, a higher percentage (approximately 75%) of neurons were X-gal positive. These data concurs with that suggesting that over 80% of nodose ganglia neurons are nociceptive (D. Weinreich, personal communication).

Benn *et al.,* (Benn et al., 2001) examined the expression of $Na_V1.8$ *in utero*. They reported a low level of $Na_V1.8$ transcript and protein in E15 rats that increased until P0. In this study, positive X-gal staining was first seen at E13; since Benn *et al.,* did not look for $Na_V1.8$ expression earlier than E15, it is not possible to say whether the results differ. However, it is important to note the relatively early onset of Cre expression when using the mouse for nociceptor specific target gene deletion. Benn *et al.,* also examined the pattern of $Na_V1.8$ expression within the DRG in E17, P0, P7, P21 and adult animals. They found that, within the small diameter neuronal population, the protein was primarily expressed in peptidergic TrkA-positive neurons at E17, with little expression in non-peptidergic IB_4 positive neurons. The relative percentage of TrkA positive neurons expressing $Na_V1.8$ then decreased, since some of these neurons differentiate into IB_4 positive, GDNF-responsive neurons from birth onwards.

Zhou *et al.,* (Zhou et al., 2002) recently reported the generation of a transgenic line in which Cre expression was restricted to peripheral neurons. Cre expression was driven by 5.8kb of the 5'-flanking region of the peripherin gene. Seven founders were selected, of which five showed germ line transmission of the transgene, and in all but one of these Cre mediated β-galactosidase activity was detected, using X-gal staining of embryos that also carried a R26R allele. At E14, positive X-gal staining was seen in the DRGs, trigeminal ganglia and olfactory epithelium. One line was

analysed later in embryogenesis, at E16, when staining was also detected in the sympathetic ganglia. The authors report that within the DRG, a subset of TrkA-, TrkB- and TrkC- dependent neurons were X-gal positive. There is no report of the expression pattern after E16. It is therefore unclear whether other tissues develop Cre expression later in ontogeny; this would be expected since peripherin is expressed within the CNS as well as in the PNS (see Section 3.1.2.). Cre expression in this line is therefore not nociceptor-specific and would not be useful to look at the role of target genes in nociception.

In this study, the ROSA26 reporter mouse was used to analyse the expression pattern of Cre. The ROSA26 locus has been used to produce several other reporter strains. Mao *et al.*,(Mao et al., 1999) generated a reporter strain by inserting a floxed 'stopper' and floxed positive selection marker (encoding resistance to puromycin) upstream of the β-gal-neomycin resistance fusion gene. Cre mediated excision of both the stopper and puromycin resistance gene resulted in activation of *lacZ* and so production of β-galactosidase. The same group have produced a line in which enhanced green fluorescent protein (EGFP) is activated by Cre (Mao et al., 2001; Thyagarajan et al., 2000). Srinivas *et al.*, (Srinivas et al., 2001) used a similar approach to insert a floxed neomycin and polyadenylation signal, followed by either enhanced yellow fluorescent protein (EYFP) or enhanced cyan fluorescent protein (ECFP) into the ROSA26 locus. These fluorescent protein reporter mice are particularly useful for detecting Cre activity in living or cultured tissues. Awatramani *et al.*, (Awatramani et al., 2001) and Possemato *et al.*, (Possemato et al., 2002) have described reporters for Flp mediated excision, in which excision of FRT-flanked neomycin/polyadenlyation signals activates alkaline phosphatase or β-galactosidase, respectively.

The other locus that has been used to produce reporter mice is the pCCAG promoter that comprises the CMV enhancer and chicken β-actin promoter (Niwa et al., 1991). Lobe *et al.*, (Lobe et al., 1999) used this to produce a double reporter in which a floxed neomycin/polyadenlyation signal cassette is placed upstream of the human placental alkaline phosphatase (hPLAP) gene. In these animals cells express *lacZ*

before Cre mediated excision, and this is replaced by hPLAP activity thereafter. The same group also report another double reporter in which the hPLAP is replaced by EGFP (Novak et al., 2000).

The data presented in this chapter provide strong evidence that Cre expression in $Na_V1.8$Cre2 mice mimics that of the target gene, and therefore that these animals express Cre in a nociceptor specific fashion.

Chapter 4

Behavioural and electrophysiological analysis of heterozygous $Na_V1.8Cre2$ mice

4.1. Introduction

$Na_V1.8$Cre2 mice will be used to delete floxed genes in nociceptors. Since animals in which the target gene had been deleted will carry one $Na_V1.8$Cre2 allele it was important to determine whether heterozygous $Na_V1.8$Cre2 mice had a behavioural phenotype, particularly in tests of nociception, which could interfere with interpretation of the phenotype of target gene deleted animals. It was also important to determine whether there was any change in the $Na_V1.8$ mediated currents in DRG neurons from these animals that contain a single functional $Na_V1.8$ allele. In the introduction, the tests used to assess for a nociceptive behavioural phenotype and the nature of the $Na_V1.8$ mediated current in DRG neurons will be described.

4.1.1. Behavioural assessment - general examination

The assessment of behavioural phenotype includes a general examination to exclude any gross abnormalities that could interfere with behavioural testing (Crawley, 2000). General appearance and behaviour of the animals is assessed as well as motor coordination and locomotor activity, since most behavioural tests require these functions. Animals should be well groomed, with healthy fur and skin, and of a normal weight. Posture should be normal and the animals should display spontaneous exploratory and feeding activity.

Motor function can be assessed using the open field test, in which spontaneous activity of the mouse is assessed over a defined period, usually 5 minutes, using an automated open field. The number of times an animal interrupts horizontal beams of infra red light emitted from the walls of an observation box is recorded.

Another test used to assess motor coordination and balance is the rotarod, a rotating cylinder, approximately 3cm in diameter, on which the animal must continuously walk forwards to avoid falling off (Jones and Roberts, 1968). The speed of rotation is increased after a given time period and the latency to falling off within a given time, usually 5 minutes, measured. The balance-beam test also assesses motor coordination; the time for an animal to cross a series of graded horizontal beams (28,

17 and 11mm diameter) and the number of times the hind feet slip off the beams are recorded. A number of other tests including the analysis of footprint pattern, stereotyped behaviours and sleep can also be performed to assess motor function (Crawley, 2000).

4.1.2 Behavioural assessment - tests of nociception

The efficacy of a potential analgesic agent and the identification of potential targets for analgesic development can be tested in rodents by assessing acute responses to a painful thermal or mechanical stimulus and by assessing these responses in models of inflammatory and neuropathic pain. Several tests have been developed, and they will be described below.

4.1.2.1. Tests of thermal sensitivity

4.1.2.1.1. Tail Flick test

In 1941, D'Amour and Smith described how the tail of a rat was placed in a groove and heat focused on its' tip from above (D'Amour, 1941). They observed a withdrawal reaction with very little variation between subjects, and for the first time reported a reliable easy test of thermal sensitivity in rodents. In the tail flick test the animal is lightly restrained and a high intensity heat-producing beam of light directed at a point close to the tip of the tail. The latency to flick the tail out of the beam is measured within a cut-off time of 10 seconds, to avoid tissue damage, and the test repeated at five minute intervals on each animal. This test assesses the spinal reflex arc.

4.1.2.1.2. Hargreaves' test

Hargreaves *et al.,* (Hargreaves et al., 1988) reported another method to assess the spinal reflex arc in which the animal is not restrained and which uses the skin of the hind paw rather than the tail. Animals are habituated in chambers and the latency of withdrawal of the hind paw from a beam of radiant heat measured. The test is repeated several times on each animal.

4.1.2.1.3. Hot plate test

The hot plate test assesses a reflex that involves higher centres (Jensen and Yaksh, 1984). The test was first described by Woolfe and MacDonald (Woolfe, 1944). Animals are placed inside a tall plastic cylinder on a metal plate that has been heated to a desired temperature, usually between 50 and 55°C. The latency to lick, shake or withdraw a hind paw is measured. Lifting of the forepaw is not assessed, since this is part of normal grooming behaviour. Wilson and Mogil (Wilson and Mogil, 2001) reported that repeating the test between 5 and 30 minutes after the first measurement results in a significant reduction in the latency, a phenomenon known as 'behavioural tolerance'.

4.1.2.2. Tests of mechanical sensitivity

Tactile hyperalgesia and allodynia are significant clinical problems, so tests in which the response to mechanical stimuli are assessed are potentially very relevant.

4.1.2.2.1. von Frey hairs

Several authors (Fuchs et al., 1999; Kim and Chung, 1992; Seltzer et al., 1990) have described the use of von Frey hairs to assess the threshold of response to a mechanical stimulus. Von Frey hairs are graded filaments of increasing rigidity that deliver logarithmic incremental forces. Mice are habituated in chambers that have nylon or metal mesh floors and von Frey hairs applied to the plantar aspect of the hind paw, until they bend slightly, for 3-5 seconds. The presence or absence of a withdrawal response is noted.

Two methods have been used to assess the response. Full battery testing (Fuchs et al., 1999) involves presenting hairs on increasing weight to the paw, each hair being applied 5 or 10 times. The percentage response is then calculated (for example, if the animal responds in 3 out of 5 applications of a given hair, the percentage response is 60%).

The second method, the up-down method, was first described by Chaplan *et al.,* (Chaplan et al., 1994) using a model described by Dixon (Dixon, 1980). This method allows the behavioural response to be assessed more quickly and results in a value for the 50% withdrawal threshold. A von Frey hair that is thought to be at the

50% threshold threshold is applied. If there is a positive withdrawal response a hair of decreased weight is presented and if there is no response, a hair of increased weight is presented. Testing is continued in this fashion until six measurements around the 50% threshold weight are obtained. This involves the presentation of between 6 and 9 hairs; more hairs are used when the 50% threshold is at a weight different from that selected for the initial presentation. The 50% withdrawal threshold is then calculated.

Chaplan *et al.,* found that there was a high correlation between the results obtained using the full battery and up-down methods, thus validating the up-down method.

4.1.2.2.2. Randall Selitto test

The Randall Selitto test involves the application of increasing mechanical force to the tail or hind paw (Takesue et al., 1969). The animal is restrained and the paw/tail placed under a 2mm diameter probe and pressure applied through the probe until the animal attempts to withdraw the paw/tail. The weight at which this occurs in measured. This apparatus was designed for use on the hind paw of rats and since this is not practicable in mice, pressure is applied to the tail.

4.1.2.3. Models of inflammatory pain

4.1.2.3.1. Formalin test

Dubuisson and Dennis (Dubuisson and Dennis, 1977) first described the formalin test in cats and rats –5% formalin (100% formalin is the aqueous solution of 37% formaldehyde (Tjolsen et al., 1992) was injected into the forepaw and behaviour observed for the next hour. Formalin elicited a spontaneous biphasic behavioural response indicative of pain. Behaviour was rated from 0, in which there was no indication of pain, to 3, in which the animal displayed licking and biting of the injected paw. The first phase lasted approximately 10 minutes and was followed by a quiescent period of about 10minutes in which there was little behaviour. The second phase lasted approximately 40minutes.

Huskaar and Fasmer (Hunskaar et al., 1985) reported the formalin test in mice, injecting into the hind paw and using licking of the injected paw as an indicator of a pain response. Since licking of the forepaw is part of normal grooming, hind paw

injection is now widely used (Tjolsen et al., 1992), and has been validated as the best behavioural measure in mice (Sufka et al., 1998). Hunskaar and Hole (Hunskaar and Hole, 1987) showed that systemic administration of opioids inhibited both phases of the response whereas systemic non-steroidal anti-inflammatory drugs and corticosteroids inhibited the second phase only. These data suggest that the first phase is caused by direct chemical activation of C-fibre nociceptors whereas in the second phase an inflammatory response occurs. There is also evidence to suggest that changes in the spinal cord induced during the first phase contribute to the second phase (Tjolsen et al., 1992).

4.1.2.3.2. Carrageenan

Carrageenans are a complex group of polysaccharides, extracted from red seaweed, made up of repeating galactose-related monomers, which form thermoreversible gels. There are three main types – lambda (λ), kappa (κ) and iota (ι) – each with different characteristics. λ-carrageenan does not form a gel at room temperature and therefore can be used for injection, resulting in a reproducible inflammatory response (Tonussi and Ferreira, 1992; Winter et al., 1962) that is maximal 3-5 hours following injection. Kayser and Guilbaud (Kayser and Guilbaud, 1987) described the behavioural response to intraplantar injection of 1% carrageenan into the hind paw of rats. Mechanical hyperalgesia and oedema of the injected paw developed within two hours and persisted for 96 hours after injection. Thermal hyperalgesia also develops.

4.1.2.3.2. Complete Freund's Adjuvant

Complete Freund's Adjuvant (CFA) is a water in oil emulsion, containing cell wall components of *mycobacterium butyricum* (<0.5mg/kg), that induces an inflammatory response following injection. CFA can be administered intradermally into the base of the tail resulting in a model of polyarthritis (Millan et al., 1986) or by intraplantar injection. Millan *et al.,* (Millan et al., 1988) described the intraplantar injection of CFA into rats, observing local inflammation and oedema that appeared within a few hours and lasted for five weeks. Thermal and mechanical hyperalgesia were confined to the injected paw and were maximal at 24 hours and persisted for the entire observation period.

4.1.2.4. Models of neuropathic pain

Several models of neuropathic pain have been developed in the rodent all involving ligation of the sciatic nerve, the motor/sensory nerve with roots from L_4, L_5 and L_6 that supplies the hind limb – see Figure 4.1. Bennett and Xie (Bennett and Xie, 1988) described the chronic constriction model in which four loose ligatures were placed around the sciatic nerve. Seltzer *et al.,* developed the sciatic nerve ligation model in which one third to one half of the sciatic nerve was tightly ligated (Seltzer et al., 1990). Kim and Chung described two experimental paradigms of spinal nerve ligation in the rat (Kim and Chung, 1992). In the first model, the L_5 and L_6 spinal nerve roots were tightly ligated and in the second, the L_5 spinal nerve only was tightly ligated. Mechanical hypersensitivity developed within a day of surgery, reached a peak 1 week after surgery and started to resolve after 14 weeks. Thermal hyperalgesia developed within three days and lasts for about 5 weeks. In addition, animals showed signs of spontaneous pain within a day of surgery.

The major drawback with the chronic constriction injury and sciatic nerve ligation models is that it is difficult to ensure that the surgical procedure performed is identical. The tension of the ligatures in the former and the numbers and types of fibres ligated in the latter are open to intra- and inter- operator variability, making interpretation of phenotypic changes more difficult.

With the Chung model the only potential variable is the normal biological variability in the proportion of the spinal segments that contribute to the sciatic nerve. This makes it a much more reproducible model. It also allows study of the contribution of injured or uninjured afferents in the generation of the hyperalgesia. The major disadvantage of this model is that the surgical procedure is much more invasive than in the other models. Recently, Honore *et al.,* (Honore et al., 2000) showed that the behavioural and neurochemical changes that occur after L_5 spinal nerve ligation in the mouse are the same as those observed in rats, validating this model for use in mice.

Decosterd and Woolf (Decosterd and Woolf, 2000) developed the spared nerve model of neuropathic pain in which two of the terminal divisions of the sciatic nerve were axotomised (the tibial and common peroneal nerves), and the third division

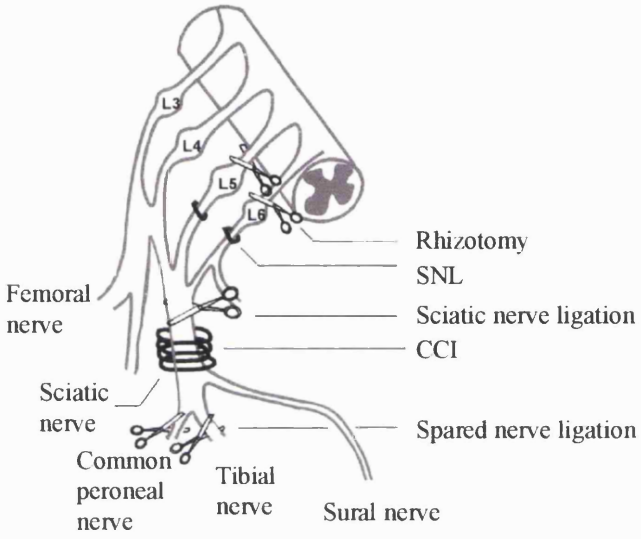

Figure 4.1: Models of neuropathic pain.
Diagram of the lumbar plexus and the nature of the injuries used to create different models of neuropathic pain (reproduced from Decosterd et al. 2002).
CCI=chronic constriction injury, SNL=spinal nerve ligation.

was spared (the sural nerve). This model is technically simpler than the other models and, as with the Chung model, the injury is clearly defined.

Other neuropathic pain models include transection, or cryoneurolysis of the sciatic nerve, dorsal horn rhizotomy, and intraperitoneal streptozocin to model diabetic neuropathy (reviewed in (Wang and Wang, 2003).

4.1.2.5. Models of visceral pain

The most widely used model of visceral pain has been the abdominal constriction or writhing test in which intraperitoneal injection of algesic agents such as acetylcholine, hypertonic saline or acetic acid evokes a characteristic abdominal stretching behaviour. Other models include intravesical injection of turpentine, colorectal distension and artificial renal calculosis (Giamberardino, 1999). Laird *et al.,* (Laird et al., 2001) recently reported a model of colitis in which chemical substances such as capsaicin or mustard oil are injected into the rectum via the anus resulting in visceral pain and referred hyperalgesia.

4.1.3. $Na_V1.8$-mediated currents in DRG neurons

There are two pharmacologically distinct types of voltage-gated sodium channels in sensory neurons, those that are sensitive to TTX and those that are resistant to TTX (reviewed in Baker and Wood 2001). Most voltage-gated sodium channels are TTX-sensitive, and at least six different TTX-sensitive α subunits are expressed in sensory neurons, inhibited by low nanomolar concentrations of TTX. These channels are rapidly activating and inactivating. The predominant current in large diameter sensory neurons is TTX-sensitive, whereas in small diameter, primarily nociceptive neurons, there is also a prominent TTX-resistant current. The TTX-resistant α subunit $Na_V1.8$ accounts for the TTX-resistant current and has much slower activation and inactivation kinetics – see Figure 4.2.

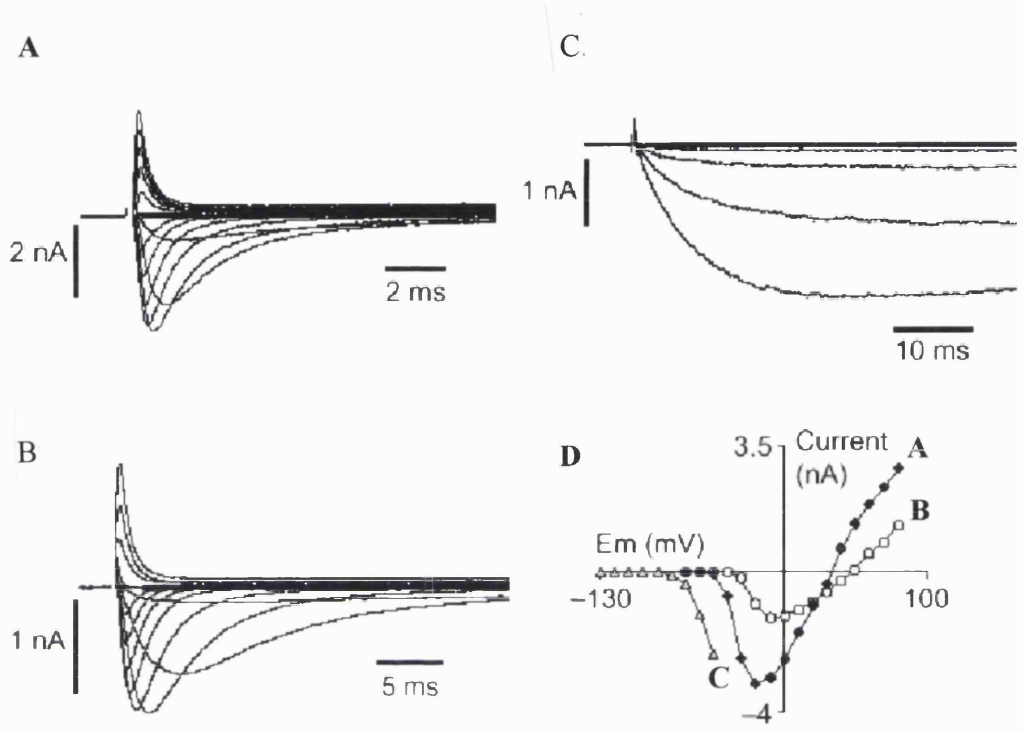

Figure 4.2: Sodium currents in small diameter DRG neurons (<25μm).

A: Fast transient TTX-sensitive Na^+ current recorded from a wild-type neuron. **B:** TTX-resistant current recorded during the continuous perfusion of TTX (250nM) from a wild type neuron. **C:** Low threshold TTX-resistant current recorded during the perfusion of TTX (500nM) from a $Na_V1.8$ -/- neuron. **D:** I/V plot of the three currents A-C (reproduced from Baker and Wood 2001).

4.2. Methods

4.2.1. Behavioural analysis

All tests were approved by the United Kingdom Home Office Animals (Scientific Procedures) Act 1986. They were performed in a Home Office designated room at 22±2°C. Experiments were performed on F3 or F4 $Na_V1.8Cre2+/-$ animals of at least 8 weeks of age. Male C57BL/6 animals of a similar age or wild type littermates were used as controls. The same observer performed all experiments and was blind to the genotype of the animals when wild type littermates were used as controls. Animals were weighed before testing.

4.2.1.1. Motor function

Motor function was assessed using the rotarod test (Ugo Basile). Animals were placed on the rod as it was rotating at 20 rpm. After one minute the rate of revolution was increased, and reached a maximum of 36 rpm within 90 secs. The length of time that each animal spent on the rod was measured, with a cut off time of 5 mins. The test was performed three times for each animal with at least 15 mins between each test.

Results were expressed as the mean time spent on the rod for each group ± the standard error of the mean (S.E.M.). The results for the two groups were compared using a Mann-Whitney rank sum test.

4.2.1.2. Thermal thresholds

Two tests were used to assess the threshold to thermal stimuli, Hargreaves' test and the hot plate test.

4.2.1.2.1. Hargreaves' test

Animals were acclimatised in the test chambers (11x8x14cm) (Ugo Basile or IITC 390) for at least 1 hour until exploratory activity had ceased. The intensity of the beam of infra-red light was set to give a withdrawal latency of around 15 secs. The latency of withdrawal to heat was recorded 4-6 times on each paw, with at least 30 secs between recordings on the same paw.

Results were expressed as the mean withdrawal latency for each group ± S.E.M. The results for the two groups were compared using an unpaired 2-tailed *t* test.

4.2.1.2.2. Hot Plate test

Animals were acclimatised to the chamber (20cm in diameter, 17.5cm high) (Ugo Basile) by placing them in it in groups of 4-6 for 15 mins before the plate was heated. The latency of withdrawal at two temperatures, 50°C and 55°C, was measured. The latency was measured once for each animal and the tests at different temperatures were separated by at least 24 hrs.

Results were expressed as the mean withdrawal latency for each group ± S.E.M. The results for the two groups were compared using an unpaired 2-tailed *t* test.

4.2.1.3. Mechanical thresholds

Two tests were used to assess the threshold to mechanical stimuli, von Frey hairs, and the Randall Selitto test.

4.2.1.3.1. von Frey hairs

Animals were acclimatised in the Perspex walled chambers (7x10x13cm) with a nylon mesh floor for at least 1hr until exploratory activity had ceased.

For the full battery method of testing (see Section 4.1.2.2.1.) six hairs, of increasing diameter, from 0.363 to 2.75g, were applied until they bent slightly, five times to the plantar aspect of each hind paw for 3 secs. The presence of a withdrawal response was recorded and the percentage response was then calculated.

Results were expressed as the mean percentage response for each group at each hair weight ± S.E.M. The results for the two groups were compared using a two-way repeated measures analysis of variance test.

For the up-down method of testing, used to assess mechanical hyperalgesia after CFA and after ligation of the sciatic nerve, a 1.66g hair was used as the first hair for baseline assessment, and a 0.603g hair used as the first hair for assessments after generation of the pain model. If application of a hair resulted in a withdrawal response, a hair of the next weakest weight was applied. If application of a hair

resulted in no response, a hair of the next strongest weight was applied. Hairs were applied until 6 responses were recorded around the 50% threshold.

The 50% threshold for each group was calculated (Chaplan et al., 1994) and the value expressed as a mean ± S.E.M.

4.2.1.3.2. Randall Selitto test

Each animal was placed in a restrainer (IITC) and left to settle for a few minutes until they stopped struggling. Force was applied approximately midway along the tail, at a point where the tail diameter was just greater than that of the probe (Ugo Basile analgesy meter). The force at which the animal attempted to withdraw the tail, vocalise or struggle was recorded. The test was repeated three times for each animal.

Results were expressed as the mean weight tolerated for each group ± S.E.M. The results for the two groups were compared using an unpaired 2-tailed *t* test.

4.2.1.4. Models of inflammatory pain

Three models of inflammatory pain were used, the Formalin test, intraplantar injection of carrageenan and intraplantar injection of Complete Freund's Adjuvant.

4.2.1.4.1. Formalin test

Animals were acclimatised in the chamber (20x20x20cm) for at least 1 hr before testing until exploratory activity had ceased. Each animal was restrained and 20µl of 5% formalin (37% formaldehyde (BDH) diluted with 0.9% saline (Sigma)) injected subcutaneously into the plantar aspect of a hind paw using a Hamilton syringe and 27g needle. The amount of time spent licking or biting the injected paw was then recorded in 5 minute periods over the next hour. Activity during the first phase, from 0-10 mins, and the second phase, from 10-60 mins, was then calculated for each animal.

Results were expressed as the mean time spent licking/biting (secs) in each phase for each group ± S.E.M. The results for the two groups were compared using an unpaired 2-tailed *t* test.

4.2.1.4.2. Intraplantar carrageenan

Baseline thermal thresholds for one paw were recorded for each animal using Hargreaves' test. 20μl of either 0.9% saline (Sigma) or 2% λ-carrageenan (Sigma) (diluted with 0.9% saline) was then injected into the plantar aspect of a hindpaw using a Hamilton syringe and 27g needle. Thermal thresholds of the injected paw were then assessed at hourly intervals for three hours using Hargreaves' test.

Results were expressed as the relative change in the withdrawal latency (test/baseline) at each time point for each group ± S.E.M. The relative change data for the two groups were compared using a two-way repeated measured analysis of variance test.

4.2.1.4.3. Intraplantar Complete Freund's Adjuvant

Baseline thermal and mechanical thresholds for one paw were recorded for each animal using Hargreaves' test and von Frey hairs (using the up-and-down method) respectively. 20μl Complete Freund's Adjuvant (Sigma) was injected into the plantar aspect of a hindpaw using a Hamilton syringe and 27g needle. Animals were assessed 1, 2, 3, 4, and 10 days after injection. On each day thermal and mechanical thresholds of the injected paw were assessed using the same method.

Results of the thermal withdrawal latencies were expressed as the relative change in the latency at each time point after injection (test/baseline) for each group ± S.E.M. The relative change data for the two groups were compared using a two-way repeated measures analysis of variance test.

Results of the 50% withdrawal threshold were expressed as the relative change in the 50% threshold at each time point after injection (test/baseline) for each group ± S.E.M. The results for the two groups were compared using a two-way repeated measures analysis of variance test.

4.2.1.5. Chung model of neuropathic pain:

Baseline thermal and mechanical thresholds for one paw were recorded from $Na_V1.8Cre2+/-$ and wild type littermates using Hargreaves' test and von Frey hairs (using the up-down method) respectively. Animals were anaesthetised using

Halothane. A midline incision was made in the skin of the back at the L_2-S_2 levels and the left paraspinal muscles separated from the spinous processes, facet joints and transverse processes at the L_4-S_1 levels. The L_5 transverse process was removed and the left L_5 spinal nerve tightly ligated using 8-0 silk thread. These operations were performed by Dr. Elisabeth Matthews. Animals were assessed 1, 3, 6, 9, 12, 15, 19, 22, 26 and 29 days after injection. On each day thermal and mechanical thresholds were measured.

Results of the thermal withdrawal latencies were expressed as the relative change in the latency at each time point after injection (test/baseline) for each group ± S.E.M. The results for the two groups were compared using a two-way repeated measures analysis of variance test.

Results of the 50% withdrawal threshold were expressed as the relative change in the 50% threshold at each time point after injection (test/baseline) for each group ± S.E.M. The results for the two groups were compared using a two-way repeated measures analysis of variance test.

4.2.2. Electrophysiological analysis

DRG cultures were prepared from adult mice (homozygous $Na_V1.8Cre2$, heterozygous $Na_V1.8Cre2$, and wild type littermates) killed by cervical dislocation. TTX-resistant Na^+ currents in small (<25μm apparent diameter) DRG neurons were recorded in the whole-cell voltage-clamp configuration. The TTX-resistant Na^+ currents were recorded in relative isolation by including blockers of K^+ and Ca^{2+} currents in the intracellular and extracellular solutions, and by including 250 nM TTX (Sigma and Alomone Labs) in the extracellular solution. Recordings of the current attributable to $Na_V1.8$ were made from a holding potential of either –90 or –70 mV.

Na^+ current amplitude values were converted to current density by dividing the peak current value (in nA) by the cell capacitance (in pF). Data are expressed as mean ± S.E.M. Experiments were performed at room temperature (22 - 25°C).

DRG culture and electrophysiological analysis were performed by Dr. Mark Baker.

4.3. Results

4.3.1. Behavioural analysis of heterozygous $Na_V1.8Cre2$ animals

Litters were of normal size (n=4-12) and all offspring were healthy with normal gross motor and sensory function. All animals were at least 8 weeks of age at the time of behavioural testing.

The mean weights of the $Na_V1.8Cre2+/-$ and C57BL/6 control animals tested were 26.5±0.8g (n=26) and 24.1±0.4g (n=32) respectively. When analysed using an unpaired 2-tailed *t*-test, this represents a significant difference between the two groups (P=0.006). When wild type littermates were used as controls, there was no significant difference between littermates of different genotypes - mean weight of $Na_V1.8Cre2+/-$ mice (n=18) was 24.1±0.9g and mean weight of wild type littermates (n=16) was 23.9±0.8. This represents no significant difference between the groups when analysed using an unpaired 2-tailed *t*-test, P = 0.84.

4.3.1.2. Motor function Figure 4.3.A

Eight male $Na_V1.8Cre2+/-$ animals and eight male C57BL/6 animals were subjected to the rotarod test. The mean time spent on the apparatus for each group was 212.5±11.2 and 177±10.6 secs respectively. Analysis using a Mann-Whitney rank sum test revealed that this represents no significant difference between the two groups - P =0.26.

4.3.1.2. Baseline thermal sensitivity Figure 4.3.B, C.

4.3.1.2.1. Hargreaves' test

The spinal reflex arc was tested using Hargreaves' test on both hind paws on six male $Na_V1.8Cre2+/-$ animals and six male C57BL/6 animals. The mean latency of

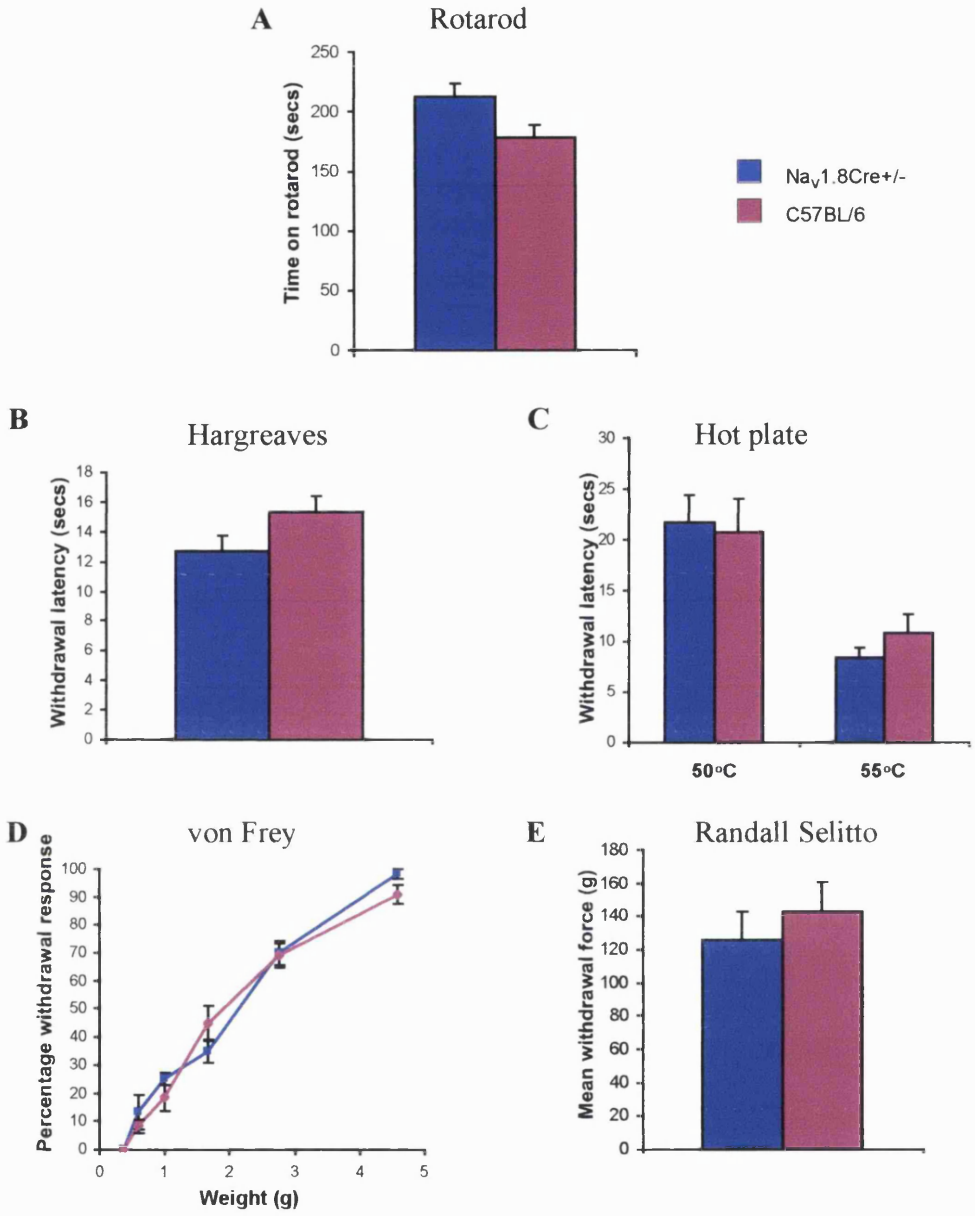

Figure 4.3: Behavioural analysis of heterozygous Na$_V$1.8Cre2 and wild type mice - acute thermal and mechanical withdrawal thresholds.

A: Mean time spent on rotarod

B: Mean latency of withdrawal from a thermal stimulus using Hargreaves' test

C: Mean latency of withdrawal from a thermal stimulus (50°C and 55°C) using the hot plate

D: Percentage response to mechanical force using von Frey's hairs

E: Mean withdrawal force to noxious mechanical stimulus using Randall Selitto test.

See text for statistical analysis.

withdrawal of the hind paw for the two groups was 12.7±1.0 and 15.3±1.1 secs respectively. This represents no significant difference between the two groups when compared using an unpaired 2-tailed *t* test – P =0.12.

4.3.1.2.2. Hot plate test Figure 4.3.C

Sixteen male $Na_V1.8Cre2+/-$ animals and eleven male C57BL/6 animals were tested using the hot plate. The mean latency to withdrawal of a hind paw at 50°C was 21.7±2.7 and 20.8±3.3 secs respectively, and, at 55°C, 8.4±0.9 and 10.9±1.8 secs respectively. This represents no significant difference between the two groups at either temperature when compared using an unpaired 2-tailed *t* test - P =0.68 at 50°C and P =0.15 at 55°C.

4.3.1.3. Baseline mechanical sensitivity Figure 4.3. D, E.

4.3.1.3.1. Von Frey's hairs

The sensitivity to mechanical stimuli was assessed using von Frey's hairs on six male $Na_V1.8Cre2+/-$ animals and twelve male C57BL/6 animals. Comparing the percentage responses of the two groups using a two way analysis of variance test with repeated measures, there was no significant difference between the groups in the percentage response to a given hair (P =0.99), although as expected, there was a highly significant effect of the hair weight on the response (P <0.001).

4.3.1.3.2. Randall Selitto test

Application of noxious mechanical pressure using the Randall Selitto apparatus also resulted in a response that was not significantly different between the two groups. Fourteen male $Na_V1.8Cre2+/-$ animals and fourteen male C57BL/6 animals were tested, and the mean weight that resulted in a withdrawal response was 126.0±16.4g and 142±17.9g respectively for the groups. When analysed using an unpaired 2-tailed t test, P =0.13.

4.3.1.4. Models of inflammatory pain

4.3.1.4.1. Formalin test Figure 4.4.A

Intraplantar injection of formalin elicited a biphasic behavioural response comprising licking and biting of the injected paw. The response of six male

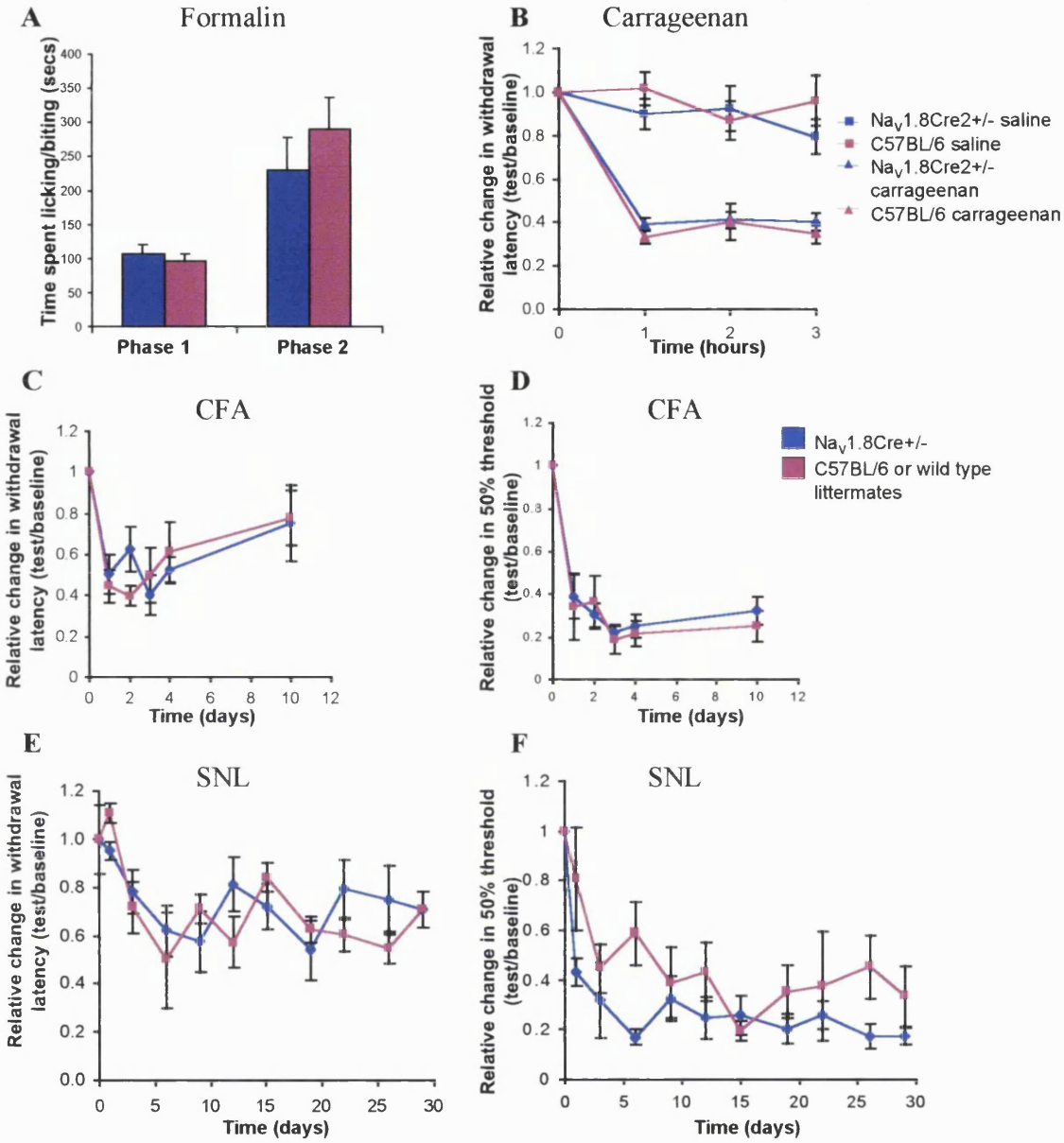

Figure 4.4. Behavioural analysis of heterozygous $Na_V1.8Cre2$ and wild type mice - inflammatory and neuropathic pain models.

A: Mean time spent licking/biting the injected paw following 20µl intraplantar formalin - phase 1=0-10 minutes, phase 2=10-60 minutes post injection.

B: Relative change in threshold of withdrawal to thermal stimulus (Hargreaves' test) following 20µl intraplantar carrageenan or saline into the hind paw.

C: Relative change in threshold of withdrawal to a thermal stimulus (Hargreaves' test) and **D:** Relative change in 50% threshold to mechanical stimulus (von Frey's hairs) following 20µl intraplantar Complete Freund's Adjuvant (CFA) into the hind paw.

E: Relative change in threshold of withdrawal to thermal stimulus (Hargreaves' test) and **F:** Relative change in 50% threshold to mechanical stimulus (von Frey's hairs) following ligation of the left L5 spinal nerve (SNL).

See text for statistical analysis.

$Na_V1.8$Cre2+/- animals was not significantly different from that of six male C57BL/6 animals. The mean licking/biting time of the $Na_V1.8$Cre2+/- and C57BL/6 animals was 107.2±12.6 and 96.1±10.3 secs respectively in the first phase and 230.8±47.7 and 290.6±45.4 secs respectively in the second phase. When analysed using an unpaired 2-tailed *t* test, P =0.51 for the first phase and P =0.38 for the second phase.

4.3.1.4.2. Intraplantar carrageenan Figure 4.4 B.

Nine $Na_V1.8$Cre2+/- and seven C57BL/6 animals received intraplantar carrageenan and eight $Na_V1.8$Cre2+/- and seven C57BL/6 animals received intraplantar saline. The latency to withdrawal from a thermal stimulus was measured before injection and hourly for three hours after injection. The baseline withdrawal latencies for all the $Na_V1.8$Cre2+/- and C57BL/6 mice were 14.06±0.37 and 12.91±0.7 seconds respectively (P=0.15 when compared using an unpaired t-test). Intraplantar injection of carrageenan induced thermal hyperalgesia within 1 hour of injection and this was sustained for the three time points measured.

Injection of saline resulted in little change in the thermal withdrawal threshold at any time point. As expected, the difference between the response to carrageenan and to saline was highly significant for both the $Na_V1.8$Cre2+/- and C57BL/6 animals (P <0.001 at each time point for both groups – analysis using two way analysis of variance with repeated measures).

For further analysis, the data were normalised by dividing the mean latency at a given time point after carrageenan injection by the baseline latency for each mouse. A two way analysis of variance test with revealed that there was no significant difference in the response to carrageenan or saline between the $Na_V1.8$Cre2+/- and C57BL/6 animals at a given time point after injection; for carrageenan, P =0.31 and for saline, P=0.42. In addition, there was no significant difference in the responses at each time point after injection between the $Na_V1.8$Cre2+/- and C57BL/6 animals - P=0.63 for carrageenan, and P=0.43 for saline.

4.3.1.4.3. Intraplantar CFA Figure 4.4 C, D.

Intraplantar injection of CFA resulted in thermal and mechanical hyperalgesia that developed within 24 hours of injection in both the $Na_V1.8$Cre2+/- animals (n=6) and

wild type littermates (n=6). The hyperalgesia was most pronounced three days after CFA injection in both groups and thereafter returned towards baseline levels. The baseline thermal withdrawal thresholds were 12.76±0.62 secs and 10.67±0.7 secs for the $Na_V1.8Cre2+/-$ mice and wild type littermates respectively (P=0.05 when compared using an unpaired t-test). The baseline 50% withdrawal thresholds to mechanical stimuli were 2.24±0.34g and 2.02±0.28g for the $Na_V1.8Cre2+/-$ mice and wild type littermates respectively (P=0.64 when compared using an unpaired t-test).

For analysis, the withdrawal latency and mean 50% response data were normalised as described for carrageenan, and compared using two way repeated measures analysis of variance. There was no difference in the relative change in either the latency of withdrawal to a thermal stimulus or the 50% withdrawal threshold to a mechanical stimulus between the $Na_V1.8Cre2+/-$ animals and wild type littermates at any time point: P =0.79 and 0.74 respectively.

4.3.1.5. Chung model of neuropathic pain Figure 4.4, E, F.

Six $Na_V1.8Cre2+/-$ animals and four wild type littermates underwent ligation of the left L_5 spinal nerve and developed thermal and mechanical hyperalgesia that began within one day of surgery and reached maximal levels at six days. The thermal hyperalgesia observed was less pronounced than the mechanical hyperalgesia and gradually returned towards baseline levels, whereas the mechanical hyperalgesia was sustained throughout the duration of assessment. The baseline thermal withdrawal thresholds were 11.81±0.42 secs and 11.19±1.15 secs for the $Na_V1.8Cre2+/-$ mice and wild type littermates respectively (P=0.58 when compared using an unpaired t-test). The baseline 50% withdrawal thresholds to mechanical stimuli were 2.69±0.65g and 1.58±0.32g for the $Na_V1.8Cre2+/-$ mice and wild type littermates respectively (P=0.23 when compared using an unpaired t-test).

Data was normalised as described for injection of carrageenan, and when compared, using two way analysis of variance with repeated measures, there was no significant difference in the relative change in either the latency of withdrawal to a thermal stimulus or the 50% withdrawal threshold to a mechanical stimulus between the

$Na_V1.8$Cre2+/- animals and wild type littermates at any time point: P =0.76 and 0.1 respectively.

4.3.2 $Na_V1.8$-mediated currents in small diameter sensory neurons from heterozygous $Na_V1.8$Cre2 mice. Figure 4.5.

In small diameter neurons from wild type mice, 22 of 23 neurons expressed functional $Na_V1.8$ current. Similarly, 22 of 24 neurons from $Na_V1.8$Cre2+/- mice generated the current – see Figure 4.5. For those neurons in which the current was recorded, the $Na_V1.8$ current density in wild type neurons was $65.00 \times 10^{-3} \pm 22.51 \times 10^{-3}$ nA/pF (n = 22), and this was not different from the current density in $Na_V1.8$Cre2+/ - neurons - $77.34 \times 10^{-3} \pm 11.80 \times 10^{-3}$ nA/pF (n = 22) (P = 0.63 Student's t-test). In 26 neurons from $Na_V1.8$Cre2-/- mice, no currents attributable to $Na_V1.8$ were recorded. These data suggest that the functional loss of a single copy of the $Na_V1.8$ gene following targeting of Cre does not affect the TTX-resistant current density in small diameter DRG neurons, and that $Na_V1.8$Cre2-/- animals are effectively $Na_V1.8$ null mutants.

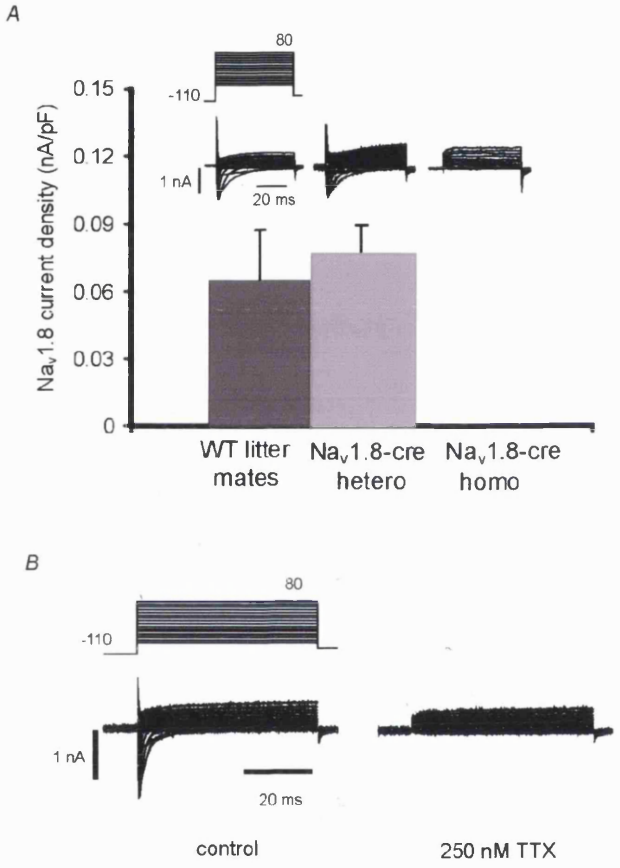

Figure 4.5: TTX-resistant current in small diameter neurons from $Na_V1.8$Cre2 -/-, +/- and +/+ littermates.

A: Mean $Na_V1.8$ current density is unchanged with the functional loss of one $Na_V1.8$ gene, whereas no TTX-resistant Na^+ currents were found in neurons from $Na_V1.8$Cre2 -/- mice. Inset: left, centre and right panels - example currents recorded from wild type, $Na_V1.8$Cre2 heterozygous and homozygous DRG neurons respectively. Left panel includes pulse protocol (mV). **B:** In neurons from $Na_V1.8$Cre2 -/- mice, only TTX-sensitive transient Na^+ currents remain. Left hand panel - currents recorded without external TTX, , right hand panel - currents recorded after superfusion of 250 nM TTX.

4.4. Discussion

The results of the behavioural and electrophysiological experiments presented in this chapter show that heterozygous F3 and F4 $Na_V1.8$Cre2 mice have a similar phenotype to C57BL/6 or wild type littermate controls in tests of thermal and mechanical thresholds, in models of inflammatory and neuropathic pain and in the nature of the $Na_V1.8$ mediated current in small diameter neurons. The data confirm that there is no gene dose effect with $Na_V1.8$ in line with data presented by Akopian *et al.,* on heterozygous $Na_V1.8$ null mutant mice (Akopian et al., 1999).

The nociceptive behavioural phenotype observed in this study is similar to that of wild type mice reported by other groups (e.g. (Abbadie et al., 2003; Akopian et al., 1999; Mogil et al., 1999a; Saegusa et al., 2001). The only difference was in the weights of $Na_V1.8$Cre2+/- mice when compared to that of C57BL/6 control mice - $Na_V1.8$Cre2+/- mice were significantly heavier. This difference may be because inbred mice are lighter than hybrid mice, or because C57BL/6 mice of 8 weeks of age were ordered specifically for the behavioural experiments whereas some of the heterozygous mice used were 2-3 weeks older than this. Alternatively, the insertion of Cre has an effect on the weight of the animals. The latter factor is unlikely since there was no difference in weight when $Na_V1.8$Cre2+/- and wild type littermates were compared.

In the last few years some attention has been focused on the genetic and environmental factors that can confound interpretation of an observed behavioural phenotype in genetically modified mice, particularly when assessing for a nociceptive behavioural phenotype. As in this project, gene targeting is usually carried out in ES cells derived from a 129 substrain since these cells are easily derived from 129 mice, are stable during manipulation in culture, and remain able to contribute to the germline after injection into blastocysts (Simpson et al., 1997). The host strain most commonly used is C57BL/6 since this inbred strain favours competition from the injected 129 ES cells. The resulting chimera are crossed to C57BL/6 animals and if there is germ line transmission of the 129 derived genes, half of the resulting progeny will be

heterozygous for the 129 derived genome, including the targeted gene. The heterozygous animals are then interbred to produce F2 null mutant, heterozygous and wild type offspring. The genomes of the F2 offspring are differing random hybrids of 129 and C57BL/6 at all loci except the target locus. Since it is known that these two mouse strains are associated with different behavioural phenotypes, this can lead to the incorrect attribution of a particular phenotype to the targeted gene mutation when in fact it is due to differences in the background. Lariviere *et al.,* reviewed the two major mechanisms by which this occurs (Lariviere et al., 2001). Firstly, the 'hitchhiking donor gene confound' refers to the genetically linked material that surrounds the targeted gene, derived from the donor 129 genome, present in the heterozygous animals. In the wild type littermates this material is derived from the C57BL/6 genome. Therefore it is possible that an observed phenotype is due to one of these 129-derived hitchhiking genes rather than the targeted mutation. Although back crossing with C57BL/6 animals reduces the contribution of the 129 genome, a significant amount (~1%) is still present after as many as 12 backcrosses (Lariviere et al., 2001). The second confounding factor is epistasis, a term that refers to the interaction between genes that influence a given trait. Thus, alleles within one genetic background may interact with the mutated gene in ways that affect the observed phenotype, whereas there may be little or no interaction with alleles from another genetic background.

Mogil *et al.,* have painstakingly described and compared the phenotypes of eleven strains of inbred mice, including the 129 and C57BL/6 strains, in over 20 nociceptive behavioural tests (Lariviere et al., 2002; Mogil et al., 1999a; Mogil et al., 1999b). Their work has revealed that there is a great variation in the sensitivity to a given nociceptive test across different strains and that there is no consistency in the sensitivity of a particular strain to different tests. 129 mice have a very different nociceptive phenotype to C57BL/6 mice, being generally more insensitive in tests of thermal and mechanical thresholds, and more sensitive in tests of thermal and mechanical hypersensitivity and to a range of analgesic agents (Lariviere et al., 2001).

As well as genetic factors, there are several environmental factors that can also contribute to a nociceptive phenotype. These include the robust phenomenon of stress-induced analgesia, to which group housing of mice, the use of restrainers, and inadequate habituation in a novel testing environment can significantly contribute (Wilson and Mogil, 2001). In addition, the test must be carefully chosen to ensure that it assesses the desired pathway, and detailed planning undertaken to ensure that the testing paradigm, including factors such as stimulus intensity, repetition of the test and enpoints measured, results in reliable data. Chesler *et al.,* recently analysed factors influencing baseline thermal nociceptive sensitivity, assessed using a single test (tail withdrawal) performed over 8000 times by a number of experimenters on a variety of strains of mice, in different conditions. They revealed that the experimenter performing the test had a greater influence on the test outcome than the genetic background of the mouse, and that factors such as season, humidity, cage density and time of experimenting can also influence the outcome (Chesler et al., 2002)

One can estimate that approximately 90% of the genome of the heterozygous F3 and F4 animals used in these experiments was of C57BL/6 origin, and when compared with C57BL/6 animals or wild type littermates there was no phenotypic difference in any of the tests. This suggests that the potential confounding genetic effects are not significant in the targeting of the $Na_V1.8$ allele. Care was taken to minimise environmental factors – all tests were performed by the same experimenter, the ambient temperature was maintained, almost all were performed in the morning, adequate habituation was allowed before commencing analysis, and tests were performed in the same physical environment. These factors may all have contributed to the nature of the data gathered.

In summary, this chapter presents data showing that the nociceptive behavioural phenotype and the $Na_V1.8$ mediated current in heterozygous $Na_V1.8Cre2$ mice, in which there is loss of a functional $Na_V1.8$ allele, is not different from that of wild type mice. These data confirm that these animals can be used to delete a floxed target gene in nociceptors and the resulting phenotype attributed to the loss of the target gene only.

Chapter 5

Final Discussion

In this project, the specific localisation of the voltage gated sodium channel, $Na_V1.8$ (Djouhri et al., 2003a) has been exploited to develop a nociceptor specific Cre expressing mouse. The Cre gene (Gagneten et al., 1997) was targeted to the translational start site of the $Na_V1.8$ gene in 129 embryonic stem (ES) cells, correctly targeted ES cells were successfully transferred to C57BL/6 blastocysts and germ line transmitting $Na_V1.8$Cre chimeras generated.

Examination of the expression pattern of functional Cre in these animals using ROSA26 reporter mice (Soriano, 1999) revealed that it follows that of the target gene, $Na_V1.8$Cre2-mediated recombination commenced at E13 and was confined primarily to small diameter neurons in dorsal root, trigeminal and nodose ganglia. Within the DRGs, expression closely followed that of $Na_V1.8$. A very low number of cells in the superior cervical ganglia also showed Cre expression. No expression was seen in non-neuronal tissue or in the central nervous system. Electrophysiological examination of the TTX-resistant current in small diameter DRG neurons in culture from heterozygous $Na_V1.8$Cre2 animals revealed that it was identical to that in small diameter DRG neurons from wild-type animals. The nociceptive behavioural phenotype of heterozygous $Na_V1.8$Cre2 animals was not different from that of wild-type control animals in measures of acute pain thresholds or in models of inflammatory and neuropathic pain.

These data suggest that the $Na_V1.8$Cre2 mouse can be used to delete genes of interest exclusively in nociceptors, particularly those with a broad expression pattern. This is achieved by crossing them to mice in which the gene of interest is floxed. The phenotype of animals that are homozygous for the floxed target gene and heterozygous for $Na_V1.8$Cre2 can be compared with that of animals that are homozygous for the floxed target gene only. Any phenotypical difference can be attributed to deletion of the target gene within the nociceptor population.

Many of the currently available adjuvant analgesic drugs used to treat neuropathic pain exert their effects by action at a number of different receptors localised in both the peripheral and central nervous system (Beydoun and Backonja, 2003). Their use is often limited by unpleasant side effects many of which are centrally mediated.

Analgesics with a more selective profile and that have a predominantly peripheral site of action are therefore needed. Development of agents that act peripherally is potentially possible because of the physiological blood brain barrier, and they are likely to have fewer adverse effects. However, before such developments can be made, evidence that a selective peripheral site of action would result in effective pain relief is required. Nociceptor-specific gene deletion using the $Na_V1.8Cre2$ mouse will provide insights into the mechanisms of pathophysiological pain and potentially provide an impetus for the development of more effective and more selective analgesics.

There are other experimental approaches that have been used to induce a regional reduction in gene expression. Antisense oligonucleotides are short single stranded DNA molecules complementary to a chosen mRNA sequence. On hybridising to their cognate sequence, they prevent translation either by inducing degradation of mRNA or by physically interfering with the translational machinery (Dias and Stein, 2002). Local administration of antisense oligonucleotides in dorsal root ganglia has been shown to induce a reduction of $P2X_3$ (Honore et al., 2002) and $Na_V1.8$ (Lai et al., 2002) in *in vivo* studies, providing insights into the role of these genes in nociception. Regional administration of small interfering RNAs (siRNA) also results in a local reduction in gene expression (McManus and Sharp, 2002). These are short lengths of double stranded RNA that bind to their cognate mRNA sequence and induce its degradation, utilising an endogenous method of post-transcriptional gene silencing. SiRNA has been shown to be effective *in vitro* in neuronal cell lines (Gan et al., 2002) but there have been no *in vivo* reports of the effects of siRNA in neuronal tissue.

Another approach, viral gene therapy, has been developed in the last ten years as a means of delivering exogenous DNA to a variety of host cells (Lundstrom, 2003). Its use to deliver Cre in order to induce a regional deletion of a floxed target gene has been demonstrated with moderate efficacy in lumbar DRGs (Rinaldi et al., 1999) and in the dorsal horn of the spinal cord (South et al., 2003).

These approaches to induce a regional reduction in gene expression are technically more simple and quick than the generation and utilisation of a site-specific Cre expressing mouse line. However, when compared, use of a Cre expressing mouse line to achieve site-specific gene deletion has several advantages. The use of a cell specific promoter to drive Cre expression ensures that gene deletion occurs within a specific cell population, whereas the site of action of antisense, siRNA or virally delivered Cre is local to the site of delivery and therefore is not cell type specific. Gene delivery using viral vectors is also dependent on the trophism of the virus. Complete deletion of a target gene is much less likely using one of the other methods because of dosage and penetration problems. In addition, Cre mediated recombination results in permanent gene deletion, whereas antisense or siRNA induce a transient reduction in gene expression only. Thus although these techniques may be useful to elucidate the role of a gene *in vivo*, they are unlikely to give as detailed insights into the function of specific gene products in nociceptors.

There are two factors that potentially limit the use of the $Na_V1.8$Cre mouse. The first is associated with the promoter chosen to drive Cre expression, $Na_V1.8$: although this promoter is expressed almost exclusively in nociceptors, there is evidence that a minority of nociceptive neurons do not express $Na_V1.8$ (Djouhri et al., 2003a), and that a minority of low threshold mechanoreceptors do express $Na_V1.8$ (Djouhri et al., 2003a; Novakovic et al., 1998; Renganathan et al., 2000). These data raise the possibility that a small percentage of nociceptors would continue to express the target gene and that there may be target gene deletion in low threshold non-nociceptive neurons.

The second limiting factor is related to the onset of Cre expression that follows that of $Na_V1.8$. In this study, Cre mediated recombination was detected at E13, and was significant by E15. This raises the possibility that onset of Cre mediated deletion of a target gene at this stage in ontogeny could induce compensatory changes in the levels of expression of related genes within this cell population and so mask a phenotype. These factors should be considered when assessing a nociceptor target gene deleted animal.

The generation of an inducible nociceptor specific Cre mouse in which both spatial and temporal expression of Cre is controlled is a potential development of this project that would circumvent the problems of compensation outlined above. There are several methods available to generate an inducible Cre. The tetracycline regulatory system, initially developed by Gossen and Bujard (Gossen and Bujard, 1992; Gossen et al., 1995), is based on the transgenic approach and involves using a promoter with the desired expression pattern to drive a transcription factor, the tetracycline transactivator, whose binding to a minimal promoter is dependent on the administration of tetracycline or its derivative doxycycline. The minimal promoter drives expression of the desired transgene, in this case Cre. Two systems have been developed – the 'tet-off' system and the 'tet-on' system. In the 'tet-off' system, in the absence of doxycycline the transactivator induces transgene transcription, and on administration of doxycycline, a conformational change occurs in the transactivator preventing transgene transcription. In the 'tet-on' system the transactivator is mutated so that transgene expression only occurs in the presence of doxycycline. Several groups have demonstrated the use of this system to control Cre expression, showing that Cre mediated deletion of floxed target genes can be induced and occurs exclusively in the target cell population following drug administration (Lindeberg et al., 2002; Saam and Gordon, 1999). However to induce Cre mediated gene deletion using this system, three mouse lines are required – one in which the tetracycline transactivator is controlled by the promoter with the desired expression pattern, one in which the minimal promoter is driving Cre expression and one in which the target gene is floxed. These three lines need to be interbred to achieve Cre mediated target gene deletion. The other limiting factors of this system include the potential for positional effects of the transgenes, for incomplete suppression of Cre expression and poor drug penetration into neuronal tissues.

In order to utilise the $Na_V1.8$Cre mouse that has been developed in this project, exploitation of the Cre-oestrogen receptor (Cre-ER) fusion protein, Cre-ER^{T2} developed by Metzger and Chambon, or another more recently described Cre-ER fusion protein, Cre-ER^{TM} (Danielian et al., 1998), is a much more suitable approach, since the targeting vector could be modified to incorporate the Cre-ER gene. In this

system, temporal control of Cre activity is achieved by fusing the *cre* gene to a mutated form of the ligand-binding domain (LBD) of the oestrogen receptor. This receptor is a member of the nuclear receptor superfamily that is sequestered in the cytoplasm until the endogenous ligand, 17β-oestrodiol, binds. Upon ligand binding, the interaction with the sequestering protein, heat shock protein 90, Hsp90, is disrupted, and the receptor is able to translocate to the nucleus. Fusion of Cre to the oestrogen receptor LBD therefore also results in sequestration of Cre in the cytoplasm preventing recombination, a nuclear event, until the ligand binds. Metzger *et al.,* first demonstrated that administration of the endogenous oestrogen agonist 17β-oestrodiol or the synthetic oestrogen antagonist 4-hydroxytamoxifen (OHT) to F9 murine embryonal carcinoma cells expressing Cre-ER resulted in induction of Cre mediated recombination (Metzger et al., 1995). The same group went on to mutate the LBD of the receptor to render it insensitive to 17β-oestradiol but sensitive to synthetic oestrogen antagonists, creating Cre-ER^T and Cre-ER^{T2}, so that the system could be used *in vivo*. Cre-ER^{T2} was shown to be 4-fold more sensitive to OHT than Cre-ER^T (Feil et al., 1997). They also used the transgenic approach to introduce Cre-ER^T *in vivo* under the control of the ubiquitous cytomegalovirus promoter (Metzger and Chambon, 2001). They examined Cre activity in lacZ expressing reporter mice and showed that there was some degree of excision after OHT administration in all tissues except the thymus with a maximum level of ~50% seen in the tail.

The generation of an inducible nociceptor specific Cre expressing mouse is clearly a potential development of the $Na_V1.8$Cre2 mouse. Replacing the Cre gene used in this project with Cre-ER^{T2} or Cre-ER^{TM} is the most attractive strategy as it would exploit the targeting vector already generated, and so the tight expression pattern of the Cre. It would be important to examine whether the presence of the Cre-fusion gene alters the expression pattern and whether there is any basal Cre expression in the absence of OHT administration. In addition detailed examination of the timing of the onset of Cre expression after OHT administration, the maximal level of Cre mediated recombination achieved, and the time for Cre to complete target gene recombination would be needed.

There is mounting evidence that the non-nociceptive afferent sensory neuron population also contributes to the generation of pathological pain states. As mentioned before, there is evidence that the upregulation of the embryonic TTX-sensitive VGSC $Na_V1.3$ in neuropathic pain occurs in myelinated sensory neurons (Kim et al., 2001). There is evidence that the phenotype of non-nociceptive $A\alpha/\beta$ neurons changes in models of inflammatory pain – substance P is released from their central terminals and they develop a nociceptive phenotype (Neumann et al., 1996). The neurotrophic factor BDNF is released centrally from nociceptive neurons but its receptors are localised on myelinated neurons (Pezet et al., 2002). Therefore the generation of a mouse in which Cre expression occurs in myelinated, predominantly non-nociceptive sensory neurons would provide valuable insights into nociception as well as complementing the results of studies in which the $Na_V1.8$Cre mouse is used. Mallucci *et al.,* used the transgenic approach to generate a mouse line in which Cre expression is driven by the control elements of the murine neurofilament-H gene (Mallucci et al., 2002). They reported that Cre mediated recombination in transmitting founder lines started approximately 10 weeks after birth and was confined exclusively to myelinated neurons. This study focused particularly on Cre mediated recombination within the central nervous system, but since neurofilament-H is a marker of myelinated sensory neurons, this mouse line could be used to examine the effects of target gene deletion within these predominantly non-nociceptive neurons. An attractive feature of this mouse line is that the onset of Cre expression occurs in adulthood, so the role of target genes before this time would not be affected. In the case of $Na_V1.3$, whose levels of expression in the central nervous system are high *in utero* but fall significantly after birth, this feature is particularly relevant.

There are many target genes that could be studied using the $Na_V1.8$Cre mouse. Neuronal plasticity underlies the development of neuropathic and inflammatory pain; a host of changes occur in primary sensory neurons, in the spinal cord and in the brain following injury. Alterations in the localisation of proteins, in their phosphorylation status and threshold for activation, and in their expression have

been reported. The changes are not consistent between different types of injury or between different cells within the sensory pathway. Neurotransmitters, receptor proteins and second messengers that are induced following injury are all potentially interesting targets for nociceptor specific gene deletion.

The peptidergic neurotransmitter substance P (SP) that is released from TrkA positive nociceptors is the ligand for the G-protein coupled neurokinin-1 (NK-1) receptor. This receptor is localised on afferent sensory neurons, within the spinal cord and in the brain. Approximately two-thirds of NK-1 expressing sensory neurons are unmyelinated and one-third are myelinated (von Banchet et al., 1999). Within the spinal cord, NK-1 receptors are found in lamina 1, and in the brain they are in the forebrain and in brainstem areas associated with pain. NK-1 receptor null mutant mice have normal baseline nociceptive thresholds but are analgesic in models of inflammatory pain. In addition they show a reduction in stress induced analgesia and in aggressive behaviour (De Felipe et al., 1998). Other studies have shown that these receptors play a role in opiate reward (Murtra et al., 2000). Use of the $Na_V1.8Cre2$ mouse to delete the NK-1 receptor in nociceptors would help to clarify their role in the development of inflammatory pain.

The utility of opioid receptor agonists in the management of chronic pain is well established (e.g. McQuay, 1999), although a significant minority of patients, particularly those with neuropathic pain, have partially or completely opioid insensitive pain. Another problem with the use of opioids in the management of pain is that it is often accompanied and/or limited by side effects, many of which are centrally mediated (Moulin et al., 1996). Opioid receptors are widely distributed throughout the central and peripheral nervous system and almost all opioid receptor agonists used clinically to relieve pain act both peripherally and centrally. Within the peripheral nervous system, afferent sensory neurons express μ, δ and κ opioid receptor transcript and protein, and receptor proteins are detectable within peripheral nerve terminals (Mousa et al., 2001). There is an upregulation of opioid receptor synthesis and expression in sensory neurons following inflammation and in models of neuropathic pain. Mousa *et al.,* (Mousa et al., 2001) reported an upregulation of μ opioid receptors in DRGs, evidence of receptor transport along the sciatic nerve and

accumulation of the receptors at peripheral nerve terminals after Complete Freud's Adjuvant induced inflammation of the hind paw. Truong *et al.,* (Truong et al., 2003) demonstrated that after chronic constriction of the sciatic nerve in rats, there is an accumulation of μ opioid receptors both proximal and distal to the site of injury and an increase in the percentage of μ opioid receptor immunopositive DRG neurons. In addition they showed that percutaneous perfusion of low dose morphine over the injury site resulted in a profound reversal of mechanical and thermal hyperalgesia. Systemic administration of the morphine at the same dose had no analgesic effect. These studies demonstrate that peripheral opioid receptors play an important role in pathophysiological pain and that further exploration using nociceptor specific deletion is warranted.

Protein kinase-A (PKA) and protein kinase-C (PKC) are induced following tissue or nerve injury, and mediate phosphorylation of various receptors in nociceptors and in the spinal cord. The resulting alteration in receptor function contributes to the generation of peripheral and central sensitisation. There are ten PKC isoforms with differing distributions. Malmberg *et al.,* generated a PKCγ null mutant mouse and demonstrated the role of this spinally located isoform in the generation of neuropathic pain (Malmberg et al., 1997). PKCε null mutant mice have also been generated and these animals have a normal baseline nociceptive phenotype but show marked analgesia in models of inflammatory pain (Khasar et al., 1999). PKCε is widely distributed throughout the peripheral and central nervous system, so although this study demonstrated an analgesic phenotype, nociceptor specific deletion would help to dissect the contribution of central and peripheral PKCε.

As discussed previously, all voltage gated sodium channel isoforms except $Na_V1.3$, 1.4 and 1.5 are constitutively expressed in afferent sensory neurons of adult mice, and all but $Na_V1.8$ and $Na_V1.9$ are also expressed in other excitable tissues. There is evidence to suggest that some of these more broadly expressed VGSCs play a role in the generation of pathophysiological pain but the lack of isoform specific inhibitors of the channels has precluded determination of their individual contributions. The TTX-sensitive VGSC $Na_V1.7$ (Toledo-Aral et al., 1997) is thought to play a role in the generation and propagation of TTX-sensitive currents in nociceptors (Djouhri et

al., 2003b; Herzog et al., 2001). $Na_V1.7$ is found in the soma and nerve terminals of large, medium and small diameter DRGs and in sympathetic ganglia. Djouhri *et al.,* (Djouhri et al., 2003b) showed that it is predominantly found in nociceptive neurons - all C, 90% of Aδ- and 40% of Aα/β fibre units expressed $Na_V1.7$ protein. Akopian *et al.,* reported that in $Na_V1.8$ null mutant mice, there is a compensatory upregulation of $Na_V1.7$ mRNA and of the TTX-sensitive current (Akopian et al., 1999). The level of thermal hyperalgesia following intraplantar carrageenan in these animals is the same as in wild type animals, but is markedly reduced by systemic administration of low dose lidocaine, that preferentially blocks TTX-sensitive voltage-gated sodium channels, in null mutants only. Further exploration of the role of $Na_V1.7$ in inflammatory pain using the $Na_V1.8$Cre2 mouse is therefore warranted and has been carried out by Dr. Mohammed Nassar in this laboratory. He used gene targeting to insert *loxP* sites around exons 14 and 15 of $Na_V1.7$, that encode most of the second domain of the channel including the voltage sensor, and successfully generated a floxed $Na_V1.7$ mouse. Null mutant $Na_V1.7$ animals were generated initially using a general Cre deletor mouse (Schwenk et al., 1995) These animals survived to term but died within 12 hours of birth, primarily because of a failure to feed. Nociceptor specific deletion of $Na_V1.7$ was then achieved using the $Na_V1.8$Cre2 mouse. The resulting animals were of normal weight and motor function. In nociceptive testing, $Na_V1.7$ nociceptor deleted animals showed a moderate analgesic phenotype in acute thermal withdrawal thresholds (Hargreaves' test), and a marked analgesic phenotype both in the Randall Selitto test of acute withdrawal thresholds to noxious mechanical pressure and in all inflammatory pain models. These data confirm that the $Na_V1.8$Cre2 mouse is able to mediate DRG-specific deletion of a floxed target gene, that this system is a means of gaining insights into the role of a broadly expressed gene whose null mutant phenotype is perinatal lethal, and highlight the role of $Na_V1.7$ in mediating inflammatory pain.

In summary the utility of the $Na_V1.8$Cre mouse has been demonstrated by the generation of a $Na_V1.7$ nociceptor specific deleted mouse providing insights into the role of this gene in inflammatory pain. There are many other exciting target genes

whose role in nociception could be explored using the $Na_V1.8$Cre mouse. In addition the development of an inducible $Na_V1.8$Cre mouse and the use of a non-nociceptor sensory neuron expressing Cre mouse are future developments of this project.

References

Abbadie, C., Lindia, J. A., Cumiskey, A. M., Peterson, L. B., Mudgett, J. S., Bayne, E. K., DeMartino, J. A., MacIntyre, D. E., and Forrest, M. J. (2003). Impaired neuropathic pain responses in mice lacking the chemokine receptor CCR2. Proc Natl Acad Sci U S A *100*, 7947-7952.

Akopian, A. N., Sivilotti, L., and Wood, J. N. (1996). A tetrodotoxin-resistant voltage-gated sodium channel expressed by sensory neurons. Nature *379*, 257-262.

Akopian, A. N., Souslova, V., England, S., Okuse, K., Ogata, N., Ure, J., Smith, A., Kerr, B. J., McMahon, S. B., Boyce, S., *et al.* (1999). The tetrodotoxin-resistant sodium channel SNS has a specialized function in pain pathways. Nat Neurosci *2*, 541-548.

Amaya, F., Decosterd, I., Samad, T. A., Plumpton, C., Tate, S., Mannion, R. J., Costigan, M., and Woolf, C. J. (2000). Diversity of expression of the sensory neuron-specific TTX-resistant voltage-gated sodium ion channels SNS and SNS2. Mol Cell Neurosci *15*, 331-342.

Amaya, F., Oh-hashi, K., Naruse, Y., Iijima, N., Ueda, M., Shimosato, G., Tominaga, M., Tanaka, Y., and Tanaka, M. (2003). Local inflammation increases vanilloid receptor 1 expression within distinct subgroups of DRG neurons. Brain Res *963*, 190-196.

Arin, M. J., Longley, M. A., Wang, X. J., and Roop, D. R. (2001). Focal activation of a mutant allele defines the role of stem cells in mosaic skin disorders. J Cell Biol *152*, 645-649.

Awatramani, R., Soriano, P., Mai, J. J., and Dymecki, S. (2001). An Flp indicator mouse expressing alkaline phosphatase from the ROSA26 locus. Nat Genet *29*, 257-259.

Baker, M. D., and Wood, J. N. (2001). Involvement of Na+ channels in pain pathways. Trends Pharmacol Sci *22*, 27-31.

Benn, S. C., Costigan, M., Tate, S., Fitzgerald, M., and Woolf, C. J. (2001). Developmental expression of the TTX-resistant voltage-gated sodium channels Nav1.8 (SNS) and Nav1.9 (SNS2) in primary sensory neurons. J Neurosci *21*, 6077-6085.

Bennett, G. J., and Xie, Y. K. (1988). A peripheral mononeuropathy in rat that produces disorders of pain sensation like those seen in man. Pain *33*, 87-107.

Beydoun, A., and Backonja, M. M. (2003). Mechanistic stratification of antineuralgic agents. J Pain Symptom Manage *25*, S18-30.

Black, J. A., Cummins, T. R., Plumpton, C., Chen, Y. H., Hormuzdiar, W., Clare, J. J., and Waxman, S. G. (1999a). Upregulation of a silent sodium channel after peripheral, but not central, nerve injury in DRG neurons. J Neurophysiol *82*, 2776-2785.

Black, J. A., Dib-Hajj, S., Baker, D., Newcombe, J., Cuzner, M. L., and Waxman, S. G. (2000). Sensory neuron-specific sodium channel SNS is abnormally expressed in the brains of mice with experimental allergic encephalomyelitis and humans with multiple sclerosis. Proc Natl Acad Sci U S A *97*, 11598-11602.

Black, J. A., Fjell, J., Dib-Hajj, S., Duncan, I. D., O'Connor, L. T., Fried, K., Gladwell, Z., Tate, S., and Waxman, S. G. (1999b). Abnormal expression of SNS/PN3 sodium channel in cerebellar Purkinje cells following loss of myelin in the taiep rat. Neuroreport *10*, 913-918.

Boucher, T. J., Okuse, K., Bennett, D. L., Munson, J. B., Wood, J. N., and McMahon, S. B. (2000). Potent analgesic effects of GDNF in neuropathic pain states. Science *290*, 124-127.

Bronson, S. K., and Smithies, O. (1994). Altering mice by homologous recombination using embryonic stem cells. J Biol Chem *269*, 27155-27158.

Buchholz, F., Angrand, P. O., and Stewart, A. F. (1998). Improved properties of FLP recombinase evolved by cycling mutagenesis. Nat Biotechnol *16*, 657-662.

Burnstock, G. (2002). Potential therapeutic targets in the rapidly expanding field of purinergic signalling. Clin Med *2*, 45-53.

Capecchi, M. R. (1989). The new mouse genetics: altering the genome by gene targeting. Trends Genet *5*, 70-76.

Caterina, M. J., Rosen, T. A., Tominaga, M., Brake, A. J., and Julius, D. (1999). A capsaicin-receptor homologue with a high threshold for noxious heat. Nature *398*, 436-441.

Caterina, M. J., Schumacher, M. A., Tominaga, M., Rosen, T. A., Levine, J. D., and Julius, D. (1997). The capsaicin receptor: a heat-activated ion channel in the pain pathway. Nature *389*, 816-824.

Catterall, W. A. (2000). From ionic currents to molecular mechanisms: the structure and function of voltage-gated sodium channels. Neuron *26*, 13-25.

Cesare, P., and McNaughton, P. (1996). A novel heat-activated current in nociceptive neurons and its sensitization by bradykinin. Proc Natl Acad Sci U S A *93*, 15435-15439.

Chaplan, S. R., Bach, F. W., Pogrel, J. W., Chung, J. M., and Yaksh, T. L. (1994). Quantitative assessment of tactile allodynia in the rat paw. J Neurosci Methods *53*, 55-63.

Chaplan, S. R., Guo, H. Q., Lee, D. H., Luo, L., Liu, C., Kuei, C., Velumian, A. A., Butler, M. P., Brown, S. M., and Dubin, A. E. (2003). Neuronal hyperpolarization-activated pacemaker channels drive neuropathic pain. J Neurosci *23*, 1169-1178.

Chen, C. C., Akopian, A. N., Sivilotti, L., Colquhoun, D., Burnstock, G., and Wood, J. N. (1995). A P2X purinoceptor expressed by a subset of sensory neurons. Nature *377*, 428-431.

Chen, C. C., England, S., Akopian, A. N., and Wood, J. N. (1998). A sensory neuron-specific, proton-gated ion channel. Proc Natl Acad Sci U S A *95*, 10240-10245.

Chen, L., and Huang, L. Y. (1992). Protein kinase C reduces Mg2+ block of NMDA-receptor channels as a mechanism of modulation. Nature *356*, 521-523.

Chesler, E. J., Wilson, S. G., Lariviere, W. R., Rodriguez-Zas, S. L., and Mogil, J. S. (2002). Identification and ranking of genetic and laboratory environment factors influencing a behavioral trait, thermal nociception, via computational analysis of a large data archive. Neurosci Biobehav Rev *26*, 907-923.

Chul Han, H., Hyun Lee, D., and Mo Chung, J. (2000). Characteristics of ectopic discharges in a rat neuropathic pain model. Pain *84*, 253-261.

Costigan, M., and Woolf, C. J. (2000). Pain: molecular mechanisms. J Pain *1*, 35-44.

Crawley, J. N. (2000). General Health. In What's wrong with my mouse? (New York, Wiley-Liss), pp. 31-46.

Cummins, T. R., Black, J. A., Dib-Hajj, S. D., and Waxman, S. G. (2000). Glial-derived neurotrophic factor upregulates expression of functional SNS and NaN sodium channels and their currents in axotomized dorsal root ganglion neurons. J Neurosci *20*, 8754-8761.

D'Amour, F. E., Smith, D. L. (1941). A method for determining loss of pain sensation. Journal of Pharmacology and Experimental Therapeutics *41*, 74-79.

Danielian, P. S., Muccino, D., Rowitch, D. H., Michael, S. K., and McMahon, A. P. (1998). Modification of gene activity in mouse embryos in utero by a tamoxifen-inducible form of Cre recombinase. Curr Biol *8*, 1323-1326.

de Boer, J., Williams, A., Skavdis, G., Harker, N., Coles, M., Tolaini, M., Norton, T., Williams, K., Roderick, K., Potocnik, A. J., and Kioussis, D. (2003). Transgenic mice with hematopoietic and lymphoid specific expression of Cre. Eur J Immunol *33*, 314-325.

De Felipe, C., Herrero, J. F., O'Brien, J. A., Palmer, J. A., Doyle, C. A., Smith, A. J., Laird, J. M., Belmonte, C., Cervero, F., and Hunt, S. P. (1998). Altered nociception, analgesia and aggression in mice lacking the receptor for substance P. Nature *392*, 394-397.

Decosterd, I., Ji, R. R., Abdi, S., Tate, S., and Woolf, C. J. (2002). The pattern of expression of the voltage-gated sodium channels Na(v)1.8 and Na(v)1.9 does not change in uninjured primary sensory neurons in experimental neuropathic pain models. Pain *96*, 269-277.

Decosterd, I., and Woolf, C. J. (2000). Spared nerve injury: an animal model of persistent peripheral neuropathic pain. Pain *87*, 149-158.

Dias, N., and Stein, C. A. (2002). Antisense oligonucleotides: basic concepts and mechanisms. Mol Cancer Ther *1*, 347-355.

Dib-Hajj, S., Black, J. A., Felts, P., and Waxman, S. G. (1996). Down-regulation of transcripts for Na channel alpha-SNS in spinal sensory neurons following axotomy. Proc Natl Acad Sci U S A *93*, 14950-14954.

Dib-Hajj, S. D., Tyrrell, L., Black, J. A., and Waxman, S. G. (1998). NaN, a novel voltage-gated Na channel, is expressed preferentially in peripheral sensory neurons and down-regulated after axotomy. Proc Natl Acad Sci U S A *95*, 8963-8968.

Dixon, W. J. (1980). Efficient analysis of experimental observations. Annu Rev Pharmacol Toxicol *20*, 441-462.

Djouhri, L., Fang, X., Okuse, K., Wood, J. N., Berry, C. M., and Lawson, S. N. (2003a). The TTX-resistant sodium channel Nav1.8 (SNS/PN3): expression and correlation with membrane properties in rat nociceptive primary afferent neurons. J Physiol *550*, 739-752.

Djouhri, L., Newton, R., Levinson, S. R., Berry, C. M., Carruthers, B., and Lawson, S. N. (2003b). Sensory and electrophysiological properties of guinea-pig sensory neurones expressing Nav 1.7 (PN1) Na+ channel alpha subunit protein. J Physiol *546*, 565-576.

DOH (2000). The NHS Cancer Plan (Department of Health, NHS).
Dower, W. J., Miller, J. F., and Ragsdale, C. W. (1988). High efficiency transformation of E. coli by high voltage electroporation. Nucleic Acids Res *16*, 6127-6145.

Dubuisson, D., and Dennis, S. G. (1977). The formalin test: a quantitative study of the analgesic effects of morphine, meperidine, and brain stem stimulation in rats and cats. Pain *4*, 161-174.

Dunn, P. M., Zhong, Y., and Burnstock, G. (2001). P2X receptors in peripheral neurons. Prog Neurobiol *65*, 107-134.

Dymecki, S. M. (1996). Flp recombinase promotes site-specific DNA recombination in embryonic stem cells and transgenic mice. Proc Natl Acad Sci U S A *93*, 6191-6196.

Ernstrom, G. G., and Chalfie, M. (2002). Genetics of sensory mechanotransduction. Annu Rev Genet *36*, 411-453.

Evans, M. J., and Kaufman, M. H. (1981). Establishment in culture of pluripotential cells from mouse embryos. Nature *292*, 154-156.

Fang, X., Djouhri, L., Black, J. A., Dib-Hajj, S. D., Waxman, S. G., and Lawson, S. N. (2002). The presence and role of the tetrodotoxin-resistant sodium channel Na(v)1.9 (NaN) in nociceptive primary afferent neurons. J Neurosci *22*, 7425-7433.

Farley, F. W., Soriano, P., Steffen, L. S., and Dymecki, S. M. (2000). Widespread recombinase expression using FLPeR (flipper) mice. Genesis *28*, 106-110.

Feil, R., Wagner, J., Metzger, D., and Chambon, P. (1997). Regulation of Cre recombinase activity by mutated estrogen receptor ligand-binding domains. Biochem Biophys Res Commun *237*, 752-757.

Ferri, G. L., Sabani, A., Abelli, L., Polak, J. M., Dahl, D., and Portier, M. M. (1990). Neuronal intermediate filaments in rat dorsal root ganglia: differential distribution of peripherin and neurofilament protein immunoreactivity and effect of capsaicin. Brain Res *515*, 331-335.

Fiering, S., Epner, E., Robinson, K., Zhuang, Y., Telling, A., Hu, M., Martin, D. I., Enver, T., Ley, T. J., and Groudine, M. (1995). Targeted deletion of 5'HS2 of the murine beta-globin LCR reveals that it is not essential for proper regulation of the beta-globin locus. Genes Dev *9*, 2203-2213.

Fitzgerald, E. M., Okuse, K., Wood, J. N., Dolphin, A. C., and Moss, S. J. (1999). cAMP-dependent phosphorylation of the tetrodotoxin-resistant voltage-dependent sodium channel SNS. J Physiol *516 (Pt 2)*, 433-446.

Friedrich, G., and Soriano, P. (1991). Promoter traps in embryonic stem cells: a genetic screen to identify and mutate developmental genes in mice. Genes Dev *5*, 1513-1523.

Fuchs, P. N., Roza, C., Sora, I., Uhl, G., and Raja, S. N. (1999). Characterization of mechanical withdrawal responses and effects of mu-, delta- and kappa-opioid agonists in normal and mu-opioid receptor knockout mice. Brain Res *821*, 480-486.

Fukuoka, T., Kondo, E., Dai, Y., Hashimoto, N., and Noguchi, K. (2001). Brain-derived neurotrophic factor increases in the uninjured dorsal root ganglion neurons in selective spinal nerve ligation model. J Neurosci *21*, 4891-4900.

Gagneten, S., Le, Y., Miller, J., and Sauer, B. (1997). Brief expression of a GFP cre fusion gene in embryonic stem cells allows rapid retrieval of site-specific genomic deletions. Nucleic Acids Res *25*, 3326-3331.

Gan, L., Anton, K. E., Masterson, B. A., Vincent, V. A., Ye, S., and Gonzalez-Zulueta, M. (2002). Specific interference with gene expression and gene function mediated by long dsRNA in neural cells. J Neurosci Methods *121*, 151-157.

Giamberardino, M. A. (1999). Recent and forgotten aspects of visceral pain. Eur J Pain *3*, 77-92.

Gold, M. S., Weinreich, D., Kim, C. S., Wang, R., Treanor, J., Porreca, F., and Lai, J. (2003). Redistribution of Na(V)1.8 in uninjured axons enables neuropathic pain. J Neurosci *23*, 158-166.

Goldin, A. L., Barchi, R. L., Caldwell, J. H., Hofmann, F., Howe, J. R., Hunter, J. C., Kallen, R. G., Mandel, G., Meisler, M. H., Netter, Y. B., *et al.* (2000). Nomenclature of voltage-gated sodium channels. Neuron *28*, 365-368.

Gong, S., Zheng, C., Doughty, M. L., Losos, K., Didkovsky, N., Schambra, U. B., Nowak, N. J., Joyner, A., Leblanc, G., Hatten, M. E., and Heintz, N. (2003). A gene expression atlas of the central nervous system based on bacterial artificial chromosomes. Nature *425*, 917-925.

Gossen, M., and Bujard, H. (1992). Tight control of gene expression in mammalian cells by tetracycline-responsive promoters. Proc Natl Acad Sci U S A *89*, 5547-5551.

Gossen, M., Freundlieb, S., Bender, G., Muller, G., Hillen, W., and Bujard, H. (1995). Transcriptional activation by tetracyclines in mammalian cells. Science *268*, 1766-1769.

Greene, L. A. (1989). A new neuronal intermediate filament protein. Trends Neurosci *12*, 228-230.

Gu, H., Marth, J. D., Orban, P. C., Mossmann, H., and Rajewsky, K. (1994). Deletion of a DNA polymerase beta gene segment in T cells using cell type-specific gene targeting. Science *265*, 103-106.

Gu, H., Zou, Y. R., and Rajewsky, K. (1993). Independent control of immunoglobulin switch recombination at individual switch regions evidenced through Cre-loxP-mediated gene targeting. Cell *73*, 1155-1164.

Guo, H., Mao, C., Jin, X. L., Wang, H., Tu, Y. T., Avasthi, P. P., and Li, Y. (2000). Cre-mediated cerebellum- and hippocampus-restricted gene mutation in mouse brain. Biochem Biophys Res Commun *269*, 149-154.

Gureje, O., Von Korff, M., Simon, G. E., and Gater, R. (1998). Persistent pain and well-being: a World Health Organization Study in Primary Care. Jama *280*, 147-151.

Hargreaves, K., Dubner, R., Brown, F., Flores, C., and Joris, J. (1988). A new and sensitive method for measuring thermal nociception in cutaneous hyperalgesia. Pain *32*, 77-88.

Heintz, N. (2001). BAC to the future: the use of bac transgenic mice for neuroscience research. Nat Rev Neurosci *2*, 861-870.

Herzog, R. I., Cummins, T. R., and Waxman, S. G. (2001). Persistent TTX-resistant Na+ current affects resting potential and response to depolarization in simulated spinal sensory neurons. J Neurophysiol *86*, 1351-1364.

Holt, S. J., and Sadler, P. W. (1958). Studies in enzyme cytochemistry. III. Relationships between solubility, molecular association and structure in indigoid dyes. Proc R Soc Lond B Biol Sci *148*, 495-505.

Honore, P., Kage, K., Mikusa, J., Watt, A. T., Johnston, J. F., Wyatt, J. R., Faltynek, C. R., Jarvis, M. F., and Lynch, K. (2002). Analgesic profile of intrathecal P2X(3) antisense oligonucleotide treatment in chronic inflammatory and neuropathic pain states in rats. Pain *99*, 11-19.

Honore, P., Rogers, S. D., Schwei, M. J., Salak-Johnson, J. L., Luger, N. M., Sabino, M. C., Clohisy, D. R., and Mantyh, P. W. (2000). Murine models of inflammatory, neuropathic and cancer pain each generates a unique set of neurochemical changes in the spinal cord and sensory neurons. Neuroscience *98*, 585-598.

Hudson, L. J., Bevan, S., Wotherspoon, G., Gentry, C., Fox, A., and Winter, J. (2001). VR1 protein expression increases in undamaged DRG neurons after partial nerve injury. Eur J Neurosci *13*, 2105-2114.

Hunskaar, S., Fasmer, O. B., and Hole, K. (1985). Formalin test in mice, a useful technique for evaluating mild analgesics. J Neurosci Methods *14*, 69-76.

Hunskaar, S., and Hole, K. (1987). The formalin test in mice: dissociation between inflammatory and non-inflammatory pain. Pain *30*, 103-114.

Hunt, S. P., and Mantyh, P. W. (2001). The molecular dynamics of pain control. Nat Rev Neurosci *2*, 83-91.

Hunt, S. P., Pini, A., and Evan, G. (1987). Induction of c-fos-like protein in spinal cord neurons following sensory stimulation. Nature *328*, 632-634.

Iadarola, M. J., Douglass, J., Civelli, O., and Naranjo, J. R. (1988). Differential activation of spinal cord dynorphin and enkephalin neurons during hyperalgesia: evidence using cDNA hybridization. Brain Res *455*, 205-212.

IASP (1994). Classification of chronic pain (Seattle).

Jensen, T. S., and Yaksh, T. L. (1984). Spinal monoamine and opiate systems partly mediate the antinociceptive effects produced by glutamate at brainstem sites. Brain Res *321*, 287-297.

Ji, R. R., Kohno, T., Moore, K. A., and Woolf, C. J. (2003). Central sensitization and LTP: do pain and memory share similar mechanisms? Trends Neurosci *26*, 696-705.

Jin, X. L., Guo, H., Mao, C., Atkins, N., Wang, H., Avasthi, P. P., Tu, Y. T., and Li, Y. (2000). Emx1-specific expression of foreign genes using "knock-in" approach. Biochem Biophys Res Commun *270*, 978-982.

Jones, B. J., and Roberts, D. J. (1968). A rotarod suitable for quantitative measurements of motor incoordination in naive mice. Naunyn Schmiedebergs Arch Exp Pathol Pharmakol *259*, 211.

Joyner, A. L., and Guillemot, F. (1994). Gene targeting and development of the nervous system. Curr Opin Neurobiol *4*, 37-42.

Julius, D., and Basbaum, A. I. (2001). Molecular mechanisms of nociception. Nature *413*, 203-210.
Jung, S., Rajewsky, K., and Radbruch, A. (1993). Shutdown of class switch recombination by deletion of a switch region control element. Science *259*, 984-987.

Kayser, V., and Guilbaud, G. (1987). Local and remote modifications of nociceptive sensitivity during carrageenin-induced inflammation in the rat. Pain *28*, 99-107.

Khasar, S. G., Lin, Y. H., Martin, A., Dadgar, J., McMahon, T., Wang, D., Hundle, B., Aley, K. O., Isenberg, W., McCarter, G., *et al.* (1999). A novel nociceptor signaling pathway revealed in protein kinase C epsilon mutant mice. Neuron *24*, 253-260.

Kidd, B. L., and Urban, L. A. (2001). Mechanisms of inflammatory pain. Br J Anaesth *87*, 3-11.

Kim, C. H., Oh, Y., Chung, J. M., and Chung, K. (2001). The changes in expression of three subtypes of TTX sensitive sodium channels in sensory neurons after spinal nerve ligation. Brain Res Mol Brain Res *95*, 153-161.

Kim, D. S., Choi, J. O., Rim, H. D., and Cho, H. J. (2002). Downregulation of voltage-gated potassium channel alpha gene expression in dorsal root ganglia following chronic constriction injury of the rat sciatic nerve. Brain Res Mol Brain Res *105*, 146-152.

Kim, S. H., and Chung, J. M. (1992). An experimental model for peripheral neuropathy produced by segmental spinal nerve ligation in the rat. Pain *50*, 355-363.

Kozak, M. (1986). Point mutations define a sequence flanking the AUG initiator codon that modulates translation by eukaryotic ribosomes. Cell *44*, 283-292.

Lai, J., Gold, M. S., Kim, C. S., Biana, D., Ossipov, M. H., Hunterc, J. C., and Porreca, F. (2002). Inhibition of neuropathic pain by decreased expression of the tetrodotoxin-resistant sodium channel, NaV1.8. Pain *95*, 143-152.

Laird, J. M., Martinez-Caro, L., Garcia-Nicas, E., and Cervero, F. (2001). A new model of visceral pain and referred hyperalgesia in the mouse. Pain *92*, 335-342.

Lakso, M., Sauer, B., Mosinger, B., Jr., Lee, E. J., Manning, R. W., Yu, S. H., Mulder, K. L., and Westphal, H. (1992). Targeted oncogene activation by site-specific recombination in transgenic mice. Proc Natl Acad Sci U S A *89*, 6232-6236.

Lariviere, W. R., Chesler, E. J., and Mogil, J. S. (2001). Transgenic studies of pain and analgesia: mutation or background genotype? J Pharmacol Exp Ther *297*, 467-473.

Lariviere, W. R., Wilson, S. G., Laughlin, T. M., Kokayeff, A., West, E. E., Adhikari, S. M., Wan, Y., and Mogil, J. S. (2002). Heritability of nociception. III. Genetic relationships among commonly used assays of nociception and hypersensitivity. Pain *97*, 75-86.

Lawson, S. N. (2002). Phenotype and function of somatic primary afferent nociceptive neurones with C-, Adelta- or Aalpha/beta-fibres. Exp Physiol *87*, 239-244.

Lawson, S. N., and Waddell, P. J. (1991). Soma neurofilament immunoreactivity is related to cell size and fibre conduction velocity in rat primary sensory neurons. J Physiol *435*, 41-63.

Le, Y., Gagneten, S., Tombaccini, D., Bethke, B., and Sauer, B. (1999). Nuclear targeting determinants of the phage P1 cre DNA recombinase. Nucleic Acids Res *27*, 4703-4709.

Leffler, A., Cummins, T. R., Dib-Hajj, S. D., Hormuzdiar, W. N., Black, J. A., and Waxman, S. G. (2002). GDNF and NGF reverse changes in repriming of TTX-sensitive Na(+) currents following axotomy of dorsal root ganglion neurons. J Neurophysiol *88*, 650-658.

Lewandoski, M. (2001). Conditional control of gene expression in the mouse. Nat Rev Genet *2*, 743-755.

Lin, F. L., Sperle, K., and Sternberg, N. (1985). Recombination in mouse L cells between DNA introduced into cells and homologous chromosomal sequences. Proc Natl Acad Sci U S A *82*, 1391-1395.

Lindeberg, J., Mattsson, R., and Ebendal, T. (2002). Timing the doxycycline yields different patterns of genomic recombination in brain neurons with a new inducible Cre transgene. J Neurosci Res *68*, 248-253.

Lobe, C. G., Koop, K. E., Kreppner, W., Lomeli, H., Gertsenstein, M., and Nagy, A. (1999). Z/AP, a double reporter for cre-mediated recombination. Dev Biol *208*, 281-292.

Loonstra, A., Vooijs, M., Beverloo, H. B., Allak, B. A., van Drunen, E., Kanaar, R., Berns, A., and Jonkers, J. (2001). Growth inhibition and DNA damage induced by Cre recombinase in mammalian cells. Proc Natl Acad Sci U S A *98*, 9209-9214.

Lu, W. Y., Xiong, Z. G., Lei, S., Orser, B. A., Dudek, E., Browning, M. D., and MacDonald, J. F. (1999). G-protein-coupled receptors act via protein kinase C and Src to regulate NMDA receptors. Nat Neurosci *2*, 331-338.

Lundstrom, K. (2003). Latest development in viral vectors for gene therapy. Trends Biotechnol *21*, 117-122.

Luo, Z. D., Calcutt, N. A., Higuera, E. S., Valder, C. R., Song, Y. H., Svensson, C. I., and Myers, R. R. (2002). Injury type-specific calcium channel alpha 2 delta-1 subunit up-regulation in rat neuropathic pain models correlates with antiallodynic effects of gabapentin. J Pharmacol Exp Ther *303*, 1199-1205.

Malhotra, J. D., Kazen-Gillespie, K., Hortsch, M., and Isom, L. L. (2000). Sodium channel beta subunits mediate homophilic cell adhesion and recruit ankyrin to points of cell-cell contact. J Biol Chem *275*, 11383-11388.

Mallucci, G. R., Ratte, S., Asante, E. A., Linehan, J., Gowland, I., Jefferys, J. G., and Collinge, J. (2002). Post-natal knockout of prion protein alters hippocampal CA1 properties, but does not result in neurodegeneration. Embo J *21*, 202-210.

Malmberg, A. B., Chen, C., Tonegawa, S., and Basbaum, A. I. (1997). Preserved acute pain and reduced neuropathic pain in mice lacking PKCgamma. Science *278*, 279-283.

Mansour, S. L., Thomas, K. R., and Capecchi, M. R. (1988). Disruption of the proto-oncogene int-2 in mouse embryo-derived stem cells: a general strategy for targeting mutations to non-selectable genes. Nature *336*, 348-352.

Mao, X., Fujiwara, Y., Chapdelaine, A., Yang, H., and Orkin, S. H. (2001). Activation of EGFP expression by Cre-mediated excision in a new ROSA26 reporter mouse strain. Blood *97*, 324-326.

Mao, X., Fujiwara, Y., and Orkin, S. H. (1999). Improved reporter strain for monitoring Cre recombinase-mediated DNA excisions in mice. Proc Natl Acad Sci U S A *96*, 5037-5042.

Martin, G. R. (1981). Isolation of a pluripotent cell line from early mouse embryos cultured in medium conditioned by teratocarcinoma stem cells. Proc Natl Acad Sci U S A *78*, 7634-7638.

Matise, M. P., Auerbach, W., Joyner, A. L., (2000). Production of targeted embryonic stem cells. In Gene Targeting, A. L. Joyner, ed. (New York, Oxford university Press), pp. 101-132.

Matsuda, Y., Yoshida, S., and Yonezawa, T. (1978). Tetrodotoxin sensitivity and Ca component of action potentials of mouse dorsal root ganglion cells cultured in vitro. Brain Res *154*, 69-82.

McManus, M. T., and Sharp, P. A. (2002). Gene silencing in mammals by small interfering RNAs. Nat Rev Genet *3*, 737-747.

McQuay, H. (1999). Opioids in pain management. Lancet *353*, 2229-2232.

Metzger, D., and Chambon, P. (2001). Site- and time-specific gene targeting in the mouse. Methods *24*, 71-80.

Metzger, D., Clifford, J., Chiba, H., and Chambon, P. (1995). Conditional site-specific recombination in mammalian cells using a ligand-dependent chimeric Cre recombinase. Proc Natl Acad Sci U S A *92*, 6991-6995.

Meuser, T., Pietruck, C., Radbruch, L., Stute, P., Lehmann, K. A., and Grond, S. (2001). Symptoms during cancer pain treatment following WHO-guidelines: a longitudinal follow-up study of symptom prevalence, severity and etiology. Pain *93*, 247-257.

Mezey, E., Toth, Z. E., Cortright, D. N., Arzubi, M. K., Krause, J. E., Elde, R., Guo, A., Blumberg, P. M., and Szallasi, A. (2000). Distribution of mRNA for vanilloid receptor subtype 1 (VR1), and VR1-like immunoreactivity, in the central nervous system of the rat and human. Proc Natl Acad Sci U S A *97*, 3655-3660.

Millan, M. J., Czlonkowski, A., Morris, B., Stein, C., Arendt, R., Huber, A., Hollt, V., and Herz, A. (1988). Inflammation of the hind limb as a model of unilateral, localized pain: influence on multiple opioid systems in the spinal cord of the rat. Pain *35*, 299-312.

Millan, M. J., Millan, M. H., Czlonkowski, A., Hollt, V., Pilcher, C. W., Herz, A., and Colpaert, F. C. (1986). A model of chronic pain in the rat: response of multiple opioid systems to adjuvant-induced arthritis. J Neurosci *6*, 899-906.

Mogil, J. S., Wilson, S. G., Bon, K., Lee, S. E., Chung, K., Raber, P., Pieper, J. O., Hain, H. S., Belknap, J. K., Hubert, L., *et al.* (1999a). Heritability of nociception I: responses of 11 inbred mouse strains on 12 measures of nociception. Pain *80*, 67-82.

Mogil, J. S., Wilson, S. G., Bon, K., Lee, S. E., Chung, K., Raber, P., Pieper, J. O., Hain, H. S., Belknap, J. K., Hubert, L., *et al.* (1999b). Heritability of nociception II. 'Types' of nociception revealed by genetic correlation analysis. Pain *80*, 83-93.

Moulin, D. E., Iezzi, A., Amireh, R., Sharpe, W. K., Boyd, D., and Merskey, H. (1996). Randomised trial of oral morphine for chronic non-cancer pain. Lancet *347*, 143-147.

Mousa, S. A., Zhang, Q., Sitte, N., Ji, R., and Stein, C. (2001). beta-Endorphin-containing memory-cells and mu-opioid receptors undergo transport to peripheral inflamed tissue. J Neuroimmunol *115*, 71-78.

Muller, U. (1999). Ten years of gene targeting: targeted mouse mutants, from vector design to phenotype analysis. Mech Dev *82*, 3-21.

Murtra, P., Sheasby, A. M., Hunt, S. P., and De Felipe, C. (2000). Rewarding effects of opiates are absent in mice lacking the receptor for substance P. Nature *405*, 180-183.

Nagy, A. (2000). Cre recombinase: the universal reagent for genome tailoring. Genesis *26*, 99-109.

Neumann, S., Doubell, T. P., Leslie, T., and Woolf, C. J. (1996). Inflammatory pain hypersensitivity mediated by phenotypic switch in myelinated primary sensory neurons. Nature *384*, 360-364.

Niwa, H., Yamamura, K., and Miyazaki, J. (1991). Efficient selection for high-expression transfectants with a novel eukaryotic vector. Gene *108*, 193-199.

Noda, M., Suzuki, H., Numa, S., and Stuhmer, W. (1989). A single point mutation confers tetrodotoxin and saxitoxin insensitivity on the sodium channel II. FEBS Lett *259*, 213-216.

Novak, A., Guo, C., Yang, W., Nagy, A., and Lobe, C. G. (2000). Z/EG, a double reporter mouse line that expresses enhanced green fluorescent protein upon Cre-mediated excision. Genesis *28*, 147-155.

Novakovic, S. D., Tzoumaka, E., McGivern, J. G., Haraguchi, M., Sangameswaran, L., Gogas, K. R., Eglen, R. M., and Hunter, J. C. (1998). Distribution of the tetrodotoxin-resistant sodium channel PN3 in rat sensory neurons in normal and neuropathic conditions. J Neurosci *18*, 2174-2187.

Olson, E. N., Arnold, H. H., Rigby, P. W., and Wold, B. J. (1996). Know your neighbors: three phenotypes in null mutants of the myogenic bHLH gene MRF4. Cell *85*, 1-4.

Osoegawa, K., Tateno, M., Woon, P. Y., Frengen, E., Mammoser, A. G., Catanese, J. J., Hayashizaki, Y., and de Jong, P. J. (2000). Bacterial artificial chromosome libraries for mouse sequencing and functional analysis. Genome Res *10*, 116-128.

Patapoutian, A., Peier, A. M., Story, G. M., and Viswanath, V. (2003). ThermoTRP channels and beyond: mechanisms of temperature sensation. Nat Rev Neurosci *4*, 529-539.

Peier, A. M., Reeve, A. J., Andersson, D. A., Moqrich, A., Earley, T. J., Hergarden, A. C., Story, G. M., Colley, S., Hogenesch, J. B., McIntyre, P., *et al.* (2002). A heat-sensitive TRP channel expressed in keratinocytes. Science *296*, 2046-2049.

Pelletier, J., and Sonenberg, N. (1988). Internal initiation of translation of eukaryotic mRNA directed by a sequence derived from poliovirus RNA. Nature *334*, 320-325.

Pezet, S., Malcangio, M., and McMahon, S. B. (2002). BDNF: a neuromodulator in nociceptive pathways? Brain Res Brain Res Rev *40*, 240-249.

Pham, C. T., MacIvor, D. M., Hug, B. A., Heusel, J. W., and Ley, T. J. (1996). Long-range disruption of gene expression by a selectable marker cassette. Proc Natl Acad Sci U S A *93*, 13090-13095.

Possemato, R., Eggan, K., Moeller, B. J., Jaenisch, R., and Jackson-Grusby, L. (2002). Flp recombinase regulated lacZ expression at the ROSA26 locus. Genesis *32*, 184-186.

Price, M. P., McIlwrath, S. L., Xie, J., Cheng, C., Qiao, J., Tarr, D. E., Sluka, K. A., Brennan, T. J., Lewin, G. R., and Welsh, M. J. (2001). The DRASIC cation channel contributes to the detection of cutaneous touch and acid stimuli in mice. Neuron *32*, 1071-1083.

Ramirez-Solis, R., Liu, P., and Bradley, A. (1995). Chromosome engineering in mice. Nature *378*, 720-724.

Renganathan, M., Cummins, T. R., Hormuzdiar, W. N., and Waxman, S. G. (2000). alpha-SNS produces the slow TTX-resistant sodium current in large cutaneous afferent DRG neurons. J Neurophysiol *84*, 710-718.

Renganathan, M., Gelderblom, M., Black, J. A., and Waxman, S. G. (2003). Expression of Nav1.8 sodium channels perturbs the firing patterns of cerebellar Purkinje cells. Brain Res *959*, 235-242.

Rickert, R. C., Roes, J., and Rajewsky, K. (1997). B lymphocyte-specific, Cre-mediated mutagenesis in mice. Nucleic Acids Res *25*, 1317-1318.

Rinaldi, A., Marshall, K. R., and Preston, C. M. (1999). A non-cytotoxic herpes simplex virus vector which expresses Cre recombinase directs efficient site specific recombination. Virus Res *65*, 11-20.

Rodriguez, C. I., Buchholz, F., Galloway, J., Sequerra, R., Kasper, J., Ayala, R., Stewart, A. F., and Dymecki, S. M. (2000). High-efficiency deleter mice show that FLPe is an alternative to Cre-loxP. Nat Genet *25*, 139-140.

Rugiero, F., Mistry, M., Sage, D., Black, J. A., Waxman, S. G., Crest, M., Clerc, N., Delmas, P., and Gola, M. (2003). Selective expression of a persistent tetrodotoxin-resistant Na+ current and NaV1.9 subunit in myenteric sensory neurons. J Neurosci *23*, 2715-2725.

Saam, J. R., and Gordon, J. I. (1999). Inducible gene knockouts in the small intestinal and colonic epithelium. J Biol Chem *274*, 38071-38082.

Saegusa, H., Kurihara, T., Zong, S., Kazuno, A., Matsuda, Y., Nonaka, T., Han, W., Toriyama, H., and Tanabe, T. (2001). Suppression of inflammatory and neuropathic pain symptoms in mice lacking the N-type Ca2+ channel. Embo J *20*, 2349-2356.

Sah, D. W., Ossipo, M. H., and Porreca, F. (2003). Neurotrophic factors as novel therapeutics for neuropathic pain. Nat Rev Drug Discov *2*, 460-472.

Samad, T. A., Sapirstein, A., and Woolf, C. J. (2002). Prostanoids and pain: unraveling mechanisms and revealing therapeutic targets. Trends Mol Med *8*, 390-396.

Sanchez, J. F., Krause, J. E., and Cortright, D. N. (2001). The distribution and regulation of vanilloid receptor VR1 and VR1 5' splice variant RNA expression in rat. Neuroscience *107*, 373-381.

Sangameswaran, L., Delgado, S. G., Fish, L. M., Koch, B. D., Jakeman, L. B., Stewart, G. R., Sze, P., Hunter, J. C., Eglen, R. M., and Herman, R. C. (1996). Structure and function of a novel voltage-gated, tetrodotoxin-resistant sodium channel specific to sensory neurons. J Biol Chem *271*, 5953-5956.

Sauer, B. (1998). Inducible gene targeting in mice using the Cre/lox system. Methods *14*, 381-392.

Sauer, B., and Henderson, N. (1988). Site-specific DNA recombination in mammalian cells by the Cre recombinase of bacteriophage P1. Proc Natl Acad Sci U S A *85*, 5166-5170.

Schmidt, E. E., Taylor, D. S., Prigge, J. R., Barnett, S., and Capecchi, M. R. (2000). Illegitimate Cre-dependent chromosome rearrangements in transgenic mouse spermatids. Proc Natl Acad Sci U S A *97*, 13702-13707.

Schwenk, F., Baron, U., and Rajewsky, K. (1995). A cre-transgenic mouse strain for the ubiquitous deletion of loxP-flanked gene segments including deletion in germ cells. Nucleic Acids Res *23*, 5080-5081.

Segond von Banchet, G., Petersen, M., and Schaible, H. G. (1999). Expression of neurokinin-1 receptors on cultured dorsal root ganglion neurons from the adult rat. Neuroscience *90*, 677-684.

Seltzer, Z., Dubner, R., and Shir, Y. (1990). A novel behavioral model of neuropathic pain disorders produced in rats by partial sciatic nerve injury. Pain *43*, 205-218.

Shaw, G., Osborn, M., and Weber, K. (1986). Reactivity of a panel of neurofilament antibodies on phosphorylated and dephosphorylated neurofilaments. Eur J Cell Biol *42*, 1-9.

Shimshek, D. R., Kim, J., Hubner, M. R., Spergel, D. J., Buchholz, F., Casanova, E., Stewart, A. F., Seeburg, P. H., and Sprengel, R. (2002). Codon-improved Cre recombinase (iCre) expression in the mouse. Genesis *32*, 19-26.

Simpson, E. M., Linder, C. C., Sargent, E. E., Davisson, M. T., Mobraaten, L. E., and Sharp, J. J. (1997). Genetic variation among 129 substrains and its importance for targeted mutagenesis in mice. Nat Genet *16*, 19-27.

Sindrup, S. H., and Jensen, T. S. (1999). Efficacy of pharmacological treatments of neuropathic pain: an update and effect related to mechanism of drug action. Pain *83*, 389-400.

Smith, M. R., Smith, R. D., Plummer, N. W., Meisler, M. H., and Goldin, A. L. (1998). Functional analysis of the mouse Scn8a sodium channel. J Neurosci *18*, 6093-6102.

Soriano, P. (1999). Generalized lacZ expression with the ROSA26 Cre reporter strain. Nat Genet *21*, 70-71.

Souslova, V. A., Fox, M., Wood, J. N., and Akopian, A. N. (1997). Cloning and characterization of a mouse sensory neuron tetrodotoxin-resistant voltage-gated sodium channel gene, Scn10a. Genomics *41*, 201-209.

South, S. M., Kohno, T., Kaspar, B. K., Hegarty, D., Vissel, B., Drake, C. T., Ohata, M., Jenab, S., Sailer, A. W., Malkmus, S., *et al.* (2003). A conditional deletion of the NR1 subunit of the NMDA receptor in adult spinal cord dorsal horn reduces NMDA currents and injury-induced pain. J Neurosci *23*, 5031-5040.

Srinivas, S., Watanabe, T., Lin, C. S., William, C. M., Tanabe, Y., Jessell, T. M., and Costantini, F. (2001). Cre reporter strains produced by targeted insertion of EYFP and ECFP into the ROSA26 locus. BMC Dev Biol *1*, 4.

Stein, C., Schafer, M., and Machelska, H. (2003). Attacking pain at its source: new perspectives on opioids. Nat Med *9*, 1003-1008.

Steinert, P. M., and Roop, D. R. (1988). Molecular and cellular biology of intermediate filaments. Annu Rev Biochem *57*, 593-625.

Story, G. M., Peier, A. M., Reeve, A. J., Eid, S. R., Mosbacher, J., Hricik, T. R., Earley, T. J., Hergarden, A. C., Andersson, D. A., Hwang, S. W., *et al.* (2003). ANKTM1, a TRP-like channel expressed in nociceptive neurons, is activated by cold temperatures. Cell *112*, 819-829.

Strelkov, S. V., Herrmann, H., and Aebi, U. (2003). Molecular architecture of intermediate filaments. Bioessays *25*, 243-251.

Stucky, C. L., Gold, M. S., and Zhang, X. (2001). Mechanisms of pain. Proc Natl Acad Sci U S A *98*, 11845-11846.

Sufka, K. J., Watson, G. S., Nothdurft, R. E., and Mogil, J. S. (1998). Scoring the mouse formalin test: validation study. Eur J Pain *2*, 351-358.

Takesue, E. I., Schaefer, W., and Jukniewicz, E. (1969). Modification of the Randall-Selitto analgesic apparatus. J Pharm Pharmacol *21*, 788-789.

Tate, S., Benn, S., Hick, C., Trezise, D., John, V., Mannion, R. J., Costigan, M., Plumpton, C., Grose, D., Gladwell, Z., *et al.* (1998). Two sodium channels contribute to the TTX-R sodium current in primary sensory neurons. Nat Neurosci *1*, 653-655.

te Riele, H., Maandag, E. R., and Berns, A. (1992). Highly efficient gene targeting in embryonic stem cells through homologous recombination with isogenic DNA constructs. Proc Natl Acad Sci U S A *89*, 5128-5132.

Thomas, K. R., and Capecchi, M. R. (1987). Site-directed mutagenesis by gene targeting in mouse embryo-derived stem cells. Cell *51*, 503-512.

Thompson, S. W., King, A. E., and Woolf, C. J. (1990). Activity-Dependent Changes in Rat Ventral Horn Neurons in vitro; Summation of Prolonged Afferent Evoked Postsynaptic Depolarizations Produce a d-2-Amino-5-Phosphonovaleric Acid Sensitive Windup. Eur J Neurosci *2*, 638-649.

Thyagarajan, B., Guimaraes, M. J., Groth, A. C., and Calos, M. P. (2000). Mammalian genomes contain active recombinase recognition sites. Gene *244*, 47-54.

Tjolsen, A., Berge, O. G., Hunskaar, S., Rosland, J. H., and Hole, K. (1992). The formalin test: an evaluation of the method. Pain *51*, 5-17.

Toledo-Aral, J. J., Moss, B. L., He, Z. J., Koszowski, A. G., Whisenand, T., Levinson, S. R., Wolf, J. J., Silos-Santiago, I., Halegoua, S., and Mandel, G. (1997). Identification of PN1, a predominant voltage-dependent sodium channel expressed principally in peripheral neurons. Proc Natl Acad Sci U S A *94*, 1527-1532.

Tominaga, M., Caterina, M. J., Malmberg, A. B., Rosen, T. A., Gilbert, H., Skinner, K., Raumann, B. E., Basbaum, A. I., and Julius, D. (1998). The cloned capsaicin receptor integrates multiple pain-producing stimuli. Neuron *21*, 531-543.

Tonussi, C. R., and Ferreira, S. H. (1992). Rat knee-joint carrageenin incapacitation test: an objective screen for central and peripheral analgesics. Pain *48*, 421-427.

Troy, C. M., Brown, K., Greene, L. A., and Shelanski, M. L. (1990). Ontogeny of the neuronal intermediate filament protein, peripherin, in the mouse embryo. Neuroscience *36*, 217-237.

Truong, W., Cheng, C., Xu, Q. G., Li, X. Q., and Zochodne, D. W. (2003). Mu opioid receptors and analgesia at the site of a peripheral nerve injury. Ann Neurol *53*, 366-375.

Ventafridda, V., Tamburini, M., Caraceni, A., De Conno, F., and Naldi, F. (1987). A validation study of the WHO method for cancer pain relief. Cancer *59*, 850-856.

Waldmann, R., and Lazdunski, M. (1998). H(+)-gated cation channels: neuronal acid sensors in the NaC/DEG family of ion channels. Curr Opin Neurobiol *8*, 418-424.

Wang, L. X., and Wang, Z. J. (2003). Animal and cellular models of chronic pain. Adv Drug Deliv Rev *55*, 949-965.

Watkins, L. R., Milligan, E. D., and Maier, S. F. (2001). Glial activation: a driving force for pathological pain. Trends Neurosci *24*, 450-455.

Welsh, M. J., Price, M. P., and Xie, J. (2002). Biochemical basis of touch perception: mechanosensory function of degenerin/epithelial Na+ channels. J Biol Chem *277*, 2369-2372.

WHO (2003). The World Health Report 2003 (Geneva, World Health Organization).

Wilson, S. G., and Mogil, J. S. (2001). Measuring pain in the (knockout) mouse: big challenges in a small mammal. Behav Brain Res *125*, 65-73.

Winter, C. A., Risley, E. A., and Nuss, G. W. (1962). Carrageenin-induced edema in hind paw of the rat as an assay for antiiflammatory drugs. Proc Soc Exp Biol Med *111*, 544-547.

Woolf, C. J., and Mannion, R. J. (1999). Neuropathic pain: aetiology, symptoms, mechanisms, and management. Lancet *353*, 1959-1964.

Woolf, C. J., and Salter, M. W. (2000). Neuronal plasticity: increasing the gain in pain. Science *288*, 1765-1769.

Woolfe, G., MacDonald, A.D. (1944). The evaluation of the analgesic action of pethidine hydrochloride (Demerol). Journal of Pharmacology and Experimental Therapeutics *80*, 300-307.

Xiang, Z., Bo, X., and Burnstock, G. (1998). Localization of ATP-gated P2X receptor immunoreactivity in rat sensory and sympathetic ganglia. Neurosci Lett *256*, 105-108.

Zambrowicz, B. P., Imamoto, A., Fiering, S., Herzenberg, L. A., Kerr, W. G., and Soriano, P. (1997). Disruption of overlapping transcripts in the ROSA beta geo 26 gene trap strain leads to widespread expression of beta-galactosidase in mouse embryos and hematopoietic cells. Proc Natl Acad Sci U S A *94*, 3789-3794.

Zhou, L., Nepote, V., Rowley, D. L., Levacher, B., Zvara, A., Santha, M., Mi, Q. S., Simonneau, M., and Donovan, D. M. (2002). Murine peripherin gene sequences direct Cre recombinase expression to peripheral neurons in transgenic mice. FEBS Lett *523*, 68-72.